

**EDITORIAL BOARD****Editor-in-Chief****B.E. Paton***Scientists of PWI, Kiev***S.I. Kuchuk-Yatsenko** (*vice-chief ed.*),**V.N. Lipodaev** (*vice-chief ed.*),**Yu.S. Borisov, G.M. Grigorenko,****A.T. Zelnichenko, V.V. Knysh,****I.V. Krivtsun, Yu.N. Lankin,****L.M. Lobanov, V.D. Poznyakov,****I.A. Ryabtsev, K.A. Yushchenko***Scientists of Ukrainian Universities***V.V. Dmitrik**, NTU «KhPI», Kharkov**V.V. Kvasnitsky**, NTUU «KPI», Kiev**V.D. Kuznetsov**, NTUU «KPI», Kiev*Foreign Scientists***N.P. Alyoshin**

N.E. Bauman MSTU, Moscow, Russia

**Guan Qiao**

Beijing Aeronautical Institute, China

**A.S. Zubchenko**

DB «Gidropress», Podolsk, Russia

**M. Zinigrad**

Ariel University, Israel

**V.I. Lysak**

Volgograd STU, Russia

**Ya. Pilarczyk**

Welding Institute, Gliwice, Poland

**U. Reisgen**

Welding and Joining Institute, Aachen, Germany

**G.A. Turichin**

St. Petersburg SPU, Russia

**Founders**

E.O. Paton Electric Welding Institute, NASU

International Association «Welding»

**Publisher**

International Association «Welding»

**Translators**

A.A. Fomin, O.S. Kurochko, I.N. Kutianova

*Editor*

N.G. Khomenko

*Electron galley*

D.I. Sereda, T.Yu. Snegiryova

**Address**

E.O. Paton Electric Welding Institute,

International Association «Welding»

11 Kazimir Malevich Str. (former Bozhenko Str.),

03680, Kiev, Ukraine

Tel.: (38044) 200 60 16, 200 82 77

Fax: (38044) 200 82 77, 200 81 45

E-mail: journal@paton.kiev.ua

www.patonpublishinghouse.com

State Registration Certificate

KV 4790 of 09.01.2001

ISSN 0957-798X

**Subscriptions**

\$348, 12 issues per year,

air postage and packaging included.

Back issues available.

All rights reserved.

This publication and each of the articles contained  
herein are protected by copyright.Permission to reproduce material contained in this  
journal must be obtained in writing from the Publisher.**CONTENTS****SCIENTIFIC AND TECHNICAL**

- Yushchenko K.A., Bulat A.V., Skorina N.V., Marchenko A.E., Samojlenko V.I. and Kakhovsky N.Yu.* Effect of binder type on manufacturability and properties of E-08Kh20N9G2B type coated electrodes ..... 2
- Ermolenko D.Yu. and Golovko V.V.* Computation and experimental evaluation of formation of primary structure in weld metal with refractory inoculants ..... 10
- Vlasov A.F., Makarenko N.A. and Volkov D.A.* Intensification of arc and electroslog processes of welding by means of exothermal mixture introduction ..... 14
- Marchenko A.E.* Experimental studies of electrode coating thickness variation at pressing ..... 20
- Levchenko O.G. and Bezushko O.N.* Mathematical modeling of chemical composition of welding fumes in manual arc welding with high-alloyed electrodes ..... 28
- Prilutsky V.P., Akhonin S.V., Shvab S.L., Petrichenko I.K., Radkevich I.A., Rukhansky S.B. and Antonyuk S.L.* Restoration surfacing of parts of titanium alloy VT22 ..... 32
- Zhudra A.P., Voronchuk A.P., Kochura V.O. and Fedosenko V.V.* Effect of flux-cored strip surfacing modes on geometric parameters of deposited beads ..... 36
- Marchenko A.E., Skorina N.V., Kiselev M.O. and Trachevsky V.V.* Nuclear magnetic spectroscopy study of the structure of liquid glasses for welding electrodes ..... 41

**INDUSTRIAL**

- Slobodyanyuk V.P.* Production of welding consumables by enterprises of corporation «PlazmaTek» ..... 46
- Sidlin Z.A.* Control of granulometric composition of powders applied in manufacture of welding consumables ..... 50
- Babinets A.A. and Ryabtsev I.A.* Flux-cored wire for wear-resistant surfacing of thin-sheet structures ..... 54
- Kostin A.M., Martynenko V.A., Maly A.B. and Kvasnitsky V.V.* Adhesion-active high-temperature wear-resistant surfacing consumables KMKh and KMKhS ..... 58
- Pustovojt S.V., Skorina N.V. and Petruk V.S.* State-of-the art and tendencies in development of welding electrode market in Ukraine ..... 62

**NEWS**

- Production of flux-cored wires in «TM.VELTEK» Company ..... 68

*This issue of journal contains scientific-technical papers and papers dedicated to industrial points, prepared by the specialists in the field of development, production and application of welding and surfacing consumables. Among the authors are the apprentices and followers of Prof. I.K. Pokhodnya, heads and specialists of a series of enterprises manufacturing welding consumables. Readers of the journal will also be able to familiarize with current market of welding consumables in Ukraine, examples of successful organization of production and realization of the products, recommendations on increase the competitiveness of domestic welding consumables.*

*Editorial note*

## EFFECT OF BINDER TYPE ON MANUFACTURABILITY AND PROPERTIES OF E-08Kh20N9G2B TYPE COATED ELECTRODES

K.A. YUSHCHENKO, A.V. BULAT, N.V. SKORINA, A.E. MARCHENKO, V.I. SAMOJLENKO and N.Yu. KAKHOVSKY

E.O. Paton Electric Welding Institute, NASU  
11 Kazimir Malevich Str., 03680, Kiev, Ukraine. E-mail: office@paton.kiev.ua

The results of investigations of the properties of electrode compounds, coatings and electrodes of rutile-basic type were set forth and analyzed. These electrodes are designed for welding of high-strength Cr–Ni steels depending on composition of lithium-containing liquid glass. It is shown that application of Li–Na–K liquid glass for manufacture of such electrodes allows significantly improving their hygiene and sanitary properties due to reduction of specific emissions of hexavalent chromium high-toxic compounds. Simultaneously, application of Li–Na–K glass results in significant decrease of hygroscopic capacity of the coating, at that its strength and crack resistance in welding do not deteriorate, and ductility and impact toughness of weld metal is somewhat improved. The workability indices and welding-technological characteristics of compared electrodes are at the same level. The results of the investigations allowed upgrading coating composition and production technology of ANV-35 electrodes. 23 Ref., 9 Tables, 2 Figures.

**Keywords:** *high-alloy Cr–Ni steels, arc welding, coated electrodes, binders, processing characteristics of electrode compounds, strength and hygroscopic properties of electrode coatings, welding-technological and hygienic properties of electrodes, composition and structure of deposited metal, mechanical properties of weld metal*

In course of many decades the E.O. Paton Electric Welding Institute, carried out investigations under the leadership of Prof. I.K. Pokhodnya, academician of the NAS of Ukraine. They were directed on reduction of specific emissions and toxicity of the fumes, forming in welding using general designation electrodes. The main results are generalized in works [1, 2]. Under his guidance in 2013–2015 the studies were carried out on possibility of improvement of sanitary and hygiene characteristics of the general designation electrodes due to variation of types of applied binder.

Application of forced ventilation does not always help to remove the high-toxic compounds of hexavalent chromium (MAC 0.01 mg/m<sup>3</sup>) [3], contained in a welding fume (WF), from air of welder's working zone in manual arc welding of high-alloy Cr–Ni

steels. Besides, forced ventilation can not be used at all in performance of repair works inside capacitive and column equipment at the enterprises of petrochemical and chemical industry.

Experimental investigations determined a mutagenic nature of WF containing hexavalent chromium compounds. Therefore, now exceptionally large attention in the world is given to improvement of sanitary and hygiene properties of the electrodes designed for welding of high-alloy Cr–Ni steels. A successful solution of this problem, undoubtedly, depends on knowledge of fundamental characteristics as well as conditions of WF formation in welding of indicated steels.

It follows from domestic and foreign publications [4–9] that:

- chromium (the second after manganese metal on value of vapor pressure at arc welding process tem-

\*The work was carried out by initiative of Prof. I.K. Pokhodnya, academician of the NAS of Ukraine. Engineers O.I. Folbort and A.I. Radchenko participated in the work.

peratures) transfers to a welding fume solid constituent (WFSC) from the electrode and base metal as well as metallic constituents of electrode coating;

- intensity of transfer and valence of chromium in WFSC depend on its content in melted metal and electrode, real composition of slag-forming part of the coating and slag forming from it. The higher chromium content in steel and, respectively, in welding consumable, the more chromium is in WFSC. Following from the acting sanitary norms, a danger of chromium emission should be taken into account in welding of steels containing more than 5 % of chromium. Fluxing materials, as a rule, restrain chromium evaporation. Therefore, other conditions being equal, total content of chromium in WFSC in shielded-gas welding, even at high oxidizing capacity, is higher than in coated electrode welding. At that no hexavalent modification of chromium was found in it;

- according to existing classification chromium compounds in WF are divided on soluble and insoluble in water. Each of mentioned modifications includes compounds from three- or hexavalent chromium. Total portion of chromium in WFSC during coated electrode welding for stainless steels joining varies from 3 to 7 % among them from 60 to 90 % falls at its soluble compounds, representing themselves, as a rule, potassium and sodium chromates;

- the largest levels of emission of hexavalent chromium compounds in welder breath zone are observed when using the electrodes with basic coating, they are lower for rutile-basic electrodes and rutile-coated electrodes have the lowest emissions. There is no one-valued relationship between the total level of WFSC emission and content of hexavalent chromium in it. The first is related with arc voltage (power) and gas-forming capacity of the coating, the second with its oxidizing capability;

- instrumental methods proved that chromate (soluble) form of hexavalent chromium compound in the welding fume is caused by potassium and sodium silicates, being a constituent of the electrode coating or flux-cored wire core. A source of entering of alkali oxides, i.e. liquid glass, fluor spar or mica in the coating has no matter. The soluble compounds of hexavalent chromium are not detected in WFSC during welding using electrodes with lithium silicate;

- role of  $\text{CaF}_2$  in formation of the hexavalent chromium compounds is not investigated, however there is certain correlation between emission of hexavalent chromium and soluble fluorides. Reduction of  $\text{CaCO}_3/\text{CaF}_2$  relationship in the electrode coating results in increase of fume emission and content in it of  $\text{Cr}^{+6}$  compounds. Moreover, potassium chromates in WFSC were found in welding using electrodes having no  $\text{CaF}_2$  in their coating;

- electrodes, which are made based on lithium silicate for complete suppression of  $\text{Cr}^{+6}$ , show a series of sufficiently significant process and service disadvantages. In particular, arc burning stability is substantially deteriorated and as a result such electrodes can not be used for alternating current welding. Coating strength is dramatically reduced, it cracks in welding that results in worsening of protection of molten metal from environment. Based on foreign publications, indicated disadvantages of the electrodes can be eliminated by means of improvement of coating composition and adjustment of process parameters of their manufacture. Necessary lithium-containing liquid glasses [10, 11] as well as new electrode grades are developed and manufactured. However, the electrodes with improved sanitary and hygiene indices, which guarantee the requirements of commercial consumer, have not appear yet at the market.

Aim of the following work lies in the following:

- determination of a way for reduction of  $\text{Cr}^{+6}$  emission in WF due to process means of electrode manufacture, including determination of optimum relationship of lithium-sodium-potassium compounds in liquid glass binder, at which no changes in electrodes and welding process indices take place;

- specification of a role of coating constituents, in particular,  $\text{CaF}_2$  in formation of  $\text{Cr}^{+6}$  compounds in WFSC content.

**Object and experimental procedures.** Electrodes of ANV-35 (E-08Kh20N9G2B on GOST 10051-75) with rutile-basic coating were investigated. Materials corresponding to the requirements of reference documents on composition and grain-size were used for manufacture. Rod diameter is 3 mm, coating is 4.95–5.15 mm and 350 mm length. Table 1 shows the composition and characteristics of liquid glasses selected

**Table 1.** Composition (wt.%) and characteristics of liquid glasses

Type of liquid glass	Silicate module, rel. un.	$\text{SiO}_2$	$\text{Li}_2\text{O}$	$\text{Na}_2\text{O}$	$\text{K}_2\text{O}$	D.r.*	Density, $\text{g/cm}^3$ / toughness, MPa·s
K–Na	2.88	27.85	–	3.90	9.25	41.00	1.43/590
Li–Na–K	2.19	27.75	1.80	7.00	3.60	40.15	1.38/530
Li–Na	2.75	30.20	2.70	5.17	1.00	39.07	1.39/525
Li	3.60	22.80	3.15	–	–	25.95	1.25/535

\*D.r. — dry residual of liquid glass.

for planned experiments in course of preliminary experiments.

Since lithium silicates are not soluble in water, their aqueous solutions were synthetically produced by means of chemical reaction of taken in necessary relationship aqueous solution of lithium hydrate with powder of aqua silicon acid at 50–60 °C temperature. Brought up to set characteristics, they were mixed with Na and K–Na liquid glasses, produced using autoclave solving of corresponding silicate rocks.

Electrode compounds were prepared in an intensive mixer in course of 3 min. Their properties were evaluated on plastic strength  $P_m$  value, characterizing hardness of electrode compound in state of briquette and coating just applied on a rod as well as value and uniformity of flow pressure  $P_e$  through die hole of 4 mm diameter and 40 mm length. Mentioned indices were evaluated using cone aotoplastometer OB2059 and capillary viscometer OB1435, developed and manufactured at the E.O. Paton Electric Welding Institute. The procedures are described in work [12].

At that it was assumed that the coating, which is characterized by higher ductility strength at the same pressure, has the best properties.

Strength of dewatered coating of the electrodes was determined using three-point bend method of cylinder samples of 4 mm diameter and 50 mm length, made by means of extrusion of compound mass [13]. Dewatering of the samples was carried out through their drying-baking at 200, 300, 350 and 400 °C during one hour.

Hygroscopy of the coating was evaluated on kinetics of moisture sorption at short-term (8 hours) and long-term (2 weeks) exposure of the electrode samples in hydrostat at 20 °C and relative air humidity 84 %. Amount of absorbed moisture was determined by weighing of the samples with 1 and 24 hours time gap; mass increment was related to dry coating mass.

Comparative evaluation of binder effect on coating crack resistance in welding was determined using the following procedure. Welding using experimental electrodes was carried out from VDU-504 rectifier using reverse polarity ( $I_w = 90–100$  A). For each variant at least three experiments were performed by means of continuous fusion of electrodes of 350 mm length to stub of 50, 130 and 200 mm length. After cooling to room temperature the coating surface of each stub was examined and amount and length of cracks were determined in accordance with the requirements of GOST 9466–75, i.3. If no rejection signs were found, coating resistance to chips was evaluated by means of stub drop on a steel plate from 0.5 m height. The chips of any size on working part of the coating of the

tested sample (except for stub of 50 mm length) are not permitted.

Welding-technological properties of the electrodes were compared in terms of arc burning stability, weld formation quality and separation of slag crust, which were determined in welding and surfacing on plates of 12Kh18N10T steel using reverse polarity direct current from VDU 504 ( $U_{o-c} = 80$  V) rectifier.

Arc burning stability was estimated by standard deviations of current and arc voltage ( $\sigma_{I_a}$  and  $\sigma_{U_a}$ ) from statistically average indices ( $I_a^{av}$  and  $U_a^{av}$ ). They were received with the help of introduced in a welding circuit nonstationary processes analyzer of ANP-2 type [14], allowing in a real time mode reading, storing and statistically processing digital information on current and voltage changes.

Quality of metal formation was evaluated on the average values of weld geometry coefficient  $K_g^{av}$ , representing itself a relationship of weld width to its height [15]. Corresponding measurements were carried out on the beads deposited with pilot electrodes on plate surface in flat, vertical and overhead positions with transverse 7–8 mm amplitude oscillations of the electrodes.

Separation of a slag crust was determined following procedure [16] on  $\phi_{av}^0$  index, representing itself average value of enforced vee angle of plates butt joint, at which the slag crust is completely separated from a root weld surface.

Effect of binder type on composition and structure of deposited metal as well as mechanical properties of weld metal was evaluated in accordance with the requirements of GOST 9466–75. For this eight-layer deposits were made by experimental electrodes, in which content of C, Cr, Ni, Mn, Nb, S and P was determined by method of diffusion spectrometry (spectrometer DFS-51), and content of  $\alpha$ -phase ( $\delta$ -ferrite) was determined by magnetometer method (magnetometer MF-10I). Nine cylinder samples of 5 mm diameter and length were cut from upper layers for determination of content of oxygen, hydrogen and nitrogen. Analysis was carried out on LECORO-316, LECOPH-402 and LECOTN-114 units by reduction melting method [17].

Mechanical properties of weld metal were evaluated in accordance with GOST 9466–75. For this butt joints of plates of 12Kh18N10T steel were welded using the experimental electrodes. Welding was made using reverse polarity direct current ( $I_w = 80–90$  A) from VDU 504 rectifier. Three samples of II and IX type on GOST 6996–66 were cut out from the indicated joints for static tension and impact bend test, respectively. Yield strength, strength and relative elon-

**Table 2.** Process characteristics of electrode compounds (nature of flow — uniform)

Binder		Plastic strength $P_m$ , MPa	Extrusion indices	
Type	Dose, %		Pressure $P_e$ , MPa in consumption $Q$ , cm <sup>3</sup> /s	
			1	10
K-Na	23.1	0.25	32.5	37.0
Li-Na-K	24.0	0.72	33.5	35.5
Li-Na	24.0	0.75	34.0	42.5
Li	25.7	0.90	18.5	21.0

gation ( $\sigma_y$ ,  $\sigma_t$  and  $\delta_5$ ) as well as impact toughness were determined on sharp notch samples (*KCV*).

Composition of slags was determined by X-ray spectrum analysis method using X'Unique II Philips device, and specific emissions of WFSC were found by total filtration method (three experiments for each variant of the electrodes). The filters from Petryanov tissue of FPP15-1.5 grade [16] were used. WFSC samples were precipitated on AFA-KhA-18 filters [17–19] for chemical analysis. All experiments were carried out in special chamber under similar conditions in reverse polarity direct current surfacing ( $I_w = 90\text{--}100\text{A}$ ) on plates of steel 12Kh18N10T.

**Investigation results.** Results of evaluation of process indices of the electrode compounds are given in Table 2.

It can be seen that lithium-containing binders provide for higher ductility of electrode compound in comparison with potassium-sodium liquid glass, which is usually used for manufacture of ANV-35 electrodes. It becomes apparent due to almost three-fold increase of their plastic strength at equivalent extrusion pressure.

The results of coating strength tests are given in Figure 1. It can be seen that independent on binder

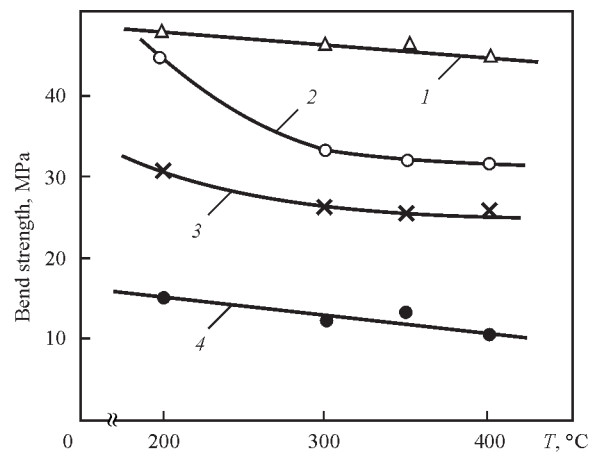


**Figure 1.** Effect of type of liquid glass and baking temperature on results of testing of coating bend strength: 1 — K-Na; 2 — Li-Na-K; 3 — Li-Na; 4 — Li

type increase of sample baking temperature results in decrease of their strength. K-Na liquid glass provides for maximum coating strength. It reduces by 11, 22 and 80 %, respectively, using Li-Na-K, Li-Na and Li types of binders. In the case of Li-Na-K and Li-Na binders, the strength reduction level is not critical in contrast to the samples, manufactured based on lithium binder.

The results of comparison of hygroscopic characteristics of the coatings, produced using different liquid glasses, are given in Figure 2.

It can be seen that in comparison with standard K-Na liquid glass the lithium-containing binder provides for lower (6–8 times) hygroscopy of the electrode coating. In this connection they have small difference from pure lithium binder. Such an effect is apparently related with compression of silicon-oxygen mesh at implantation in it of lithium ions and agrees with known virtually complete incapability of lithium ions to hydration.

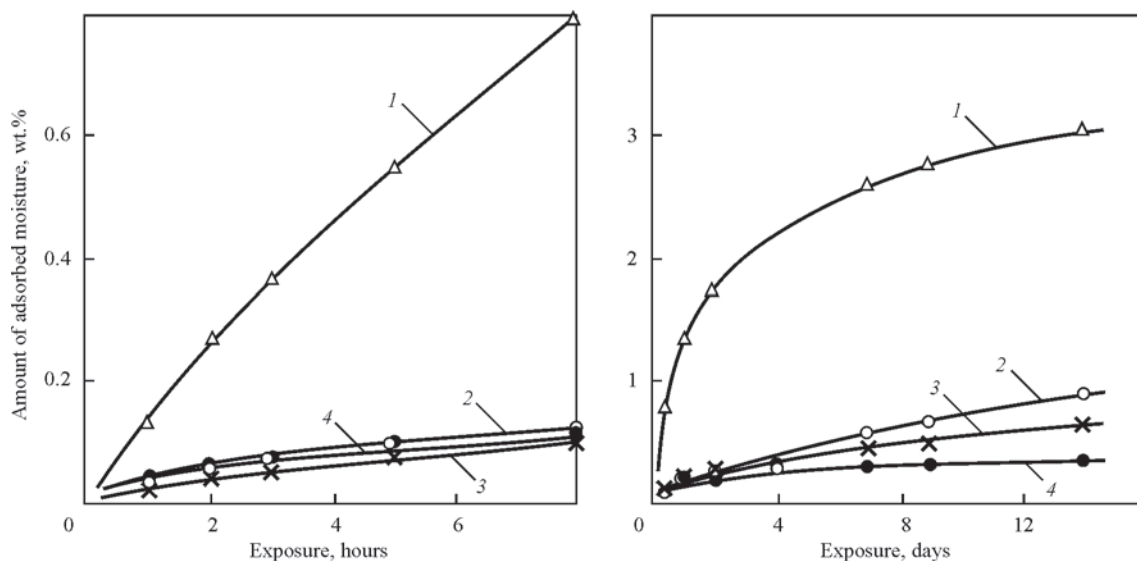


**Figure 2.** Effect of binder type on kinetics of sorption of atmospheric moisture by electrode coatings (designations are the same as in Figure 1)

**Table 3.** Effect of binder type on electrode coating susceptibility to crack in welding

Binder type	Diameters of electrode/coating, mm	Length of stub, mm	Average length of cracks, formed in electrode coating from		Nature of coating cracking
			bushing, mm	contact end, mm	
K–Na	3.0/5.00	60	–	–	Cracks are formed in 50–60 s after welding completion
		136	–	25	
		225	27	30	
Li–Na–K	3.0/5.05	62	–	–	
		134	5	27	
		222	30	38	
Li–Na	3.0/4.95	64	–	20	Cracks are formed during welding and propagate after its completion
		135	34	27	
		223	35	40	
Li	3.0/5.15	64	–	–	Excessive brittleness of coating before, during and after welding
		135	–	–	
		227	–	–	

**Table 4.** Welding-technological properties of electrodes

Type of liquid glass	Weld geometry coefficient $K_g^{av}$ in surfacing in positions			Separability of slag crust $\phi_{av}^0$	Statistical characteristics of welding mode			
	flat	vertical	overhead		$I_a^{av}$ , A	$\sigma_{I_a}$ , A	$U_a^{av}$ , V	$\sigma_{U_a}$ , V
K–Na	3.1	2.8	2.6	4	96.5	14.5	20.3	4.0
Li–Na–K	3.1	2.8	2.5	5	96.0	14.5	21.0	4.1
Li–Na	3.2	2.6	2.5	6	95.2	14.8	22.0	4.2
Li	2.8	2.5	2.3	8	94.3	18.2	23.5	5.7

**Table 5.** Composition (wt.%) and structure of deposited metal

Type of liquid glass	C	Cr	Ni	Mn	Si	Nb	S	P	$\alpha$ -phase, %
K–Na	0.053	20.1	10.2	1.3	1.0	0.7	0.011	0.022	7.5
Li–Na–K	0.053	19.6	9.9	1.3	1.1	0.7	0.010	0.021	6.5
Li–Na	0.051	19.9	10.1	1.3	1.0	0.7	0.010	0.022	6
Li	0.048	19.5	9.3	1.2	1.0	0.7	0.011	0.028	6
Requirements of GOST 10052–75	0.05–0.12	18–22	8.0–10.5	1.0–2.5	<1.3	0.7–1.3	<0.020	<0.030	2–8

Table 3 shows the results of testing of pilot electrode coating susceptibility to cracking. According to Table 3 allowable (from point of view of welding quality) susceptibility of the electrode coating to cracking is provided in use of K–Na and Li–Na–K binders. Application of Li–Na binder is unacceptable due to coating cracking in welding, and Li glass due to its excessive brittleness. It is necessary to pay attention on correlation of received results to coating strength values given in Figure 1.

Table 4 gives the indices of welding-technological properties of the electrodes. Based on them, variation of composition of the combined liquid glasses (K–Na, Li–Na–K or Na–Li) does not influence weld geometry coefficient in any welding position (difference of  $K_g^{av}$  values does not exceed 7 %).

Statistical indices of mode parameters of arc burning varies at that more systematically. Thus, increase of mass portion of lithium in the liquid glass (from 0 to 2.7 %) promotes for rise of statistically average values of voltage (from 20.3 to 22.0 V) and reduces that of current (from 96.5 to 95.2 A), while standard

deviations of current  $\sigma_{I_a}$  as well as  $\sigma_{U_a}$  at that rise from 14.5 to 14.8 and from 4.0 to 4.2 V, respectively. Nevertheless, variations of these indices do not exceed the 8 % limits that agree with the conclusions made in work [20]. Unfavorable effect of lithium, in particular on indices of arc voltage dissipation, can be considered critical only in the case of complete absence of  $Na_2O$  and  $K_2O$  in liquid glass.

Effect of liquid glass composition on slag crust separation is more noticeable. If the study is limited only with investigation of lithium-containing liquid glasses, than a separation index deteriorates with rise 1.5 time of lithium portion in liquid glass; if we take into account the results of testing of the electrodes produced only based on pure lithium glass, this index degrades 2 times.

The results of testing of chemical composition and metal structure deposited with experimental electrodes are given in Table 5, content of gases is in Table 6 and weld metal mechanical properties in Table 7. All electrodes on chemical composition and content

of  $\alpha$ -phase are virtually similar and correspond to E-08Kh20N9G2B type on GOST 10052–75. Moreover, it is determined that application of Li-containing binders results in decrease in the deposited metal of oxygen and hydrogen content and rise of nitrogen. In our opinion it is caused by increase of reduction capacity of the slags.

The average (from three results) values of mechanical properties indices of weld metal are given in Table 7. According to received data application of Li-containing binders instead of standard K–Na liquid glass allows significantly increasing relative elongation and impact toughness of weld metal that can be explained by decrease of oxygen content and rise of nitrogen in it (see Table 6).

Composition of the slags and experimental electrodes are given in Table 8. It follows from it that composition of welding slag to sufficient extent depends on type of liquid glass. The largest deviations lied in the following:

- five-fold decrease of  $K_2O$  portion in the slag at transfer from K–Na to Li-liquid glass (it is promoted, from one side, by reduction of  $K_2O$  portion in the liquid glass and, at the same time,  $K_2O$  evaporation);

**Table 7.** Mechanical properties of weld metal (temperature 20 °C)

Type of liquid glass	$\sigma_y$ , MPa	$\Sigma$ , MPa	$\delta_s$ , %	KCU, J/cm <sup>2</sup>	KCV, J/cm <sup>2</sup>
K–Na	567.1	709.5	29.5	–	88.5
Li–Na–K	513.7	702.9	35.3	–	117.7
Li–Na	535.0	713.1	33.3	–	129.3
Li	507.3	708.2	38.5	–	122.3
Requirements of GOST 10052–75	Not regulated	>55	>22	>8.0	Not regulated

**Table 8.** Composition of slags (wt.%)

Type of liquid glass	TiO <sub>2</sub>	SiO <sub>2</sub>	CaO	MgO	MnO	Fe <sub>2</sub> O <sub>3</sub>	Al <sub>2</sub> O <sub>3</sub>	Cr <sub>2</sub> O <sub>3</sub>	Nb <sub>2</sub> O <sub>5</sub>	Na <sub>2</sub> O	K <sub>2</sub> O	CaF <sub>2</sub>
K–Na (0)	30.9	16.1	15.3	1.1	5.4	1.6	5.4	7.1	1.9	1.0	2.5	11.2
Li–Na–K(1.80)	30.8	16.5	14.5	1.3	5.6	1.6	5.6	7.0	1.9	1.0	1.3	12.7
Li–Na(2.70)	30.0	16.7	11.5	1.6	5.3	1.1	5.4	7.5	1.8	1.9	0.8	16.1
Li(3.15)	31.3	16.1	10.9	1.4	5.5	1.6	5.4	7.1	1.9	–	0.5	17.9

Note. Portion of Li<sub>2</sub>O is indicated in the brackets. Portion of V<sub>2</sub>O<sub>5</sub> – 0.1 %, ZrO<sub>2</sub> – 0.4 %. Fraction relationship of chromium oxides in slags was not determined.

**Table 9.** Indices of emission and composition of WFSC

Type of liquid glass	WFSC total emission		Weight fraction, % in WFSC					
	Intensity $V_a$ , g/min	Specific $G_a$ , g/kg	Cr <sup>6+</sup>	Cr <sup>3+</sup>	Mn	Ni	F <sub>p</sub>	F <sub>np</sub>
K–Na (0 %)	0.50	11.58	1.96	2.62	4.81	1.47	11.68	1.30
Li–Na–K (0.7 %)	0.45	10.10	1.77	2.67	5.27	1.38	10.24	1.69
Li–Na–K (1.8 %)	0.35	7.28	1.44	2.82	5.69	1.29	10.35	1.88
Li–Na (2.7 %)	0.26	5.52	0.89	3.04	5.73	1.62	11.65	1.34
Li (3.2 %*)	0.20	4.52	Not detected	3.91	5.20	1.39	5.76	1.56

Note. Weight portion of Li<sub>2</sub>O in liquid glass is indicated in the brackets.

**Table 6.** Content of gases in deposited metal, wt.%

Type of liquid glass	H	N	O
K–Na	0.0015	0.067	0.062
Li–Na–K	0.0014	0.072	0.058
Li–Na	0.0012	0.079	0.051
Li	0.0010	0.082	0.045

- 1.6 time rise of CaF<sub>2</sub> portion in slag that, undoubtedly, related with decrease of escape of fluorine at transfer from K–Na to Li liquid glass;

- 1.4 time reduction of CaO portion.

The rest of constituents, including portion of Cr<sub>2</sub>O<sub>3</sub>, was kept at the same level.

Table 9 generalizes the results of testing the sanitary and hygiene characteristics of the experimental electrodes. Another set of liquid glasses was used for their manufacture.

It can be seen that application of lithium-containing binders instead of K–Na liquid glass significantly improves sanitary and hygiene indices of the electrodes. It reveals through reduction of WFSC emission and content in the fume of the most hazardous constituent, namely hexavalent chromium. The level of improvement of sanitary and hygiene indices rises with increase of a portion of lithium constituent in the liquid glass. The largest effect is reached in ap-

plication of Li–Na and Li-silicates. In comparison with K–Na analogue WFSC specific emission and its intensity reduces 2 times for Li–Na and 2.5 times for pure Li-silicate. Content of carcinogenic hexavalent chromium drops 2.2 times, and it is not revealed in WFSC at application of pure Li-binders.

Changes of slag material composition, in particular, rise of portion of  $\text{CaF}_2$  and equivalent decrease of CaO portion at transfer from K–Na to Li liquid glasses are accompanied by intensive  $\text{Cr}^{+6}$  emission in WF content.

Let's consider given results in more details. Titanous slags are characterized by special physical-chemical properties. They are formed by low titanium oxides of different valence, capable to include in their structure a large number of oxides in liquid and solid states with close parameters of crystalline lattice ( $\text{FeO}$ ,  $\text{MnO}$ ,  $\text{MgO}$ ,  $\text{NiO}$ ,  $\text{V}_2\text{O}_5$ ,  $\text{Cr}_2\text{O}_3$ ,  $\text{Al}_2\text{O}_3$ ), except for CaO, which forms perovskite with  $\text{TiO}_2$ , sufficiently refractory compound, and  $\text{SiO}_2$ , which is related with appearance of X-ray amorphous glass-like phase [21] in titanous (including welding) slags. Therefore, solidified titanous slags, even having significant difference between themselves on chemical composition, can be very similar to each other on crystalline lattice. In contrast to other welding slags they are characterized by low oxidizing capacity, and electrodes with rutile coating, designed for welding of low-carbon and low-alloy steels, are characterized by the highest sanitary and hygiene properties.

Lithium liquid glass intensifies reducing capability of titanium slags, since, based on current ideas, structure of lithium silicates does not have so called free oxygen. All oxygen is bounded with silicon atoms by strong siloxan linkages, and structure of the melt is characterized by the highest connectivity index (Q-factor)  $Q^4$  [22]. Presence of K- and Na-oxides and  $\text{CaF}_2$  in the rutile-basic type coating significantly complicates this picture, in general, suppressing favorable effect of low titanium and lithium oxides on sanitary and hygiene characteristics of the electrons.

Sodium and, in particular, potassium oxides evaporate easier from molten welding slags than lithium oxides. It can be explained through comparison of the coefficients of surface tension of alkali lithium, sodium and potassium silicates. Based on data of work [23] surface tension of  $\text{Li}_2\text{O}\cdot\text{SiO}_2$  melt ( $315 \text{ MJ/cm}^2$ ) is significantly more than of  $\text{Na}_2\text{O}\cdot\text{SiO}_2$  and  $\text{K}_2\text{O}\cdot\text{SiO}_2$  melts ( $288$  and  $236 \text{ MJ/cm}^2$ , respectively). It is without doubt that  $\text{Li}_2\text{O}\cdot\text{SiO}_2$  melt with larger surface tension will evaporate less intensively, than that of sodium and potassium silicates. Alkali oxides react with  $\text{CaF}_2$ , form volatile soluble fluorides and enrich the melt with calcium oxide. The latter forms with tita-

um oxide the perovskite, weakening the melt by titanium sesqui oxides and, thus, decreasing its reducing capacity. This, in turn, simplifies formation of ions of hexavalent chromium. To the smallest extent this scheme is realized in slags of the electrodes produced based on lithium liquid glass, and it is proved by slag compositions given in Table 8.

Carried investigations allowed correcting basic composition of ANV-35 electrode coating mainly by means of limitation in it of portion of potassium, sodium and calcium oxides and application of Li–Na–K liquid glass. Upgraded ANV-35MK electrodes significantly exceeds ANV-35 electrodes on set of characteristics, including hygienic ones.

## Conclusions

1. Effect of lithium-containing liquid glass on manufacturability, welding-technological properties of the electrodes, composition of deposited metal and mechanical properties of weld metal was studied by example of rutile-basic coated electrodes of E-08Kh20N9G2B type. It is determined that the optimum complex of technological and welding characteristics of the electrodes is provided by application of Li–Na–K binder with 1.5 % lithium constituent.

2. Application of Li–Na–K binder instead of K–Na liquid glass allows approximately 2 times reduction of emission of high-toxic  $\text{Cr}^{+6}$  compounds in WFSC composition, 7–8 times decrease of hygroscopy of electrode coating, 17 % rise of relative elongation and 30 % of weld metal impact toughness. At that, process indices and welding-technological properties of the electrodes remain unchanged.

3. Favorable effect of lithium oxides on decrease of emission of  $\text{Cr}^{+6}$  compounds in WF composition is caused by rise of slag reducing capacity due to blocking the processes of formation of potassium and sodium fluorides as well as potassium titanites.

4. Unfavorable effect of  $\text{CaF}_2$  from point of view of emission of hexavalent chromium ions is explained by the fact that reaction of potassium fluoride formation is accompanied by increase of CaO in the slag, i.e. its basicity index. This results in increase of free oxygen in the slag. At the same time, rise of CaO portion in the slag provides for decrease of reducing capacity of the slag also because larger portion of higher titanium oxides coordinates with CaO (it is proved by perovskite formation in the solidified slag), while portion of low-valent titanium oxides, characterized by lower oxidizing capacity, equivalently reduces at that.

5. Coating composition of ANV-35 grade electrodes was upgraded with a view of application of Li–Na–K binder. New modifications of the electrodes was coded as ANV-35MK. They significantly exceed

the electrodes with basic coatings on set of characteristics, including hygiene one.

1. Pokhodnya, I.K., Gorpenyuk, V.N., Milichenko, S.S. et al. (1990) *Metallurgy of arc welding: processes in arc and melting of electrodes*. Kiev: Naukova Dumka.
2. Pokhodnya, I.K., Yavdoshchin, I.R., Gubunya, I.P. (2011) Welding fume – factors of influence, physical properties and methods of analysis (Review). *The Paton Welding J.*, **6**, 33–36.
3. *GOST 12.1.007–76 SS BT*: Harmful substances. Classification and general safety requirements. Introd. 01.01.1977.
4. Yushchenko, K.A., Levchenko, O.G., Bulat, A.V. et al. (2007) Sanitary and hygienic characteristics of covered electrodes for welding high-alloy steels. *The Paton Welding J.*, **12**, 35–38.
5. Levchenko, O.G., Bulat, A.V., Bezushko, O.M. (2010) Influence of electrode coating on hygienic characteristics of fumes, formed in welding of high-alloy steels. *Visnyk NT UU KPI. Seriya Girnystvo*, Issue 19, 171–177.
6. Kawada, K., Kobayashi, M. Experimental investigations on hazard of lithium in welding fume. *IIW Doc. VIII-286–79*.
7. Kimura, I., Kobayashi, M., Godai, T. et al. (1979) Investigations on chromium in stainless steel welding fume. *Welding Res. Suppl.*, **8**, 195–204.
8. Astrom, H. (1993) Advanced development techniques for coated electrodes. *Welding Rev. Int.*, **12(2)**, 72, 74, 76.
9. Griffiths, T., Stevenson, A. (1989) Binder developments for stainless electrodes. *Welding Rev.*, **8(3)**, 192, 194, 196.
10. *Inobond*. Special silicates for welding consumables. Company brochure Van Baerle, Switzerland.
11. CristalTME. A new generation of stainless steel MMA electrodes. Company brochure AirLiquide/Oerlikon.
12. Marchenko, A.E. (1978) About rheological methods for evaluation of technological properties of electrode compounds. Information of CMEA. *Coordination Center on problems: Development of scientific basics and new technological processes of welding, surfacing and thermal cutting of materials and alloys for manufacturing of welded structures and development of efficient welding consumables and equipment*, Issue 1(**13**), 121–128.
13. Marchenko, A.E. (2010) On physical-chemical nature of strength of electrode coatings and technological means of its ensuring. In: *Proc. of 5<sup>th</sup> Int. Conf. on Welding Consumables, Technologies, Manufacturing, Quality and Competitiveness* (Artyomovsk–Kiev, Ukraine, 2010), 78–99.
14. Pokhodnya, I.K., Ofengenden, R.G., Gorpenyuk, V.N. et al. (1979) Information-measuring system for investigation of technological properties of welding consumables, equipment and processes. *Avtomatich. Svarka*, **10**, 67–68.
15. Sidlin, Z.A., Tarlinsky, V.D. (1984) *Current types of coated electrodes and their application for arc welding*. Moscow: Mashinostroenie.
16. Lipodaev, V.N., Bojko, Yu.N., Kakhovsky, Yu.N. et al. *Method of evaluation of slag crust detachability*. USSR author's cert. 407689. Publ. 28.08.1973.
17. Kalinyuk, V.V. (2011) Organizing of analysis process for titanium alloys on oxygen, nitrogen, hydrogen and carbon content. *Metrologiya ta Prylady*, **2**, 50.
18. *MU 1927–78*: Guidelines. Hygienic evaluation of welding consumables and methods of welding, surfacing and cutting of metals. Moscow: Minzdrav SSSR, 1980.
19. *MU 4945–88*: Guidelines on determination of harmful substances in welding fume (solid phase and gases). Minzdrav SSSR, 1990.
20. Slania, J., Slazak, B. (2006) Badania porownawcze elektrod otulonych wysokostopowych ERWS 19-9 L productowanych przy zastosowaniu nowego szkła wodnego modyfikowanego tlenkiem litu. *Biul. Instytutu Spawalnictwa*, **6**, 48–53.
21. Rudneva, A.V., Model, M.S. (1963) Phase transformations during reduction of titanium dioxide in slag systems. *Izvestiya AN SSSR. Metallurgiya i Gornoe Delo*, **1**, 59.
22. Marchenko, A.E., Skorina, N.V., Kiselev, M.O. (2010) Evolution of concept on nature and properties of liquid glass, being important in manufacture of welding electrodes. In: *Proc. of Int. Conf. on Welding Consumables: Technologies, Manufacturing, Quality, Competitiveness* (Agoj, 7–10 June 2010). Kiev: PWI, 2010, 100–106.
23. Perminov, A.A., Popel, S.I., Smirnov, N.S. (1961) Influence of replacement of nitrogen oxide by oxides of other metals on surface tension of silicate melts and their adhesion to hard steel. *Izvestiya Vuzov. Chyorn. Metallurgiya*, **12**, 5–8.

Received 04.07.2016

# COMPUTATION AND EXPERIMENTAL EVALUATION OF FORMATION OF PRIMARY STRUCTURE IN WELD METAL WITH REFRACTORY INOCULANTS

D.Yu. ERMOLENKO and V.V. GOLOVKO

E.O. Paton Electric Welding Institute, NASU

11 Kazimir Malevich Str., 03680, Kiev, Ukraine. E-mail: office@paton.kiev.ua

Possibility of regulation of structure and properties of weld metal of high-strength low-alloy steels was considered. It can be done with the help of introduction in a weld pool of the disperse refractory inoculants as surface-active elements. A procedure was described for performance of the experiments on introduction of the different refractory inoculants (TiC, TiN, SiC, TiO<sub>2</sub>, Al<sub>2</sub>O<sub>3</sub>, Zr<sub>2</sub>O, MgO) in the weld pool in high-strength low-alloy steel welding. The results of investigation of effect of the introduced inoculants on primary structure parameters and main mechanical properties of investigated weld metal are given. A model of interaction of refractory inoculants with solidification front was briefly discussed. Parameters of primary weld metal structure with the refractory inoculants, which were received by means of experimental investigations and computation experiment, were compared. The results of this comparison showed adequacy of a proposed model of interaction of refractory inoculant with solidification front. 9 Ref., 2 Tables, 7 Figures.

**Keywords:** arc welding, high-strength low-alloy steels, dendrite structure, primary structure, disperse refractory inoculants, solidification

Introduction in a weld pool of the refractory inoculants as surface-active particles is a perspective method for optimizing the structure and properties of weld metal of high-strength low-alloy (HSLA) steels due to regulation of structure parameters and, respectively, weld metal mechanical properties. It is known fact [1, 2] that grain size of primary structure effects nature of  $\gamma \rightarrow \alpha$  transformation processes. If nucleation of  $\alpha$ -phase in a disperse dendrite structure starts at the boundaries of austenite grains in the upper area of bainite transformation, then nucleation of ferrite inside primary grains at the interface with non-metallic inclusions at temperatures close to bainite transformation end [3, 4] are typical for coarser dendrites.

Previous works [5, 6] proposed a solidification model, which allows modelling quality changes of weld metal dendrite structure depending on surface properties of the introduced inoculants. This model was verified by experimental investigations on effect of the disperse refractory inoculants, playing a role of surface-active particles, on primary structure and mechanical properties of the weld metal of HSLA steels.

**Procedure.** The welds with different refractory inoculants were produced to study an effect of the refractory inoculants on a value of interphase energy in solidification process and formation of weld metal final structure in HSLA steels welding. Flux-cored wire of 1.6 mm diameter was used for (Ar + CO<sub>2</sub>) shielded gas welding. Assembly and welding of butt joints of 20 mm thick

St3sp(killed) steel sheets was carried out in accordance with the requirements of ISO 14171:2010 [7] using 240–250 A reverse polarity direct current at 31–32 V arc voltage. A welding rate was kept in 10–12 m/h limits. Inoculants were introduced in a wire core. 2 series of experiments were performed. TiC, TiN and SiC carbides and nitrides were introduced as refractory inoculants in the first series of the experiments, TiO<sub>2</sub>, Al<sub>2</sub>O<sub>3</sub>, ZrO<sub>2</sub> and MgO oxides were entered in the second series of the experiments. Base alloying system C–Mn–Cr–Ni–Mo–Si–Cu (without introduction of the refractory inoculants), realized in NN-0 (the first series of the experiments, heat input 20–23 J/cm) and NN-20 (the second series of the experiments, heat input 26–28 J/cm) variants, was directed on formation of the weld metal with bainite structure, which on its mechanical properties corresponds to low-alloy steels of K65 strength category (Table 1).

Selection of an inoculant type for investigations was based on their surface activity at interaction with iron-based melt. Inoculants' size was selected taking into account their further solution in the weld pool melt. Table 2 shows characteristics of the materials taken for experiments.

Weld metal primary structure was examined using optical metallography methods (optical microscope «Neophot-30») on polished samples, etched in boiling solution of sodium picrate C<sub>6</sub>H<sub>2</sub>(NO<sub>2</sub>)<sub>3</sub>ONa in water. Microstructure of the final pass of multipass weld metal (i.e. cast structure) was examined. The samples were cut out in normal to longitudinal weld axis direction in a way to observe dendrites on a microsec-

**Table 1.** Results of measurement of parameters of weld metal primary structure and mechanical properties

Inoculant type	Weld number	Average value of size of primary dendrites $\lambda_{1exp}$ , $\mu\text{m}$	Angle of inoculant wetting by iron melt $\theta$ , deg	Ultimate strength $\sigma_t$ , MPa	Impact toughness $KCV$ , J/cm <sup>2</sup>	
					+20 °C	-20 °C
–	NN-0	25.23	–	774	92	74
TiC	NN-6	26.89	125	715	112	85
TiN	NN-7	23.10	132	712	55	40
SiC	NN-9	30.20	82	726	85	65
–	NN-20	34.94	–	693	97	75
TiO <sub>2</sub>	NN-22	41.63	$\approx 0$	709	85	60
Al <sub>2</sub> O <sub>3</sub>	NN-23	31.60	40	728	82	50
MgO	NN-24	27.22	123	644	103	69
ZrO <sub>2</sub>	NN-25	29.41	102	622	120	73

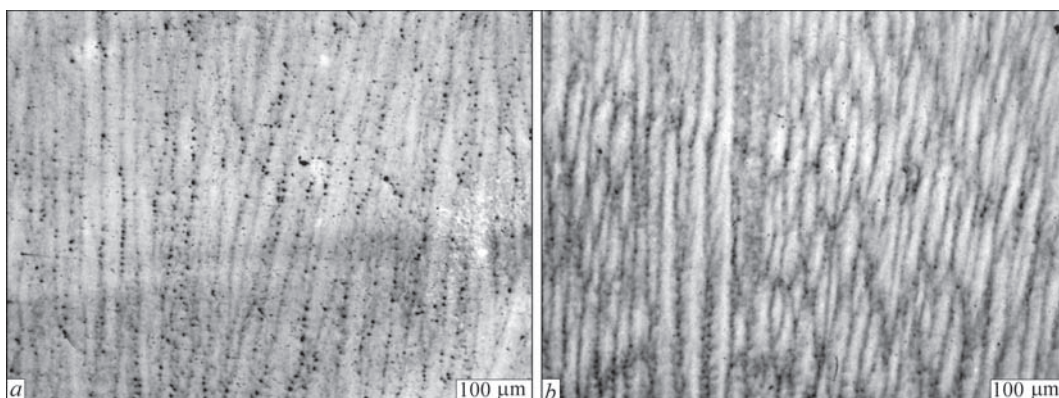
**Table 2.** Properties of refractory inoculants  $T_{mi}$  and their boundary angles of wetting by iron melt  $\theta$  [8]

Inoculant type	Melting temperature, $T_{mi}$ , °C	Surface tension of liquid phase $\sigma_l$ , mJ/m <sup>2</sup>	Boundary wetting angle $\theta$ , deg	Adhesion work $W_a$ , mJ/m <sup>2</sup>
TiC	3260	1780	125	760
TiN	2930	1780	132	590
SiC	2730	1780	82	2030
TiO <sub>2</sub>	1843	1780	$\approx 0$	3560
Al <sub>2</sub> O <sub>3</sub>	2044	1785	40	3155
ZrO <sub>2</sub>	2715	1785	102	1020
MgO	2852	1810	123	825

tion surface. These dendrites grew in a direction of the largest heat gradient in the weld pool (Figure 1). Mechanical properties of the weld metal were determined according to GOST 6996–66 [9].

Sizes of columnar dendrites ( $\lambda_1$  size in Figure 2) were determined by examination of primary structure on the images received by optical microscopy method. Sizes of secondary dendrites were not defined since they are very weakly expressed under given welding conditions. Figure 1 gives the images of typical dendrite structures of the investigated samples. The results of measurement of primary structure parameters and mechanical properties of the investigated samples are shown in Table 1.

Figures 3 and 4 show the diagrams of dependence of primary structure parameters on wetting angle of the refractory inoculants by iron melt for the first and second series of the experiments, respectively. Received results indicate the possibility of regulation of the primary structure parameters, in particular primary dendrites' size, by means of introduction of the refractory inoculants as surface-active elements in the weld pool. Decrease of a size of columnar dendrites at wetting angle rise is related with a drop of local solidification rate in refractory inoculant to weld pool melt contact zone. However, reduction of the local solidification rate in the contact zone of melt and inoculant also assumes qualitative change in morphology

**Figure 1.** Primary structure ( $\times 320$ ) of weld metal of examined samples: *a* — sample NN-23; *b* — sample NN-25

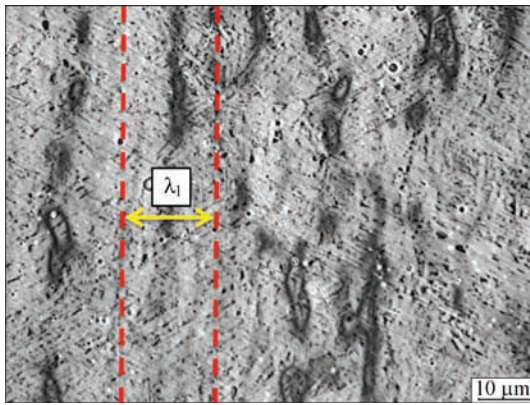


**Figure 2.** Primary structure ( $\times 1000$ ) of examined sample:  $\lambda_1$  — distance between primary dendrite axes

of the weld metal primary structure. This assumption is experimentally proved in analysis of the images of primary structure of weld metal with the inoculants having different melt wetting angles of the weld pool metal. This difference can be seen in Figure 1. Mainly straight columnar dendrites, passing through the whole visible region of the image (Figure 1, *a*), can be observed at weld metal inoculation with  $\text{Al}_2\text{O}_3$  aluminum oxide. Short columnar dendrites formed as a result of competing growth (Figure 1, *b*) are observed at weld metal inoculation with  $\text{ZrO}_2$  zirconium oxide.

**Computation experiments.** A model of interaction of refractory inoculants with solidification front relies on a data base, formed from a set of experimental results. This model describes interaction of the refractory inoculants with interface at solidification front, as a result of which change of interphase energy takes place. This leads to variation of the local rate of solidification front movement. The model assumes that the refractory inoculants are uniformly distributed in the weld pool volume with some coefficient  $\varphi$  ( $0 \leq \varphi \leq 1$ ). It is also assumed that the refractory inoculants are stable in process of solidification and have similar size, which is comparable with size of a cell

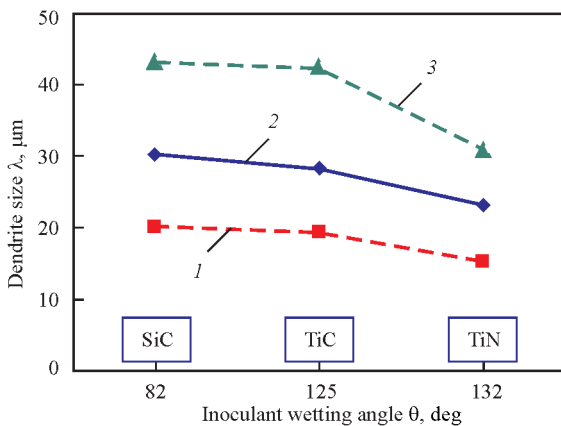


**Figure 3.** Dependence of parameters of primary structure on angle of wetting of refractory inoculants by iron melt of the first series of experiments: 1 — minimum values; 2 — averaged; 3 — maximum

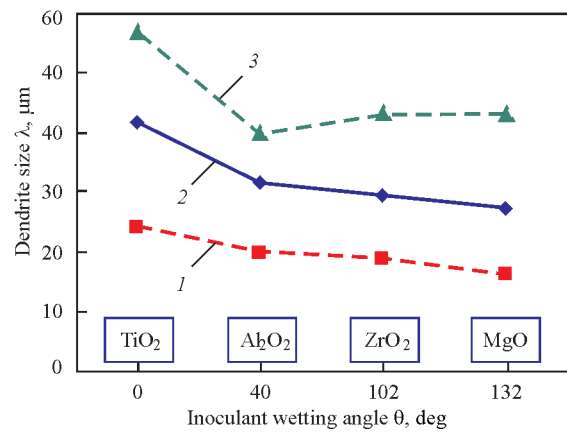


**Figure 4.** Dependence of parameters of primary structure on angle of wetting of refractory inoculants by iron melt of the second series of experiments: 1 — minimum values; 2 — averaged; 3 — maximum

of used computation mesh ( $\approx 0.4 \mu\text{m}$ ). A parameter of distribution of the refractory inoculants in the weld pool metal  $\varphi$  was taken equal 0.3 for all computations; such a choice is based on the results of work [5].

Figure 5 shows visual correspondence of dendrite structures of NN-0 and NN-20 samples, obtained in experimental and computation experiment ways. It should be noted that the structures reflecting mor-

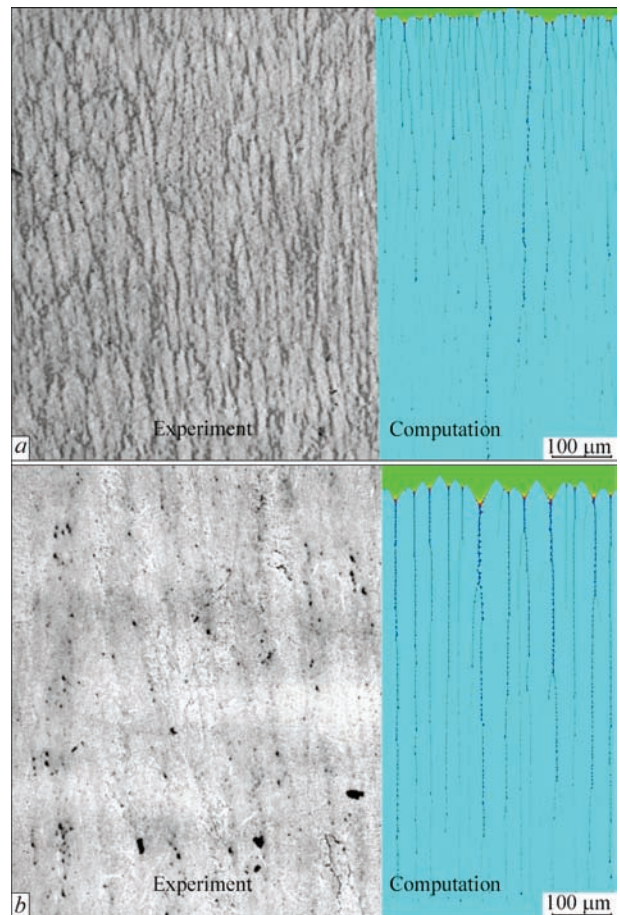


**Figure 5.** Visual correspondence of primary structure of samples NN-0 (*a*) and NN-20 (*b*) to primary structure, received by means of computation experiment

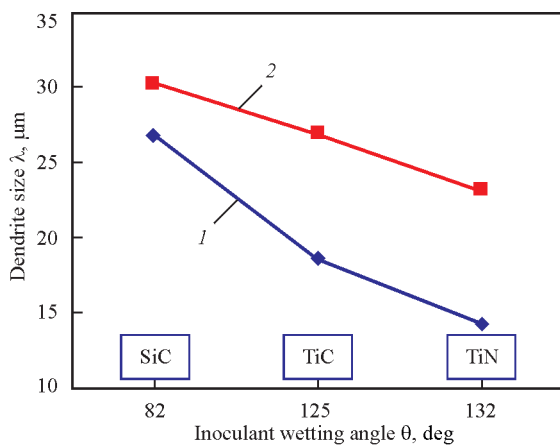


**Figure 6.** Correlation of experimental and computation results of measurement of parameters of primary structure in weld metal of first series experiment samples: 1 —  $\lambda_{1comp}$ ; 2 —  $\lambda_{1exp}$

phology of dendrite structure of the real samples were received as a result of computation.

Measurements of a distance between the axes of primary dendrites  $\lambda_{1comp}$  of the samples with addition of different refractory inoculants (TiC, TiN, SiC, TiO<sub>2</sub>, Al<sub>2</sub>O<sub>3</sub>, ZrO<sub>2</sub>, MgO), received by computation experiment, were carried out similar to a procedure of processing of primary structure images, obtained by optical metallography (Figure 2).

Figures 6 and 7 show a comparison of sizes of primary structure dendrites, received in computation  $\lambda_{1comp}$  and experimental ways  $\lambda_{1exp}$  for the samples of the first and second series, respectively. Analysis of the present dependencies allowed concluding that a tendency to distance reduction between the axes of primary dendrites at rise of the wetting angle of refractory inoculants by weld pool melt is preserved according to obtained experimental data, described above. Thus, it should be assumed that the proposed mathematical model and software developed on its basis allow receiving valid predictions of the parameters of primary structure of HSLA steel weld metal.

An average error of data, received by means of computation experiment, makes around 25 %. Such a difference in received results should be related with a parameter of refractory inoculants distribution in weld pool metal  $\varphi$ , which was taken equal 0.3. This, apparently, does not have complete correspondence to the conditions of carried experimental investigations. Insignificant growth of the error at increase of the angle of inoculant wetting by weld pool melt is related with a change of nature of their distribution in the weld metal due to qualitative change of morphology of dendrite structure at introduction of the inoculants with high wetting angles. These remarks should be taken into account for further development of the model.

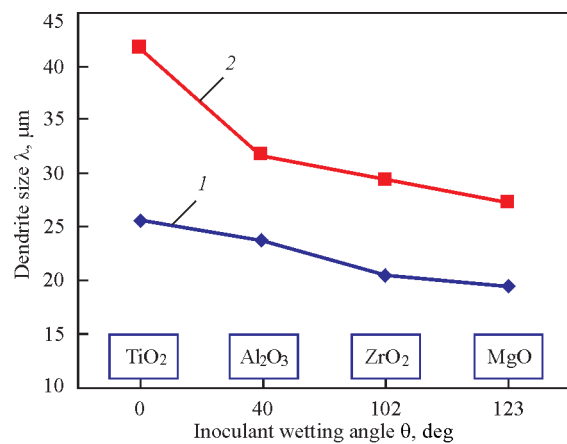


**Figure 7.** Correlation of experimental and computation results of measurement of parameters of primary structure in weld metal of second series experiment samples: 1 —  $\lambda_{1comp}$ ; 2 —  $\lambda_{1exp}$

## Conclusions

Proposed model of effect of the refractory inoculants as surface-active parts on the weld pool metal solidification process is suitable for prediction of size parameters and morphology of primary structure of HSLA steel weld metal. Software developed based on given model allows selecting the refractory inoculants and their amount for optimizing the parameters of weld metal primary structure, and, as a consequence, its mechanical properties in accordance with set requirements.

- Golovko, V.V., Stepanyuk, S.N., Ermolenko, D.Yu. (2015) Effect of titanium-containing inoculants on structure and properties of weld metal of high-strength low-alloy steels. *The Paton Welding J.*, **2**, 14–18.
- Golovko, V.V., Stepanyuk, S.N., Ermolenko, D.Yu. (2014) *Technology of welding of high-strength low-alloy steels with introduction of titanium-containing inoculants*. In: Collect. Monography: Nanosized systems and nanomaterials: Investigations in Ukraine. Ed. by A.G. Naumovets. Kiev: Akadempriodika.
- Vanovsek, W., Bernhard, C., Fiedler, M. et al. (2013) Influence of aluminum content on the characterization of microstructure and inclusions in high-strength steel welds. *Welding in the World*, **57**(Issue 1), 73–83.
- (2011) Effects of soluble Ti and Zr content and austenite grain size on microstructure of simulated heat affected zone in Fe–C–Mn–Si alloy. *ISIJ Int.*, **51**(9), 1542–1533.
- Ermolenko, D.Yu., Ignatenko, A.V., Golovko, V.V. (2016) Direct numerical modelling of formation of weld metal dendrite structure with disperse refractory inoculants, **12**, 13–20.
- Galenko, P.K., Krivilev, M.D. (2000) Isothermal growth of crystals in overcooled binary alloys. *Matematicheskoe Modelirovanie*, **12**(11), 17–37.
- ISO 26304:2011: Welding consumables. Solid wire electrodes, tubular cored electrodes and electrode-flux combinations for submerged arc welding of high strength steels. Classification.
- Panasyuk, A.D., Fomenko, V.S., Glebova, G.G. (1986) *Resistance of non-metallic materials in melts*. Kiev: Naukova Dumka.
- GOST 6996–66: Welded joints. Methods of determination of mechanical properties.

Received 19.10.2016

# INTENSIFICATION OF ARC AND ELECTROSLAG PROCESSES OF WELDING BY MEANS OF EXOTHERMAL MIXTURE INTRODUCTION

A.F. VLASOV, N.A. MAKARENKO and D.A. VOLKOV

Donbass State Machine-Building Academy  
72 Shkadinov Str., 84313, Kramatorsk, Ukraine. E-mail:sp@dgma/donetsk.ua

It is proved that introduction of up to 53.4 % of exothermal mixture in electrode coating results in increase of the following coefficients, i.e. core melting, deposition, rate of electrode melting and melting of electrode coating. Increase of thickness of electrode coating, containing 44.4 % of exothermal mixture, from 0.5 to 2.6 mm results in rise of amount of exothermal mixture and deposition coefficient, decrease of value of core melting coefficient, increase of mass rate of coating melting. It is proved that an efficient method for increase of electroslag processes efficiency is application of exothermal flux, namely scale, ferroalloys, aluminum powder and standard flux (ANF-6 etc.) in the amounts sufficient for exothermal reaction passing. This provides for emission of additional heat in a start period of exothermal processes and promotes for accelerated formation of slag pool of necessary volume on «solid» start on monofilar as well as bifilar schemes of process instead of «liquid» start. The electroslag processes using exothermal alloyed flux on «solid» start allow (in comparison with existing methods of slag pool formation) rising metal yield by 2–10 %; 1.2–1.4 kW·h economy of melting of 1 kg of standard flux; 25 % reduction of time of ESR process start period. It is determined that introduction of aluminum as a deoxidizing agent in the exothermal fluxes rises content of aluminum oxide ( $Al_2O_3$ ) in a weld pool, its resistance, and increases efficiency of electroslag process. 21 Ref., 5 Figures.

**Keywords:** *electrode, exothermal mixture, exothermal flux, slag pool, process efficiency*

Currently coated electrode manual arc welding is still one of the widely applied technological processes. Volume of works performed using manual arc welding in industrially-developed countries makes 20–25 % from total volume and in post-soviet countries it reaches 60–70 % [1–4]. Particularly high index is observed in building industry. It can exceed 80–85 % [2, 3]. This requires paying serious attention to improvement of manual arc welding. First of all, it concerns development of high-efficiency welding electrodes, one of the main factors determining process efficiency of welding [5–8].

One of the important problems of welding consumable developers is searching the new types of raw materials for their manufacture and determination of the ways for intensification of welding and metallurgical processes. One of the directions for solving this problem is application of effect of exothermal reactions through introduction of the exothermal metal-flux mixtures in welding consumable composition. They pass electric current in solid state and represent themselves mechanical mixture of scale, aluminum powder, alloying elements (in form of ferroalloys or powders) and working flux (for example, ANF-6 or other).

This problem can be solved using the effect of exothermal reactions in the electrode coating before its core melting by means of introduction in the coating

composition the materials used in form of oxidizers (scale, hematite, manganese ore etc.) and deoxidizers (ferrotitanium, ferrosilicium, aluminum powder etc.). It should be noted that data on influence of heat effect of the exothermal reactions on welding-technological properties of the electrodes are limited in the special literature [9–11].

Iron oxides introduced in the electrode coating in form of scale allow using an effect of increase of bulk weight of iron powder and its positive effect on workability of electrode production. Besides, melting of the electrode coating with exothermal mixture provokes exothermal reaction and formation of reduced iron coming into weld. This rises efficiency of welding process and due to emitted heat promotes acceleration of coating melting and electrode in whole.

It is known fact [12–14] that the exothermal reaction results in emission of additional heat power. It is determined [13] that amount of heat consumed by exothermal reaction for heating and melting of the electrode core reaches 10 kJ/s value. This is enough for uniform melting of core and shell. Melting efficiency of flux-cored strips rises by 40–60 % and that of deposition by 30 %. Besides, power saving is obtained (1500 kW·h per 1 t of the deposited metal).

The aim of this paper is intensification of manual arc welding and electroslag processes by means of development of welding consumables using exothermal mixtures in their production.

Electrodes currently applied in industry for welding and surfacing are characterized by low efficiency (deposition coefficient does not exceed 8.5–9.5 g/A·h), therefore increase of efficiency of manual arc welding (surfacing) and searching the new types of raw materials for their manufacture is one of the main problems for surfacing consumable developers.

Introduction of iron powder in composition of the electrode coating is one of the main ways increasing efficiency of manual arc welding (surfacing). Content of iron powder in the electrodes in 15–25 % range improves their welding-technological properties without significant change of the deposition coefficient. The largest efficiency is reached at content of iron powder in the electrode coating in the amount of 60–70 % at coating mass coefficient in 100–200 % range (such electrodes are called «high-efficient»). However, specific weight of the «high-efficient» electrodes used in our country (due to necessity of application in this case of power sources with increased open — circuit voltage, scarcity of iron powder, complexity in providing their quality production in continuous production lines «electrode press–conveyor calcining furnace») is very low. Further growth of efficiency of electrode advanced grades is also limited by scarcity (on the world market as well as in our country) of series of raw materials such as iron powder, rutile concentrate etc.

The aim stated in present work was solved applying exothermal metal-flux mixtures, representing themselves mechanical mixture of scale, aluminum powder, alloying elements in form of ferroalloys (ferromanganese, ferrotitanium, ferrosilicium) in manual arc welding and exothermal fluxes (exothermal mixture + standard flux) in electroslag processes.

Welding processes can be intensified by introduction of exothermal mixtures in the welding consumable composition. Carried investigations [15] determined that variation of a content of exothermal mixture in the electrode coating from 35 to 64 % provides for 1280 °C growth of temperature, which is sufficient for complete melting of ferroalloy.

Rate and efficiency of electrode melting, evaluated mainly by change of length or mass of the molten electrode core per unit of time, is an important characteristic of welding process and depends on number of factors, main of which are welding current, coating composition, current type and polarity.

Introduction in the electrode core of exothermal mixture provokes emission of additional amount of heat due to chemical reaction taking place between iron oxides and elemental-deoxidizers. The largest amount of heat is emitted at interaction of aluminum with ferrous oxide, and the lowest at manganese with ferrous oxide interaction ( $q^{Al} = 3268$ ,  $q^{Ti} = 2171.1$ ,  $q^{Si} = 2224.7$ ,  $q^{Mn} = 950.8$  J/g).

Electrodes containing in the coating marble, fluor-spar, rutile concentrate, ferromanganese, ferrotitanium, iron scale and aluminum powder and having 5.0 mm core diameter and different content of exothermal mixture at constant value of coefficient of coating mass ( $K_c = 0.6$ ) were manufactured for determination of effect of amount of exothermal mixture on indices of electrode melting. Melting of the electrodes was carried out at similar values of welding current (290 A) and its density (24.8 A/mm<sup>2</sup>) at 60 V open-circuit voltage of power source. The electrodes of 5.0 mm core diameter and coating thickness of 0.5–2.6 mm that corresponded to variation of coefficient of coating mass from 0.17 to 1.14 were manufactured for determination of effect of thickness of the electrode coating with exothermal mixture on process characteristics of their melting. Amount of exothermal mixture in the studied electrodes made 44.4 % of coating mass.

Values of experimental data are given in Figure 1. It is proved that introduction of exothermal mixture in the electrode coatings (Figure 1, *a*) results in increase of the following coefficients, namely melting of core ( $\alpha_{m.cr} = 8.7$ –11.4 g/A·h), deposition (8.0–12.5 g/A·h), electrode melting (9–19 g/A·h), and electrode melting rate (17–23 m/h) [16, 17].

Experiments showed that increase of electrode coating thickness (Figure 1, *b*) results in rise of amount of exothermal mixture, reduced iron and deposition coefficient ( $\alpha_d = 10.4$ –13.4 g/A·h), decrease of coefficient of melted core ( $\alpha_{m.cr} = 12.8$ –10.5 g/A·h) and rate of electrode melting (21.5–18.3 m/h). Reduction of  $\alpha_{m.cr}$  with rise of the coating thickness indicates that heat being formed during exothermal reaction is mainly spent for coating melting, increasing its mass rate of melting (0.18–1.03 g/s).

Determination of effect of amount of exothermal mixture and electrode coating thickness with exothermal mixture on heating of the part and electrode melting (Figure 2) was carried out using calorimetry method.

Influence of exothermal process heat effect, appearing in melting of the electrodes with exothermal mixture in the coating, was experimentally determined by melting the electrodes using reverse polarity direct current at welding current values 290 A and open-circuit voltage of power supply 60 V and statistically analyzed on «Statistica» program.

It is determined that introduction in the electrode coating of exothermal mixture up to 53.4 % (Figure 2, *a*) varies  $\eta_p$  from 0.715 to 0.815 and  $\eta_e$  from 0.28 to 0.415; at that variation is directly-proportional. Increase of amount of deposited metal ( $q_{d.m}^a = 10.5$ –21.0 g), core being melted ( $q_{m.cr}^a = 14.0$ –19.0 g) and coating ( $q_{m.c}^a = 8.5$ –11.4 g) as well as heat power of arc ( $\Delta Q_{ia}/Q_{la} = 0$ –12 %) at almost similar amount of

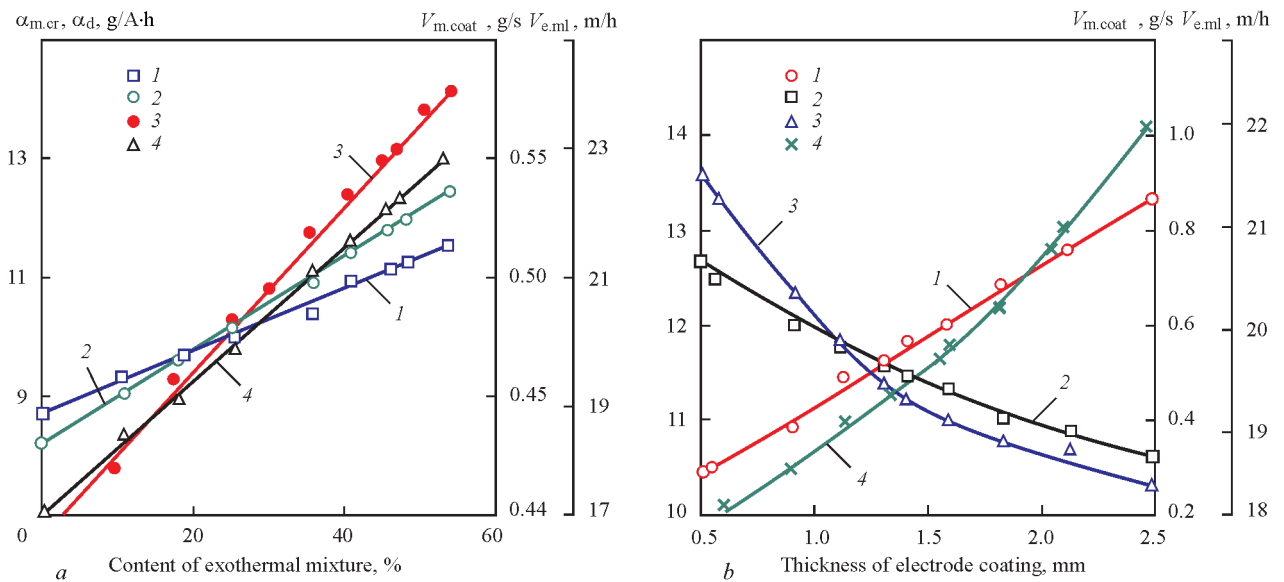


**Figure 1.** Variation of indices of electrode melting depending on amount of exothermal mixture (a) and coating thickness (b) in the coating

slag on plate ( $q_{sl}^a$ ) show that additional heating of the plate takes place mainly due to increase of amount of electrode metal per the same time interval and due to increase of arc heat power.

The investigations showed that change of the electrode coating thickness from 0.5 to 2.6·10<sup>-3</sup> m (Figure 2, b) rises content of exothermal mixture and increase amount of heat and reduced iron during exothermal reaction. Amount of deposited metal and slag on the base metal raised in calorimetry from 17.5 to 21.0 g and from 2.0 to 13.0 g, respectively, that resulted in change of  $\eta_p$  from 0.74 to 0.84; proportional increase of  $\eta_e$  from 0.31 to 0.47, regardless decrease of their melting rate, takes place due to rise of arc heat power and specific heat consumption ( $K_e + K_e^{chem}$ ) for electrode melting.

Despite of reduction of amount of melted core, rise of electrode coating thickness promotes increase of amount of deposited metal that is possible only under condition of intensive reduction of iron from its oxide. Decrease of  $\alpha_{m.cr}$  with increase of the coating thickness shows that heat, formed at exothermal reaction, is mainly spent for coating melting that rises its mass rate of melting (0.18–1.03 g/s). Besides, core gives part of heat to the coating that provokes for reduction of core heating and its melting rate. Due to the fact that percent content of exothermal mixture in all investigated compositions of the electrodes was the same, and only its mass amount was varied, we observed just increase of reduced iron from its oxides and rise of efficiency of electrode coating melting.

Due to the fact that increase of exothermal mixture content in the studied electrodes, i.e. metallic compo-

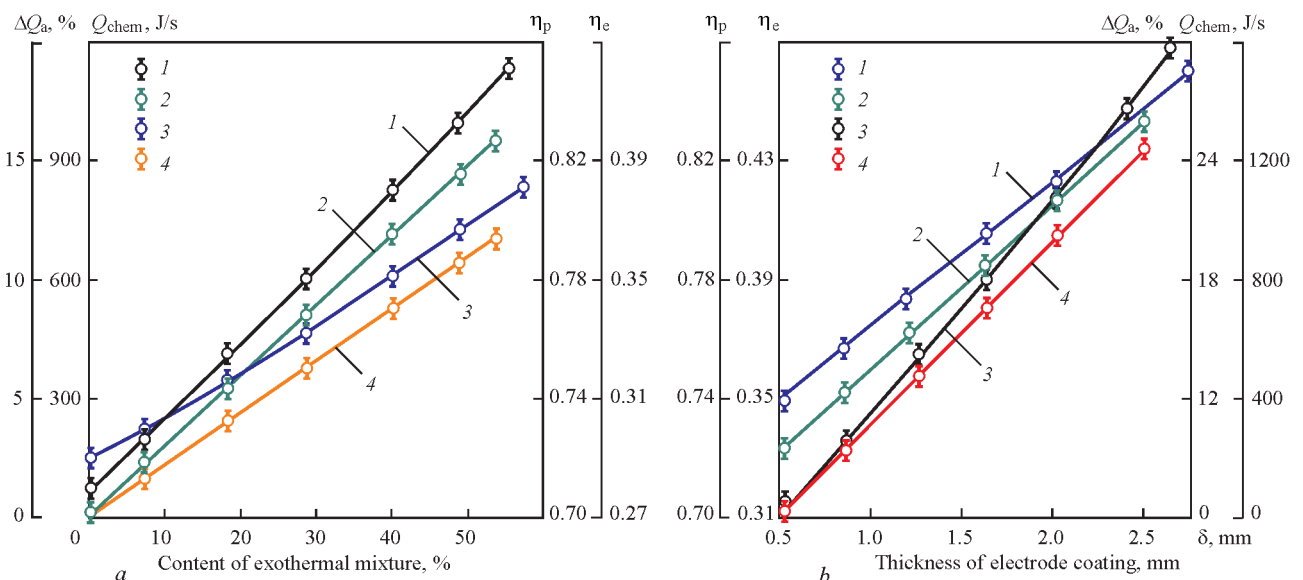


**Figure 2.** Effect of amount of exothermal mixture in the electrode coating (a) and coating thickness (b) on melting heat characteristics

ment of the coating, takes place because of respective decrease of content of gas-slag forming part of the coating, then heat expenses for coating melting are reduced, since total heat of iron is lower than that of slag, and portion of heat, spent for core melting as well as droplets heating rises.

It follows from mentioned above that the electrodes with exothermal mixture in the coating are more reasonable for application in surfacing. Deposition coefficient of the electrodes containing 44.4 % of exothermal mixture in the coating makes 11.8–12.5 g/A·h, melting rate 21.5–25 m/h, optimum welding current makes 280–300 A due to increased melting rate and absence of overheating in process of surfacing for electrodes of 5.0 mm diameter.

The statistical models were developed, which allowed determining an optimum content of exothermal mixture and electrode coating thickness. Modelling of the melting process was carried out with the help of software system Statistica 6. The experiments, in which these factors vary at two levels, i.e. experiments of  $2^k$  type, acquired the biggest distribution.

The factors are amount of exothermal mixture  $Q$  and coefficient of electrode coating mass  $K_c$ . Response is the coefficients of electrode melting  $\alpha_{e,m}$ , rate of electrode melting  $V_{e,m}$  and melting of electrode coating  $V_{coat}$  (Figure 3).

Regression equations look like:

$$\begin{aligned} \alpha_m &= 10.55238 + 2.29644K_c - 3.24688K_c^2 + \\ &+ 0.18470Q - 0.00240Q^2 + 0.05875K_cQ, \text{ g/A}\cdot\text{h}; \\ V_{e,m} &= (4.68931 - 0.0004K_c + 0.001974Q + \\ &+ 0.000553Q^2 + 0.000057K_cQ)10^{-2}, \text{ m/s}; \\ V_{coat} &= (0.475801 + 0.003526K_c - 0.003735K_c^2 + \\ &+ 0.01418Q - 0.005248Q^2 + 0.000411K_cQ), \text{ g/s}. \end{aligned} \quad (1)$$

The factors are amount of exothermal mixture  $Q$  and electrode coating thickness  $\delta_c$ ,  $Q_{chem}/Q_e$ . Response is efficiency of part and electrode heating  $\eta_p$ ,  $\eta_e$  and relationship of heats  $Q_{chem}/Q_e$  (Figure 4).

Regression equations look like:

$$\begin{aligned} \eta_e &= 0.37767 + 0.005941\delta_c + 0.008338\delta_c^2 + \\ &+ 0.002299Q + 0.00115Q^2 - 0.04041\delta_cQ; \\ \eta_p &= 0.76075 + 0.94813\delta_c + 0.93457\delta_c^2 + \\ &+ 0.00648Q + 0.00007Q^2 - 0.06425\delta_cQ; \\ Q_{chem}/Q_e &= 9.71120 + 0.4979\delta_c + 0.2795\delta_c^2 - \\ &- 0.01102Q + 0.001453Q^2 - 0.01778\delta_cQ. \end{aligned} \quad (2)$$

Electroslag processes are realized with «solid» or «liquid» start [16]. In «solid» start melting of a working flux and formation of the weld pool of necessary volume is carried out in arc mode. The method is characterized with instability (often short-circuitings), non-uniform and continuous flux melting (low efficiency). The electroslag technology for large-sized billets production is performed in bifilar or three-phase type furnaces using only «liquid» start by means of siphon casting of slag melted out of the furnace in lower part of a pocket in electroslag welding (ESW), mold

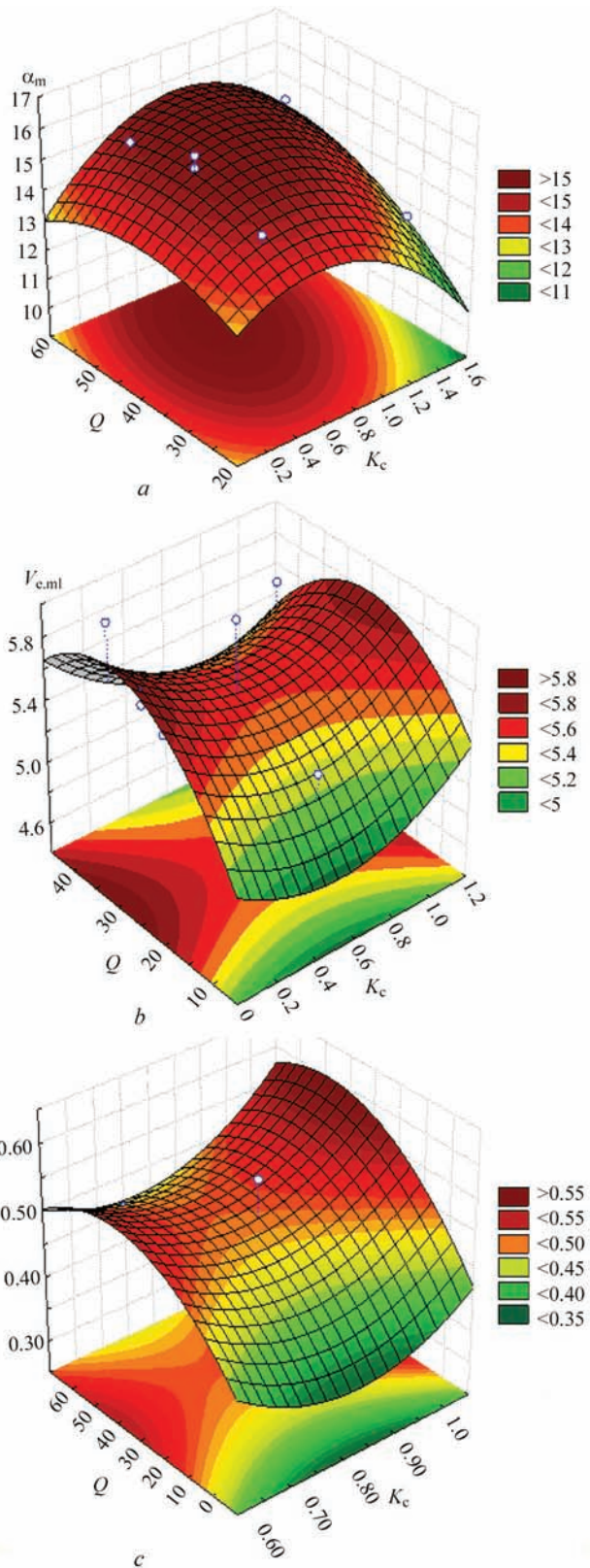


**Figure 3.** Dependence of melting coefficient  $\alpha_m$  (a), rate of electrode melting  $V_{e,m}$  (b) and electrode coating  $V_{coat}$  (c) on amount of exothermal mixture  $Q$  and coefficient of electrode coating mass  $K_c$  in electroslag remelting (ESR) or casting into crucible in electroslag die casting (EDC). However, laboriousness of ingot casting taking into account time of flux melting in flux-melting furnaces is significantly higher in comparison with «solid» start.

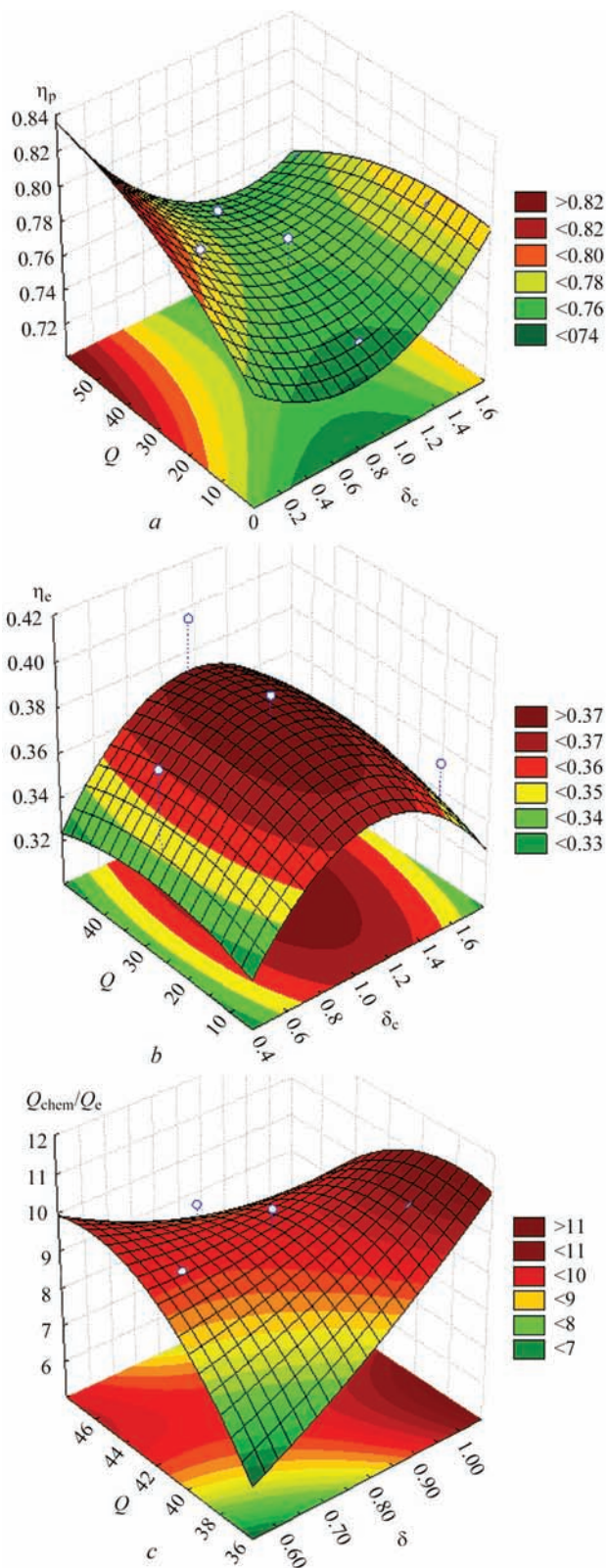


**Figure 4.** Dependence of heating efficiency of part  $\eta_p$  (a), electrode  $\eta_e$  (b) and relationship of heats  $Q_{chem}/Q_c$  (c) on amount of exothermal mixture  $Q$  and electrode coating thickness  $\delta_c$

An essence of the developed start method lies in the following (Figure 5).

Presence of exothermal mixture in the first (6) and second (5) layers provides for acceleration of working flux melting due to reduction of electric conductivity

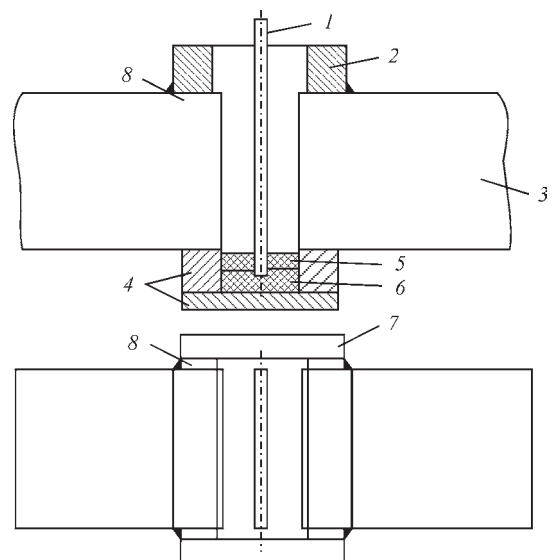


**Figure 5.** ESW scheme: 1 — plate electrode; 2 — run-off tabs; 3 — welded joint; 4 — metallic pocket; 5 — working flux; 6 — exothermal mixture; 7 — forming backgigs; 8 — side plates

ty of the slag and heat emitted at interaction of iron oxides with aluminum. In the first layer (6) exothermal reactions develop temperatures promoting quick melting of the working flux and heating of consumable electrode. Reduction of slag electric conductivity is reached through introduction in the molten flux of aluminum oxide, which is formed due to aluminum to iron oxides interaction. Constant electric mode promotes rise of slag pool temperature, increase melting efficiency and reduction of specific consumption of electric energy. Due to optimum relationship of the components in the first layer (6) it is electroconductive in a solid state and allows complete reaction of aluminum with its oxide formation. Presence of the exothermal mixture in the second layer (5) accelerates its melting without splashes and swirling.

Iron is reduced (~70 % of scale mass) in exothermal mixture melting. It precipitates to a bottom plate or dummy ingot and then removed to a crop; refined metal of consumable electrode is deposited over a layer formed from reduced iron and starts formation of sound weld or casting. As the result loss of consumable electrode is decreased to minimum and metal quality in bottom part of the ingot is improved due to that fact that electrode melting takes place in a liquid slag (similar to process with syphon slag casting).

The indices of comparative tests of the optimum variant for developed method of «solid» start and currently applied «solid» and «liquid» ESR starts are given in work [18]. The developed method of ESR start under similar conditions provides for (in comparison with existing «solid» start) 2 times increase of efficiency of flux melting and provide metal yield up to 10 % , reduce by 16 the time of start period for slag pool formation of necessary volume in compari-

son with existing «liquid» start, and rise by 2 % metal yield. Besides, melting of the exothermal flux forms a slag constituent, namely aluminum oxide ( $\text{Al}_2\text{O}_3$ ), mass of which can make to 20–30 % of necessary mass of molten working flux and 1.2–1.4 kW·h saving for melting of 1 kg of standard flux.

Heat effect of the exothermal reaction from interaction of element-deoxidizers with ferrous oxide is determined using the following formula [19]:

$$Q_{\text{chem}} = \sum_{i=1}^{i=k} \frac{G_{\text{m.cr}}}{t} K_c (Q_{\text{ie.m}}) q_{\text{ie.m}}, \text{ J/s}, \quad (3)$$

where  $G_{\text{m.cr}}$  is the mass of melted electrode core, g;  $Q_{\text{ie.m}} - Q_{\text{ie.m}}^{\text{Al}}, Q_{\text{ie.m}}^{\text{Ti}}, Q_{\text{ie.m}}^{\text{Si}}, Q_{\text{ie.m}}^{\text{Mn}}$  is the portion of exothermal mixture in the electrode coating at interaction of  $i^{\text{th}}$  element-deoxidizer with ferrous oxide, %;  $K_c$  is the coefficient of coating mass;  $q_{\text{ie.m}}$  are the heat effects (J/g) of exothermal mixture for a reaction of titanium, silicon and manganese with ferrous iron.

Compositions of the exothermal fluxes were developed. They are applied to electrosag processes and provide in their melting conformity of physical-chemical properties of electrosag metal to base metal, electric conductivity in solid state and possibility to carry the processes using mono-, bifilar or three-phase schemes applicable to 9KhF, 9Kh2MF and 60Kh2SMF steels [17, 18].

## Conclusions

1. It is proved that an effective method to increase the efficiency of manual arc welding (surfacing) and electrosag processes is application of the exothermal metal-flux mixtures representing themselves mechanical mixture of scale, aluminum powder, alloying elements in form of ferroalloys (ferromanganese, ferrotitanium, ferrosilicium) in manual arc welding (surfacing) and exothermal fluxes («exothermal mixture + standard flux») in electrosag processes in amount sufficient for exothermal reaction.

2. It is determined in experimental way that introduction of exothermal mixture in the electrode coating rises electrode melting rate thanks to heat being emitted in the exothermal reaction (0–11.5 %); provides for reduction of costs for melting of gas-slag-forming part of the coating and improvement of arc process characteristics.

3. It is proved that up to 53.4 % content of exothermal mixture in the electrode coating results in change of efficiency of part heating  $\eta_p$  from 0.715 to 0.815 and that of electrode  $\eta_e$  from 0.28 to 0.415; at that the change has a direct-proportional nature. Rise of thickness of electrode coating increases content of

exothermal mixture; increase amount of heat and reduced iron in the exothermal reaction that results in variation of  $\eta_p$  from 0.74 to 0.84 and  $\eta_e$  from 0.31 to 0.47 due to increase of arc heat power and specific heat consumptions ( $K_e + K_e^{\text{chem}}$ ) for electrode melting.

4. The statistical models were developed. They allow determining optimum content of the exothermal mixture and electrode coating thickness providing minimum losses of electrode metal.

1. Mazur, A.A., Pustovojt, S.V., Petruk, V.S. et al. (2014) Ukrainian market of welding consumables. *The Paton Welding J.*, **6/7**, 46–52.
2. Doria, J.G. (2001) Welding consumables: Market trends. Istanbul: European Welding Association.
3. Nassau, L. van (2001) *Expert report stick electrodes 2000*: Stick electrodes. Istanbul: European Welding Association.
4. (1998) *Materials and applications*: Welding handbook. Miami, USA, Vol. 4, Pt 2.
5. Shlepakov, V.N. (2011) Current consumables and methods of fusion arc welding (Review). *The Paton Welding J.*, **10**, 26–29.
6. (2011) *Welding consumables*. In: Coll. of papers in The Paton Welding J. for 2006–2010. Comp. by V.N. Lipodaev. Kiev: PWI.
7. (2012) *Metallurgy of arc welding and welding consumables*: Collect. of NASU, PWI. Comp. by I.K. Pokhodnya, A.S. Kotelchuk. Kiev: Akadempriodika.
8. Pokhodnya, I.K. (2003) Welding consumables: State-of-the-art and tendencies of development. *The Paton Welding J.*, **3**, 2–13.
9. Ioffe, I.S., Kuznetsov, O.M., Pitsersky, V.M. (1980) Effect of titanium thermite mixture in electrode coating on increase of welding efficiency. *Svarochn. Proizvodstvo*, **3**, 26–28.
10. Karpenko, V.M., Vlasov, A.F., Bilyk, G.B. (1980) Indices of melting of welding electrodes with exothermal mixture in coating. *Svarochn. Proizvodstvo*, **9**, 23–25.
11. Vlasov, A.F., Makarenko, N.A., Kushchy, A.M. (2014) Heating and melting of electrodes with exothermic mixture in coating. *The Paton Welding J.*, **6/7**, 147–150.
12. Chigarev, V.V., Zarechensky, D.A. (2006) Examination of indices of exothermal mixtures burning. *Visnyk Pryazov. DTU*, 1–4.
13. Chigarev, V.V., Zarechensky, D.A., Belik, A.G. (2007) Peculiarities of melting of flux-cored strips with esothermic mixtures contained in their filler. *The Paton Welding J.*, **2**, 46–48.
14. Zarechensky, A.V., Leshchinsky, L.K., Chigarev, V.V. (1985) Peculiarities of melting of flux-cored strips with exothermal mixtures. *Svarochn. Proizvodstvo*, **8**, 39–41.
15. Vlasov, A.F., Karpenko, V.M., Leshchenko, A.I. (2006) Experimental determination of exothermic process in heating and melting of electrodes. *Visnyk Donbas. Derzh. Mashyn. Akademii*, **4(2)**, 65–68.
16. Latash, Yu.V., Medovar, B.I. (1970) *Electrosag remelting*. Kiev: Metallurgiya.
17. Makarenko, N.A., Vlasov, A.F., Volkov, D.A. et al. (2015) Study and development of composition of exothermic fluxes for electrosag processes. *Sovremennaya Elektrometallurgiya*, **2**, 10–16.
18. Vlasov, A.F., Makarenko, N.A., Kushchy, A.M. (2016) Application of exothermal mixtures in manual arc welding and electrosag processes. *Svarochn. Proizvodstvo*, **8**, 7–14.
19. Vlasov, A.F., Kushchy, A.M. (2011) Technological characteristics of electrodes with exothermal mixture in coating for surfacing of tool steels. *Ibid.*, **4**, 10–15.

Received 26.10.2016

## EXPERIMENTAL STUDIES OF ELECTRODE COATING THICKNESS VARIATION AT PRESSING\*

A.E. MARCHENKO

E.O. Paton Electric Welding Institute, NASU  
11 Kazimir Malevich Str., 03680, Kiev, Ukraine. E-mail: office@paton.kiev.ua

Oscillographic and mathematical statistics methods were applied to study the regularities of formation of coating thickness variation in experimental electrodes UONI 13/55 with 4 mm rod diameter at their manufacture in angle hydraulic press under the conditions maximum close to production ones. It is found that coating thickness variation is a continuous, multistage, nonmonotonic (wavelike) and harmonic process, in which disturbances, arising at the starting stage, can be felt in subsequent stages of electrode pressing. Coating thickness variation is caused, primarily, by violation of elasticity and viscosity balance, on which the consistency of electrode coating masses depends. At the same time the probability of appearance of coating thickness variations is essentially influenced by the features of forming path of electrode coating press. 15 Ref., 7 Figures.

**Keywords:** arc welding, coated electrodes, pressing, coating thickness variation, oscillography, mathematical statistics

Viscoelasticity of electrode coating masses should be considered as the main cause for coating thickness variation. In terms of weld quality this is the most dangerous defect, arising, primarily, from quick discharge of elastic stresses, accumulated by coating mass during its application on the rods [1–5]. A lot of the suggested causes for coating thickness variation, the most often discussed in publications earlier, for instance [1, 6, 7], are not always the main ones. Nonetheless, many of them can, to a certain extent, facilitate appearance of coating thickness variation, caused by the above-mentioned elastic turbulence of coating masses.

Another important cause to be considered is the natural tendency of coating mass to find a coating shell cross-sectional configuration during interaction with the elastic rod in the press chamber, which would minimize energy consumption for flowing. It, apparently, proceeds by hydrodynamic, i.e. more complex mechanism, than does the traditional (as, for instance, in [1]), schematic of elastic deformation of the rod overhanging part under the impact of the coating mass, pumped into the press chamber. Otherwise, it would be difficult to explain why coating thickness variation arises in manufacture of electrodes in continuous-flow presses.

In the most unfavourable cases accumulation and discharge of elastic stresses proceed continuously, run

very quickly and unpredictably. Coating thickness changes just as quickly. Application of its examination methods of equivalent speed should help understand this stochastic process. Such methods include oscillography, combined with mathematical statistics treatment of the recorded results.

Oscillographic studies of thickness variation were started at PWI long ago [8]. However, many of the obtained results could be analyzed and explained in terms of excess of elasticity over viscosity only now, when viscoelastic nature of coating masses can be regarded as quite well established by rheological studies [2–5].

**Object and methods of investigation.** Investigations were performed at manufacture of experimental electrodes UONI 13/55 with participation of personnel of PWI Experimental Production in commercial equipment with which it is fitted.

Material composition of electrode coating charge (wt.%) was as follows: marble — 51.5; fluorite concentrate — 19; quartz sand — 6; medium-carbon ferromanganese — 6.5; ferrosilicium FC-45 — 7; ferrotitanium — 7; mica-muscovite — 3; and purified Na-CMC — 1 (above 100).

In preparation of equipment, and optimizing the electrode manufacturing process, procedure of thickness variation oscillography, oscillogram digitizing and statistical treatment of results, the following fractional composition of the mixture was used, ex-

\*Based on materials of the paper presented at IXth International Conference «Arc Welding. Materials and Quality» (May 31–June 3, 2016, Volgograd, Russia).

pressed as the total weight balance on 0315, 02, 016, 01 and 0063 grids to GOST 6613-86: 2, 10, 15, 25 and 35 wt.%, respectively. 65 % passed through 0063 mesh. Coating mass was prepared using NaK liquid glass with 3.05 module,  $1.435 \text{ g.cm}^{-3}$  density and  $900 \text{ mPa}\cdot\text{s}$  viscosity, glass dose was 30 wt.%.

Dry mixture for the charge was prepared in cylindrical plough mixer of intensive type, and coating mass was prepared in single-roller mixer.

Electrodes were produced in hydraulic electrode coating press of Havelock Engineering Company with angular feed of coating mass ( $90^\circ$ ). Electrode rod diameter was 4 mm, coating thickness was 1.1–1.2 mm. Pressing speed was 420 electrodes per minute.

Wire and coating materials met the requirements of respective GOSTs, and allowances for deviations of forming tool dimensions complied with the requirements of acting normative documentation. Dies, rod guide tips and rod feeding rollers were not used for any other purpose, except for experiments performed in this work.

Coating mass flow, preliminarily turned along the rod guide, is reduced three times in Havelock Engineering press:

- in two-channel slot mass feeder, fixing the rod guide;
- in press chamber, located between the edge of rod guide tip and calibration sleeve cone;
- in calibration sleeve channel.

Turning of mass flow and each of its above-mentioned reductions are performed in transition flow regime, so that they are sources of hydrodynamic disturbances in it. Average gradient of shear rate, which determines the resistance, overcome by the mass during reduction, is proportional to jet reduction ratio and is dependent on the characteristic dimension of forming channel. For circular cylindrical channel, as in the calibration sleeve, this is the diameter, and for a flat or annular (slot) channel, as in mass feeder, this is its width. Moreover, acceleration of mass flow in two-channel mass feeder changes two more times, depending on whether the mass consistency allows passing through both parts of slotted channel at once, or just one of them. Standard gap between rod guide tip edge and calibration sleeve is 1.5 mm.

Continuous recording of coating thickness variation during electrode pressing was performed using specialized monitor with electromagnetic transducer block, supplied with Havelock Engineering Company press. Together with the calibration sleeve, the block is fastened on base seat, envisaged for this purpose in the press. Calibration sleeve position, also during travel, is adjusted by four bolts with the known thread pitch. Figure 1 gives the general view of the instrument in the working position [9].

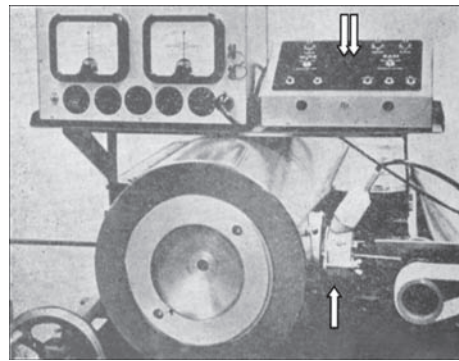


**Figure 1.** Head-sensor for measuring coating thickness variation in Havelock Engineering press (marked by an arrow)

Electromagnetic signals, proportional to horizontal and vertical coordinate components of electrode coating thickness variation vector (CC CTVV) formed in the monitor electronic block, are read from scales of two control pointer instruments in standard configuration. Actual state of thickness variation is determined by pointer deviation from zero. We used loop oscillograph 8SO-4 for continuous recording of these deviations. Recording was performed on aerial film, 120 mm wide, with sensitivity of 1200 units to GOST 100691–63. The film develops very quickly in the light. Recording speed was selected during preliminary experiments and was equal to 10 mm/s. Data recorded on the film were digitized during its subsequent processing, and coordinates of points separated from each other by a distance of 5–6 mm on the curves were determined.

Coating mass was prepared in the quantity of 50 or 100 kg (batch), briquetted and divided into three press charges, each of not more than two briquettes. During pressing out of the first charge, adjustment of coating mass and rod feeding to avoid the relative misalignment of the axes of calibration sleeve and the rods, and of loopback beam position was performed, as well as tuning of film recording. During pressing out of the second charge the main records of 50 to 360 s duration were made. The last charge was used as the reference one, and if required, the briquettes were soaked for up to one hour to check the «viability» of coating mixture. They were stored under the conditions, traditionally used in production to prevent moisture loss.

During pressing one electrode was selected every 7–10 s. They were instantly controlled in a portable concentrimeter (shown in Figure 1 by a double arrow). Results were immediately recorded on film (casual inspection). At the end of the charge, single samples were taken in the quantity of not less than 10 electrodes, which were marked, and then controlled, and the results were statistically generalized in the laboratory (group control).

Results of casual and group control were used to correct the settings of the press and oscilloscope, in

order to precise the position of zero lines ( $X_0, Y_0$ ) on the film, designed for counting of CTVV horizontal ( $x_i$ ) and vertical ( $y_i$ ) components. Shifting of  $x_i$  up or down from zero meant thickening of coating shell right or left half. Similar shifting of  $y_i$  was indicative of thickening of its upper or lower parts.

Values of  $x_i$  and  $y_i$  were used to calculate individual values of coating thickness variation vector ( $e_i$ ) and angle of its orientation in the section, normal to electrode axis ( $\text{tg}\alpha_i = x_i/y_i$ ), then  $e_i$  map was plotted in comparison with the lines of mean ( $e_{im}$ ) and boundary values, specified by GOST 9466–75.

Values and angle of orientation of  $e_i$  are random quantities. The need for application of statistical methods for their assessment and presentation became clear already during preliminary experiments. With this purpose, individual  $e_i$  values found from 100 measurements, were grouped into conditional samples, each of five  $e_i$  values. Sample number was 20 pcs. Sample average ( $e_{av}$ ), standard deviations ( $s_p$ ) and ranges ( $R$ ), as well as their general average of 20 samples ( $E_{av}, S_p$  and  $R_{av}$ ) were calculated. Presented graphically, these data more accurately reflect the variability of the processes and their tendencies, than do individual indexes [10].

**Nature of CC CTVV oscillograms.** Curves of CCTV horizontal and vertical components, similar to extrusion curves of coating masses, obtained in capillary plastometer OB 1435 [3], reflect the starting, structural, steady-state and final stages of pressing.

In the majority of experiments, recording was begun not right after starting the rod-feeder machine. Therefore, in short oscillograms, which reflect the pressing process during 15–35 s, the starting stage is not recorded, as a rule. Sometimes, the film captured only the final part of its structural (downward) branch, going into, so to speak, steady-state branch. As follows from Figure 2, in coating mass, used by us for procedure optimization, the starting portion of CC CTVV oscillograms has a clearly pronounced oscillating form. Here, for vertical component this is an almost ideal sinusoid with mild extremality of center line, gradually attenuating and even-

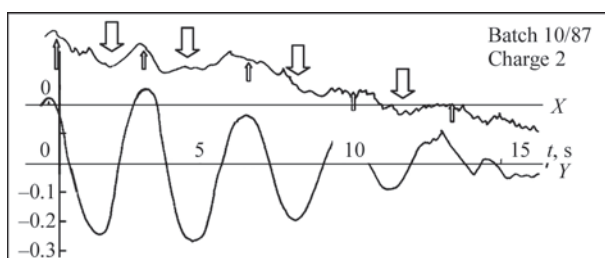


**Figure 2.** CC CTVV oscillograms obtained during pressing of UONI 13/55 electrodes ( $X$  — horizontal,  $Y$  — vertical components; arrows show responses of vertical component to a change of horizontal component)

tually taking the shape of irregular oscillations, while the horizontal one is like that from the very start. The disturbances recorded on vertical component oscillogram, as beam shifting upwards or downwards from the loop, are almost synchronously reflected on the oscillogram of horizontal deflections as the respective beam shifting to the right-left (marked by arrows in Figure 2). This is attributable to relatively elastic consistency of the studied coating mass, and configuration of the forming zone of the used press, in particular, vertical location of two mass-feeding slots, which enables the viscoelastic coating mass periodically changing the flow path, jumping from the upper window into the lower one, and vice versa. Horizontal component further reflects the consequences of hydrodynamic disturbances, arising even before the coating mass has passed through mass-feeder slots, which are caused by flow turning by  $90^\circ$ . Cycles, associated with alternative passing of coating mass through the above-mentioned two slot channels of mass-feeder, are superimposed on them.

The extent of sinusoidal portion of vertical oscillogram depends on the change of coating mass consistency, caused by briquette soaking before use. This stage could not be recorded for the first, freshest charge, because of prolonged setting-up of the press (just a stationary portion of 45 s duration was obtained). Duration of sinusoidal portion in the second charge was equal to 15 s, and that of the third one, which had been soaked longer than the other ones before application, was two times longer.

Results of calculation of attenuation in sinusoidal amplitudes, recorded at pressing electrodes from the second and third charges of coating mass, are given in Figure 3. It is seen that despite the relatively short soaking of coating mass in the briquette state, its relaxation period increased 3 times. Coating mass consistency changed, because of structure formation processes, which had occurred in it during this time.

We established the following general regularities of changing of the shape of CC CTVV curves, depending on consistency of coating masses for low-hydrogen electrodes during their manufacture in Havelock Engineering press. For highly elastic masses, both the oscillograms  $x_i = f(t)$  and  $y_i = f(t)$  at the starting stage of pressing have the form of sinusoids, although not always as ideal in shape, as in Figure 2. Further on they gradually degrade into oscillating curves of an irregular shape, and for  $x_i = f(t)$  oscillograms this often occurs earlier than for  $y_i = f(t)$ .

For coating masses close in their consistency to the one presented in this work, only  $y_i = f(t)$  oscillogram is sinusoidal, and that only at the start of pressing. For even softer coating masses  $y_i = f(t)$  almost merges with zero line, while  $x_i = f(t)$  curve preserves its irreg-

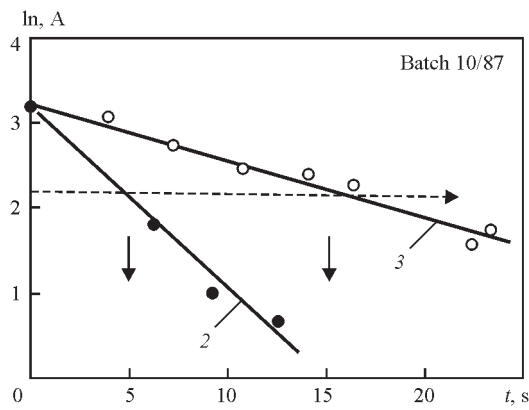


**Figure 3.** Comparison of oscillation amplitudes of vertical component of coating thickness variation vector during starting stage of pressing electrodes from second (2) and third (3) charge of coating mass

ular shape longer. For fluid-like masses both the oscillograms have the shape of low-amplitude sinusoids from the very start.

**Curves of evolution of coating thickness variation vector.** Evolution of individual values of the vector of coating thickness variation is given in Figure 4. At the starting stage, it looks like not as perfect a sinusoid, as CTVV vertical component. Alongside that, one or two weak amplitudes are wedged between high amplitudes in some places. Both gradually attenuate (similar to CC CTVV sinusoids) that is indicative of relaxation nature of the process they reflect. Then they evolve into a kind of harmonic functional dependence with more than two variables. So far four harmonics could be singled out with oscillation frequency from 1 up to  $0.04 \text{ s}^{-1}$ .

CTVV changes in the pulsed mode not only by value, but also by its orientation in space. This can be judged by observing the changes of CTVV «trace», as  $e_i$  projection on a plane, normal to electrodes coming out of the press head. Figure 5 shows the form of this kind of phase trajectories obtained during the start-

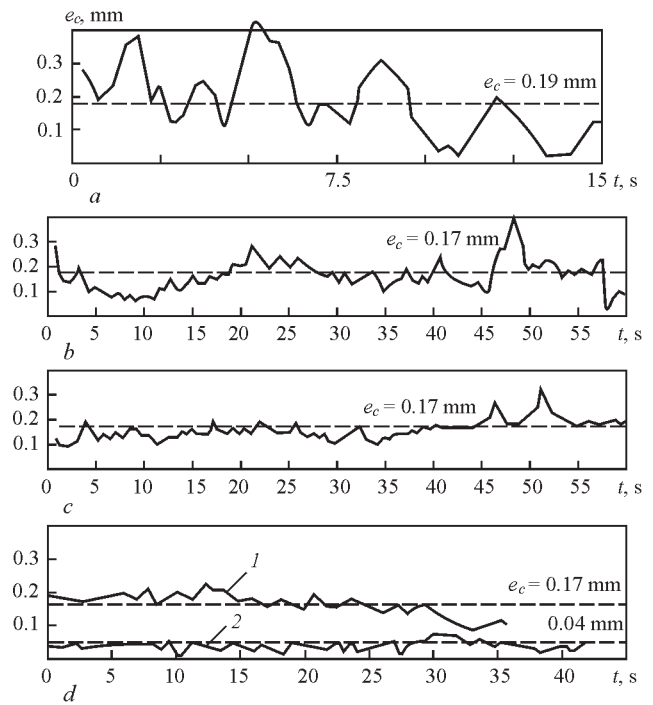


**Figure 4.** Evolution of CTVV of electrodes made during pressing of coating mass second charge: starting (a), stationary (b, c) and final (d) stage from first (1) and second (2) coating mass charge;  $e_i, e_{i,av}$  — individual and sample average values of coating thickness variation

ing stage of electrode pressing. Initial point of each sample is marked with a cross, the final one — with an arrow. The first two samples consist of 20, and the third one — of 10 electrodes.

As we can see, pulsing amplitude by  $y_i$  (particularly, its positive part) decreases simultaneously with less noticeable decrease of  $x_i$ . This results in overall compression of  $x_i$  and  $y_i$  and, therefore, its gradual shifting to zero area takes places simultaneously with decrease of  $e_i$  value.

Further variations of  $e_i$  value and orientation were assessed by the following ten samples of electrodes,

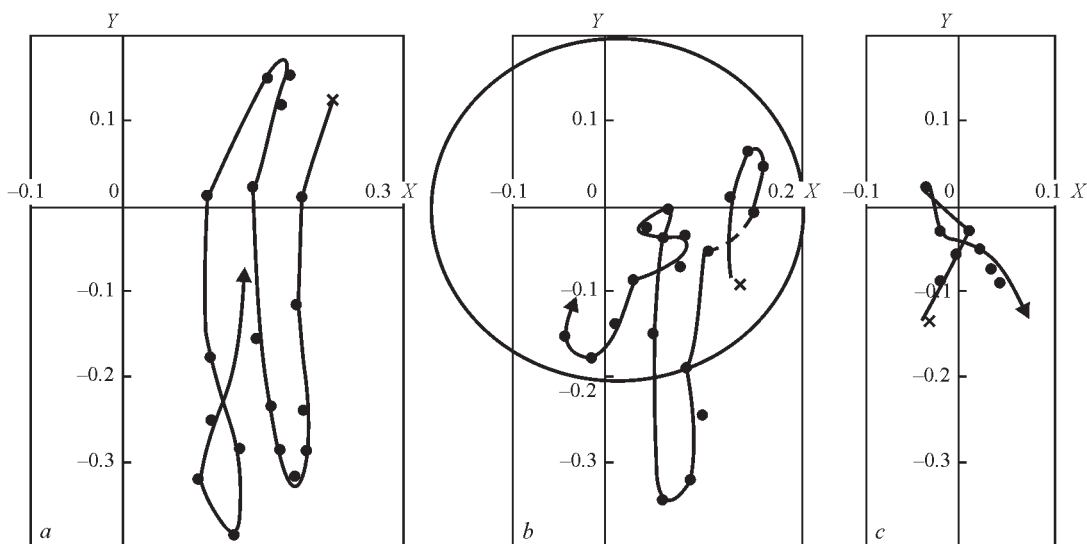


**Figure 5.** Appearance of phase trajectories of coating thickness variation vector during starting stage of electrode pressing. Numbers of coating thickness measurements, included into samples: a — 1–20; b — 21–40; c — 41–50

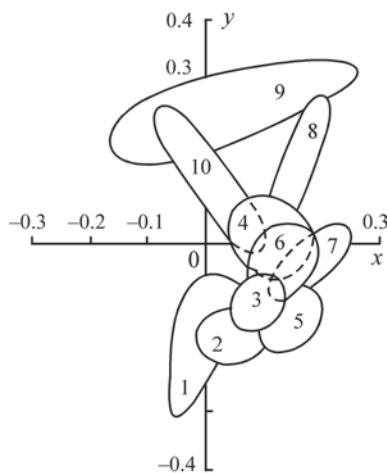


**Figure 6.** Nature of change of characteristics of coating thickness variation in electrodes pressed from coating mass of charge 2. Figures mark number of the sample, each of 10 electrodes

selected from the stationary stage. They are shown in Figure 6 in the form of lobes, including 10 individual  $x_i$  and  $y_i$  values from each sample.

Together with Figure 4, it shows that in terms of CTVV evolution, this stage can only be called stationary with great reserve. Vector of coating thickness variation for electrodes pressed during this stage, first decreases, and then abruptly increases, while dislocation changes by pulsing spiral, in the form of successive rotational transitions from III to IV, I, II and then again to IV quadrant. It occurs nonmonotonically within each sample, as well as at transition from sample to sample, with different rate within just 60 seconds. Considering that 420 electrodes came out of the press head every minute, the rate of these changes is indeed huge, and it cannot be explained in terms of just variation of coating mass viscosity, as many have attempted to do up to now. For this purpose it is necessary to take into account in a timely manner the variation of relevant coating mass elasticity characteristic.

**Evolution of statistical selective CTVV characteristics.** Figure 7 reflects variations of sample averages and ranges of coating thickness variation during the «stationary» stage, compared to average sample values for each group, namely initial, middle and final. They more clearly reflect the general evolution of coating thickness variation, than does  $e_r$ . Consequences of the process starting stage are quite evident in electrodes of initial group (a). Decrease of  $e_r$ , occurring at the end of the starting stage, was followed by two spikes, separated by a short period of stabilization. On the whole, average sample values of thickness variation rise, and this increase is continued in the new series of samples (b), also in a wavelike, even though somewhat quieter manner. Signs of this characteristic decreasing appeared only at the final (c) stage, but, probably, only as the next descending branch of the wave. Constancy of general average value  $E_{av}$  on the level of 0.17 mm is an indirect confirmation of it.

Nonetheless, the process gradually calms down that is indicated by the reflected in Figure 7 decrease of oscillations and general sample average values of ranges ( $R_{av} = 0.090$  mm in the initial and 0.025 mm in the final series of samples).

We do not give sample standard deviations of  $e_r$ , although we also calculated them alongside the ranges, and took them into account in analysis of obtained results. The nature of their variation is similar to that of the ranges. Absolute values, however, are 2 to 3 times lower. If there is the need to assess the share of hidden rejects by  $e_r$ ,  $s_r$  value must be taken into account [10].

Constancy of  $E_{av}$  in the above analyzed samples of electrodes from charge 2 should not be regarded as an indication of the possibility of their value decreasing further. Results obtained when studying the electrodes of the first charge, given in Figure 4, d for comparison show that in this case,  $E_{av}$  eventually dropped to values of 0.04 mm (in charge 2), compared to 0.17 mm. The difference can also be to some extent linked to the change of coating thickness consistency during its soaking in briquettes.

**Discussion of results.** Presented investigation results show that unstable flow of coating mass is the main cause for coating thickness variation. Instabilities in the pressure flow usually arise when elasticity accumulated during coating mass deformation exceeds the level, which can be damped by its viscosity before it comes into contact with the rod in the press chamber. Coating thickness variation is exactly one of undesirable kinds of rapid discharge of excess elasticity during formation of coating shell on the rod. The other kind is discussed below.

Accumulation and relaxation of elastic stresses in the pressure flow of coating mass, from which electrode coating is formed in the press head, should be regarded as a continuous process, which starts at the moment, when coating mass flow begins, and which can go on until mass charge has been used completely. Results of conducted studies show that this is:

- on the whole, a relaxation process, in which statistical average value and scattering indices of thickness variation gradually decrease, i.e. overall balance of viscosity and elasticity improves, primarily, due to elastic stress relaxation;
- multistage process, characterized by elasticity and viscosity levels and ratios, which are different at different stages;
- «hereditary» process, in which disturbances, arising in its previous stages, are felt at its subsequent stages, including both the starting and final stages in the most unfavourable case;
- nonmonotonic and, most probably, wavelike process, during which the thickness variation, decreasing

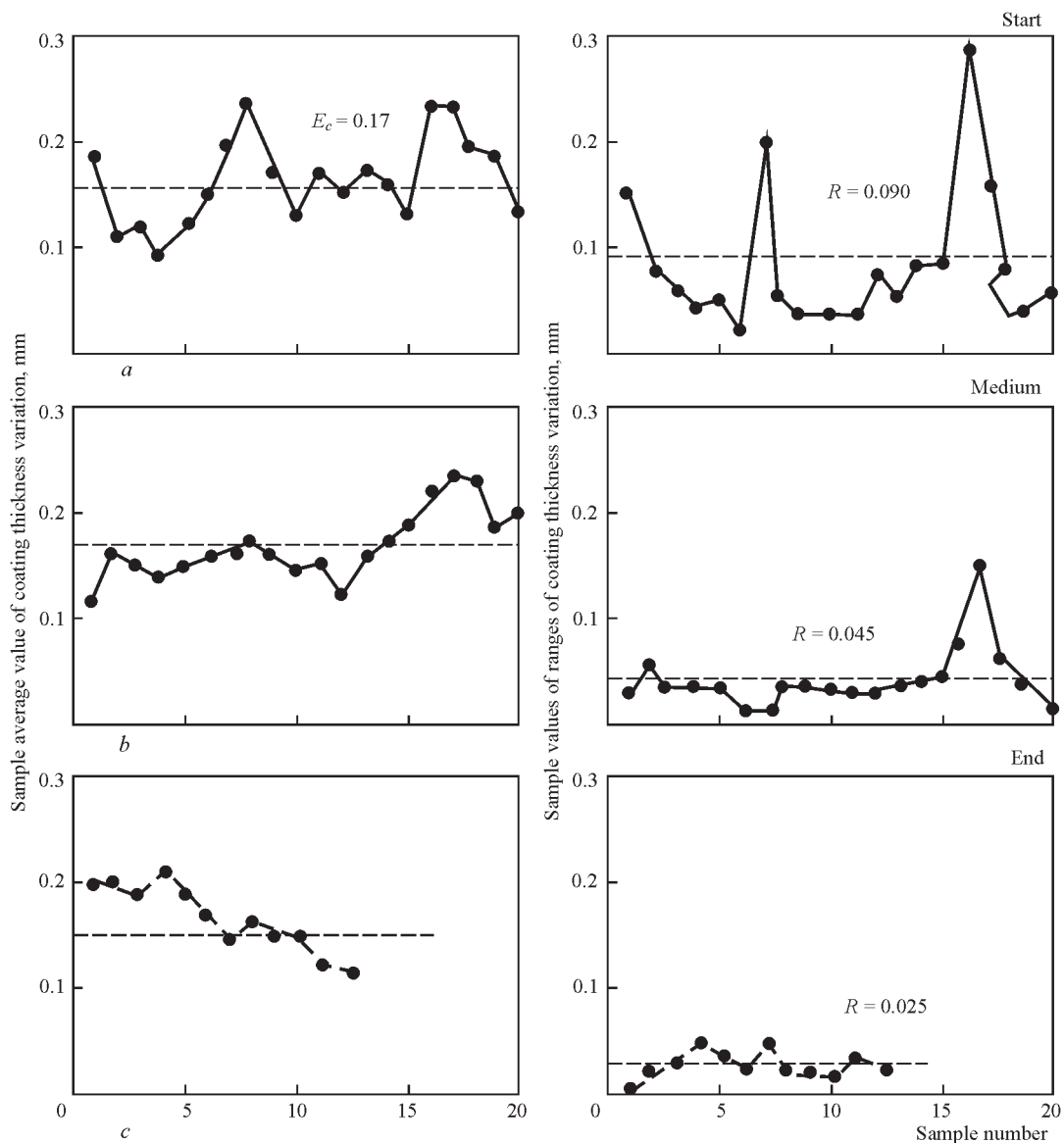


**Figure 7.** Measurement of CTVV statistical characteristics during electrode pressing from coating mass in charge 2 (for *a-c* see the text)

with time, increases again, having reached the next minimum, up to the previous or somewhat lower level;

- harmonic process, as short cycles with lower pulsing amplitudes run within the long cycle.

The main sources of elasticity are the starting deformation of coating mass, which is caused by its volumetric compression, on the one hand, and turning of coating mass flow through 90 degrees, on the other hand, significantly accelerating the layers in its outer contour. The action of the first source starts, when the piston is brought from the travel to working speed. Relaxing, they continue acting after switching on the rod-feeding machine and stop after complete relaxation of starting elasticity. The second source is, probably, active during the entire pressing cycle.

Elastic stresses, arising during this period, relax in different ways and with different speed in mass feeder channels, press chamber and calibration sleeve. Being superposed on each other, they are manifested

as harmonics on the curve of evolution of thickness variation characteristic. Owing to reduction of coating mass flow, additional elastic energy is generated in each of them. Its relaxation occurs at subsequent stages of flow formation.

In this complicated pattern of origin and relaxation of elastic stresses, provoking thickness variation, the actual causes of nonmonotonic evolution of its values during electrode pressing need to be clarified. For this purpose, the known postulates of hydrodynamics of a Newtonian fluid flowing through an annular channel formed by two stationary non-concentric tubes should be précised, allowing for viscoelastic nature of electrode coating masses. Alongside that, instead of a stationary inner tube, an elastic rod should be considered, which is also prone to reversible deformations, is moving in synchronism with the shell, and which has a certain degree of freedom of the transverse displacements, while being inside the shell.

In keeping with hydrodynamic theory of fluid flow, volumetric rate of fluid flow through a circular tube with inner core of a round cross-section depends on axial displacement of the core relative to the outer tube.

In the case of their concentric position, the fluid in the annular gap flows, while enveloping the core by a layer with symmetric velocity profile. The more is the core shifted from the concentric position, the higher the volumetric rate (flow rate) of the fluid over the wide section of the gap, despite the fact that the size of overall cross-section, through which the fluid flows, remains unchanged [11, 12].

This conclusion is valid for pressure flows of Newtonian simple and complex fluids, as well as for viscoplastic materials, such as Bingham body. It, in principle, is independent on whether the coating and rod non-axiality is caused by careless pre-setting of press chamber elements, or whether it arises as a natural shifting of elastic rod due to coating mass elasticity. In either case increase of the degree of non-axiality leads to increase of the statistical scatter index of thickness variation. Thus, the tendency of coating mass circular flow to disturb the coaxial position of calibration sleeve with the rod should be regarded as a quite natural phenomenon. This conclusion does not lose its significance also for electrode coating masses, which are not fluids by their rheological properties and which move in synchronism with the rod, and not as an axially stationary core, as was considered above.

Our studies of rheological properties of electrode coating masses show that there are a number of reasons, why the «coating mass-rod» system, brought out of the concentric state, usually does not preserve its maximum thickness variation, at which the most favourable energy conditions for its pressure flow are achieved. The system comes out of this state with a certain periodicity, gradually approaching the stationary state. First of all, it should be taken into account that increase of volumetric rate of coating mass flow, caused by violation of sleeve and rod coaxiality, is accompanied by increase of the shear rate gradient  $\dot{\gamma}$  in the mode of  $\dot{\gamma} = \text{const}$ , in which its greatest dissipative heating occurs [13].

Both factors decrease shear viscosity of coating mass  $\eta$ , and, to a much greater extent,  $\xi$  — first difference coefficient of normal stresses. It characterizes the rate of coating mass elasticity decrease under the impact of increasing shear rate gradient [5]. Thus, with  $\dot{\gamma}$  increase, caused by increase in thickness variation, the coating mass ability to dampen its elastic characteristics should be also enhanced, i.e. the probability of further increase of coating thickness variation decreases with time. As a result, every time the period of  $e_i$  increase is followed by its decrease, «rod-coating»

system is discharged from elastic stresses, and gradually reaches the next minimum of thickness variation.

This is followed by beginning of its new cycle, as  $\dot{\gamma}$  and  $T$  reached here will promote accumulation of elastic stresses.

It should not be overlooked that elastic stresses in pressure flow can relax not only in transverse ( $x_i$  and  $y_i$ ) directions, but also along the moving electrode ( $z_i$  direction) with consequences which are not recorded by oscillographic method, accepted by us. They can be assessed indirectly. Imagine an electrode in the form of a two-layer stratified flow, in which the steel rod is replaced by coating mass, which differs from coating mass in the outer layer by elasticity and viscosity ratio. For example, let us choose marble powder as coating mass filler for the inner layer, and let coating charge be the coating mass filler for the outer layer, and vice versa. Consistency of the compared coating masses is different: plastic strength and extrusion pressure for the first, softer coating mass are  $P_m = 0.35$  MPa, and  $P_{extr} = 6.0$  MPa, and for the second, tougher one, they are 1.95 and 23.5 MPa, respectively. Let us first imagine that the softer coating mass is inside the two-layer briquette, and the elastic one is outside, axially relative to it. Experiment shows that in the extrusion produced from such a billet the inner layer is torn into cylindrical pieces, brought apart to almost equal distances from each other along the axis by outer layer material. Now, if the softer component is placed outside the two-layer briquette with the elastic one inside it, the extrusion interface remains continuous, but acquires a wavelike shape. In the actual electrode the interface cannot deform like that. However, periodical longitudinal discharge of elastic stresses accumulated during deformation of coating mass, enveloping the steel rod, can be realized as jet restoration [14] by coating shell slipping along the rod surface. This results in violation of adhesion of coating shell with the rod.

The finer the coating mass filler, the higher the strength of baked sample of extrusion from it, but the lower the strength of coating shell from it in baked electrodes [15], particularly, when the coating mass is prepared using high-modulus liquid glass of low viscosity.

Thus, there are grounds to believe that elasticity of coating mass, accumulated in it at electrode pressing, not only causes thickness variation, but may also promote lowering of final coating strength in baked electrode, through weakening of coating adhesion to the rod as a result of elasticity relaxation.

## Conclusions

1. Oscillographic and mathematical statistics methods were applied to study the regularities of formation of

coating thickness variation in experimental electrodes UONI 13/55 with 4 mm rod diameter at their manufacture in angle hydraulic press under conditions maximum close to production environment. Values of vertical and horizontal components of thickness variation vector were recorded on aerial film, moving with  $10 \text{ mm}\cdot\text{s}^{-1}$  speed, at pressing speed of 420 electrodes per minute. Duration of observation in the experiment was varied from 30 to 240 s.

2. Results of conducted experiments suggest that coating thickness variation is caused by disbalance of elasticity and viscosity characteristics of coating masses, arising during coating mass application onto rods by extrusion. Elasticity should be regarded as a characteristic provoking appearance of coating thickness variation as a result of instant relaxation of accumulated elastic stresses, and viscosity — as a damping factor, weakening or suppressing the role of elasticity unfavourable from this point of view.

3. Accumulation and relaxation of elastic stresses in pressure flow of coating mass, from which electrode coating is formed in the press head, is a continuous multistage, nonmonotonic (wavelike) and harmonic process. In it, the disturbances, responsible for appearance of thickness variation, which arose in the previous stages, are felt at subsequent pressing stages, including, in the most unfavourable case, even the final stage.

4. Probability of formation of coating thickness variation is determined by coating mass consistency, and depends on design features of forming path of electrode coating press. Proneness to non-symmetrical configuration of the shell from coating mass on the rod is the result of its tendency to provide the most favourable energy conditions for the flow. Degree of rod deviation from the position coaxial relative to the shell depends on the nature of the change of elasticity and viscosity ratio as a result of such a deviation. Under real non-isothermal conditions, the influence of viscous heating of coating mass is superimposed on evolution of this ratio, alongside speed, resulting in evolution becoming more cyclic. Harmonics within each cycle reflect the influence of elasticity generation centers on it, which cause disturbance of stable flow of coating masses (for instance, acceleration, turning, reduction, separation and stratification of the flow). Number and kind of these centers depend on design features of forming head of electrode coating press.

5. Coating thickness variation, on the one hand, subtly responds to changes of coating mass consisten-

cy and forming path configuration, and, on the other hand, its value markedly and unpredictably changes by extent and orientation. As a result, process monitoring by this characteristic to improve product quality, can be highly problematic. In terms of coating mass rheology, lowering of coating masses tendency to elasticity accumulation in pressure flow state should become the main direction of their improvement in order to reduce coating thickness variation.

- Vornovitsky, I.N. (1989) Thickness variation as a basic factor of electrode quality. *Svarochn. Proizvodstvo*, **4**, 7–9.
- Marchenko, A.E. (2000) Thickness variation as a factor of process state and quality of manufacture of welding electrodes. In: Proc. of Scient.-Techn. Seminar on Electrode Manufacturing at the Turn of New Millennium (St.-Petersburg, 22-26 May, 2000). Cherepovets: Association «Elektrod», 124–125.
- Marchenko, A.E. (2014) Thickness difference of electrode coatings caused by elastic turbulence of electrode compounds under condition of nonisothermal pressure flow. *The Paton Welding J.*, **67**, 177–189.
- Marchenko, A.E. (2015) Investigation of elasto-plastic characteristics of electrode coating masses in the state of pressure flow through cylindrical forming nozzles. In: *Proc. of Int. Sci.-Techn. Conf. on Welding Consumables. Petranievsky readings* (St.-Petersburg, 15–17 Oct. 2015), 79–89.
- Marchenko, A.E. (2016) Rheological investigations of non-isothermal pressure flows of coating mixtures for welding electrodes. *The Paton Welding J.*, **1**, 1–19.
- Stepanosov, A.R. (1989) Expert evaluation of causes of thickness variation in welding electrode coating. *Svarochn. Proizvodstvo*, **4**, 9–11.
- Vornovitsky, I.N. (2001) *Quality control of welding electrodes in their manufacture process*. Moscow: IKAR.
- Marchenko, A.E. (1993) Peculiarities of formation of coating thickness variation detected by oscillography. In: *Abstr. of Pap. of Int. Sci.-Techn. Conf. on Welding Metallurgy and Consumables* (St.-Petersburg, 1–2 June 1993), 98–100.
- Paton, B.E., Pokhodnya, I.K. (1961) Welding equipment in Great Britain. *Avtomatich. Svarka*, **6**, 75–92.
- Sakata Shiro (1980) *Practical guidelines on quality control*. Ed. by V.I.Gostev. Moscow: Mashinostroenie.
- Redderger, P.J., Charles, M.E. (1962) Axial laminar flow in a circular pipe with a fixed core. *J. of Chemical Engineering*, Aug., 148–151.
- Happel, J. (1976) *Hydrodynamics at Reynolds small numbers*. Moscow: Mir.
- Marchenko, A.E. (2015) On heat pattern created by viscous heating of electrode coating mass in the zone of pressure flow forming. In: *Proc. of Int. Sci.-Techn. Conf. on Welding Consumables. Petranievsky readings* (St.-Petersburg, 15–17 Oct. 2015), 65–78.
- Vinogradov, G.V., Malkin, A.Ya. (1977) *Rheology of polymers*. Moscow: Khimiya.
- Marchenko, A.E. (2010) On physical-chemical nature of electrode coating strength and technological ways ensuring it. In: *Proc. of 5<sup>th</sup> Int. Conf. on Welding Consumables. Technologies. Manufacturing. Quality. Competitiveness* (Artyomovsk, 7–11 June, 2010). Kiev, 2010, 78–99.

Received 28.11.2016

# MATHEMATICAL MODELING OF CHEMICAL COMPOSITION OF WELDING FUMES IN MANUAL ARC WELDING WITH HIGH-ALLOYED ELECTRODES

O.G. LEVCHENKO<sup>1</sup> and O.N. BEZUSHKO<sup>2</sup>

<sup>1</sup>NTUU «Igor Sikorsky KPI»

37 Pobedy Prosp., 03056, Kiev, Ukraine

<sup>2</sup>E.O. Paton Electric Welding Institute, NASU

11 Kazimir Malevich Str., 03680, Kiev, Ukraine. E-mail: office@paton.kiev.ua

A mathematical model of convective evaporation of metal from the melt surface was proposed for prediction of the composition of fumes formed in manual arc welding. Numerical analysis of the characteristics of the flow of multicomponent metal vapour in welding with high-alloyed chromium-nickel electrodes was performed. Rates of evaporation of welding fume components at application of electrodes for high-alloyed steel welding were established. Obtained mathematical model enables calculation of not only the relative mass fraction of toxic component in the fume, as it was possible up to now, but also of convective flows of welding fume components. 12 Ref., 2 Tables, 4 Figures.

**Keywords:** electric arc welding, coated electrodes, welding fumes, chemical composition, evaporation intensity, mathematical modeling

Manual arc welding is characterized by high values of temperature in the arc gap. A considerable part of the surface of metal of electrode drops and weld pool is in the boiling state and evolves a large amount of metal vapours into the arc zone, from which fumes harmful for the welder's body form as a result of vapour condensation and oxidation in working zone air.

The objective of this work was mathematical simulation of the composition of welding fumes (WF) forming in manual arc welding with high-alloyed

chromium-nickel electrodes based on physico-chemical properties of weld pool components.

Vapour pressure of different substances becomes higher with temperature rise. After a significant vapour pressure equal to atmospheric pressure (101325 Pa) has been reached, the substance starts boiling [1]. Dependence of saturated vapour pressure  $p_i$  near the molten metal surface on its temperature can be determined, using Kleiperon–Klausius equation [2]

$$p_s = p_0 \exp \left[ \frac{\lambda}{k} \left( \frac{1}{T_v} - \frac{1}{T_s} \right) \right], \quad (1)$$

where  $p_s$  is the saturated vapour pressure above the metal surface;  $p_0$  is the atmospheric pressure,  $T_b$  is the metal boiling temperature (temperature, at which saturated vapour pressure of this metal is equal to atmospheric pressure);  $T_s$  is the surface temperature,  $\lambda$  is the work function of atom in the melt,  $k$  is the Boltzmann constant. This equation holds, provided the vapour follows the ideal gas law, and molar volume of liquid  $V_l$  is much smaller than molar volume of vapour  $V_v$ .

Plotted graphic dependencies of saturated vapour flow of individual toxic elements, included into welding electrode composition (chromium, manganese, nickel and iron), on evaporating alloy surface temperature, according to equation (1) at  $T_s = 1500$ – $3500$  K, are given in Figure 1. Analysis of the given data shows that during open arc welding process man-

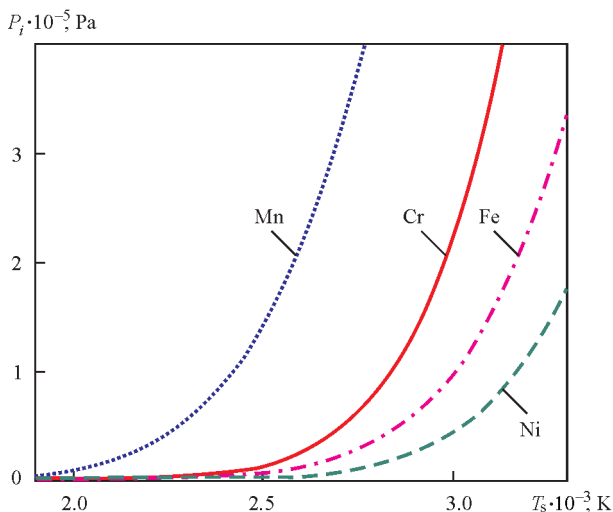


**Figure 1.** Dependence of pressure of saturated vapours of chromium, nickel, manganese and iron on temperature

ganese will be the first to evaporate the most intensively, followed by chromium, iron and nickel.

Calculations were performed using the values of atom work function  $\lambda$  and boiling temperature  $T_b$ , at which pressure of the respective element saturated vapour is equal to atmospheric pressure [3, 4] (see Table 1).

Let us evaluate the resulting pressure of saturated vapours over the surface of an alloy, which is in the liquid state [5]. We will regard this alloy as a weak solution of chromium, manganese and nickel in iron. We will determine resulting pressure  $p_v$  as a sum of saturated vapour pressures above the alloy  $i$ -th component  $p_{is}$ , allowing for activity of the  $i$ -th component in the solution  $\alpha_i$

$$p_v = \sum_i \alpha_i p_{is}. \quad (2)$$

Iron activity can be determined, using Raoult law [2, 5]

$$\alpha_{Fe} = X_{Fe}, \quad (3)$$

where  $X_{Fe}$  is the molar (atomic) fraction of Fe in the respective alloy. Note that Raoult law is applicable practically only for weak solutions, in which the saturated vapour behaves as an ideal gas, i.e. it is fulfilled the better, the lower the vapour pressure.

We will apply Henry's law to determine the activity of the vapour of dissolved substances Cr, Mn, Ni [2, 5]. Let us present impurity activities in the following form:

$$\alpha_{Cr, Mn, Ni} = \gamma_i X_{Cr, Mn, Ni}, \quad (4)$$

where  $\gamma_i$  is the coefficient of activity of the  $i$ -th element;  $X_{Cr, Mn, Ni}$  is the molar (atomic) fraction of the respective dissolved element, i.e. its concentration in the alloy. In view of lack of data, let us assume that all the coefficients of activity are equal to a unity.

Thus, considering relationship (3) and assuming that  $\alpha_{Cr, Mn, Ni} = X_{Cr, Mn, Ni}$ , formulas (1) and (2) can be used to assess the saturated vapour pressure above the surface of an alloy, which is in the molten state, depending on  $T_s$ . Molar fraction of an element in the melt is calculated by the following relationship:

$$X_{im} = \frac{C_{im} : M_i}{\sum C_{im} : M_i}, \quad (5)$$

where  $M_i$  is the atomic mass;  $C_{im}$  is the mass fraction of  $i$ -th element in the melt.

Let us study the features of evaporation of a multi-component alloy in the case of high-alloyed electrodes of E-08Kh20N9G2B type (20 % Cr, 2 % Mn, 9 % Ni). Pressure of multicomponent saturated vapour over the melt for Cr, Mn, Ni and Fe is given in Figure 2.

Let us apply Knight model to determine the quantitative characteristics of the evaporation process (density, temperature and outflow velocity of the vapour)

**Table 1.** Physical properties of molten metal components

Physical properties	Chemical element			
	Cr	Mn	Ni	Fe
Atom work function in the melt, $\lambda$ , erg·10 <sup>-12</sup>	5.79	3.73	6.31	5.65
Metal boiling temperature, $T_b$ , K	2840	2424	3173	3008

[6]. The model is based on the assumption that the vapour flow is one-dimensional and stationary. This model is actively applied for performance of numerical analysis of thermal and gas-dynamic characteristics of the vapor flow in laser welding [6–9]. Information about its application for manual arc welding is not available.

According to this model, there is a Knudsen layer of the thickness of several free path lengths vapour particles near the evaporated metal surface, beyond which (in the gas-dynamic flow region) a thermodynamic equilibrium is established. In [6–9] the following relationships were proposed, which relate density  $\rho_v$  and temperature  $T_v$  of vapour on Knudsen layer boundary with saturated vapour density  $\rho_{s,v}$  and evaporating surface temperature  $T_s$

$$\frac{T_v}{T_s} = 1 + \frac{m^2 \pi}{32} \left( 1 - \sqrt{1 + \frac{64}{m^2 \pi}} \right), \quad (6)$$

$$\frac{\rho_v}{\rho_{s,v}} = \sqrt{\frac{T_s}{T_v}} \left[ \left( m^2 + \frac{1}{2} \right) e^{m^2} \operatorname{erfc}(m) - \frac{m}{\sqrt{\pi}} \right] + \frac{1}{2} \frac{T_s}{T_v} (1 - \sqrt{\pi} m e^{m^2} \operatorname{erfc}(m)), \quad (7)$$

where  $\operatorname{erfc}(m)$  is the probability integral. Value  $m$  is calculated by the following formula

$$m = \left( \frac{M_v u^2}{2kT_v} \right)^{1/2}, \quad (8)$$

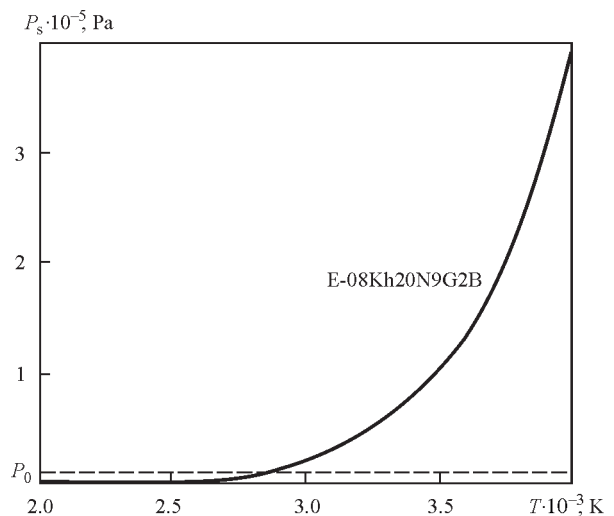


**Figure 2.** Temperature dependence of saturated vapour pressure above the surface of metal melt of E-08Kh20N9G2B type electrodes ( $X_{Cr} = 0.213$ ;  $X_{Mn} = 0.02$ ;  $X_{Ni} = 0.085$ ;  $X_{Fe} = 0.683$ )

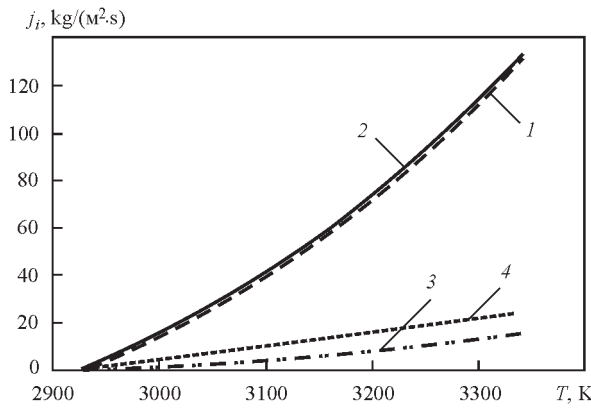


**Figure 3.** Dependence of convective vapour flows of chromium (1), iron (2), manganese (3), and nickel (4) on drop surface temperature

where  $u$  is the weight-average velocity of outflow from the metal surface.

Weight-average velocity of outflow from the metal surface was calculated by the following formula

$$u = \frac{s_0 \left( \frac{p_m^0}{p_0} - 1 \right)}{\gamma_0 \sqrt{1 + \frac{\gamma_0 + 1}{2\gamma_0} \left( \frac{p_m^0}{p_0} - 1 \right)}}, \quad (9)$$

where  $p_0$  is the atmospheric pressure;  $\gamma_0 = 1.4$  is the constant of air adiabatic;  $s_0 = 331.5$  m/s is the velocity of sound in the air;  $p_m^0$  is the vapour pressure on Knudsen layer boundary.

Calculation of convective flow of vapour was performed by the following formula:

$$J_{p,i} = \alpha_i \frac{p_s}{p_v} \frac{M_i}{M_v} j_p, \quad (10)$$

where  $p_v$  is the resultant pressure, calculated by formula (2);  $p_i$  is the saturated vapour pressure over the  $i$ -th component from formula (1);  $\alpha_i$  is the activity of the  $i$ -th component, calculated by formulas (3, 4);  $M_v$  is the average mass of an atom of multicomponent vapour  $M_v = \sum_{i=1}^n M_i \frac{\alpha_i p_s}{p_v}$ ,  $j_p$  is the full evaporation flow  $j_p = \rho_v M_s \approx \rho_v u$ .

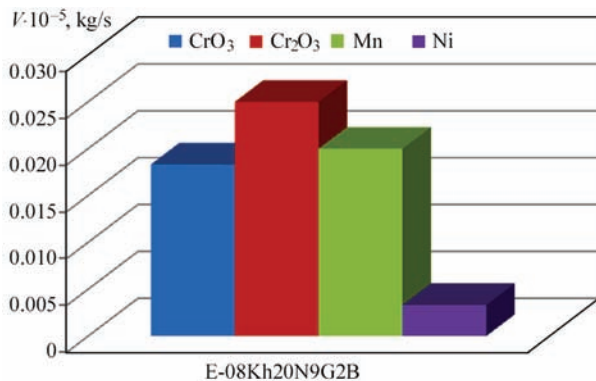


**Figure 4.** Intensity of formation of WF toxic components in welding with coated electrodes of E-08Kh20N9G2B type

**Table 2.** Intensity of WF component formation in welding with coated electrodes of E-08Kh20N9G2B type

Electrode type — E-08Kh20N9G2B (ANV-65u grade)	Formation intensity, $V_a \cdot 10^{-5}$ , kg/s			
	CrO <sub>3</sub>	Cr <sub>2</sub> O <sub>3</sub>	Mn	Ni
	0.018337	0.025005	0.020004	0.003334

Obtained graphic dependencies of convective flows  $J_i$  of chromium, manganese, nickel and iron on drop surface temperature are given in Figure 3.

As is seen from Figure 3, in the temperature range from 2900 to 3400 K, the highest evaporation flow is characteristic for chromium and iron. To determine the evaporation intensity of these elements, we will assume that the drop evaporation area is the same as that of a sphere with a diameter equal to electrode diameter. Diameter of electrodes, used to perform experimental welding, was equal to 4 mm. Then, the area of a spherical welding drop was calculated by formula  $S_{\text{drop}} = \pi d^2$  and was equal to  $5.0265 \cdot 10^{-5}$  m<sup>2</sup>.

We will write the evaporation flow of the  $i$ -th element in the following form

$$J_i = V_i / S_{\text{drop}}. \quad (11)$$

Hence,  $V_i = J_i / S_{\text{drop}}$ .

Experimental data [10] of the intensity of formation (precipitation) of chromium, manganese, nickel and iron in welding with coated electrodes of E-08Kh20N9G2B type, are given in Table 2.

Experimental data were used to plot the diagrams of the intensity of WF component formation.

As is seen from the obtained results, the summary value of the intensity of chromium compound formation prevails over the values of other harmful components that is confirmed by calculated data of the intensity of chromium evaporation (Figure 4).

Using the proposed mathematical model, it is possible to predict the intensity of formation of the above WF components in welding with high-alloyed chromium-nickel electrodes. Here, it should be taken into account that the vapour formed from molten metal drop is transferred into the weld pool, where is partially condenses, and the rest is dissipated beyond the arc, forming fumes as a result of vapour condensation in air. Thus, the results of experimental determinations of the quantity of evolved WF show just that part of metal vapour from which the fumes form. Therefore, in order to precise the actually predicted value of the intensity of WF component evolution, we will use the coefficient of  $K_{vi}$  ratio of experimental value of evolution intensity of  $i$ -th element  $V_{i\text{exp}}$  to its calculated evaporation intensity  $V_{i\text{calc}}$

$$K_{vi} = V_{i\text{exp}} / V_{i\text{calc}}$$

Calculated value of evaporation intensity  $V_{i\text{calc}}$  was used at the temperature of  $T_v = 3000$  K. As experi-

mental values of chromium evaporation intensity are given for trivalent and hexavalent chromium, we will sum them up for their comparison with calculated data. Obtained data of the coefficients of evaporation intensity of the  $i$ -th element  $K_{vi}$  for chromium, manganese and nickel, respectively, in welding with electrodes of 08Kh20N9G2B type with basic coating with metal deoxidation-alloying through the electrode rod are as follows:  $K_{vCr} = 6.08 \cdot 10^{-4}$ ;  $K_{vMn} = 9.09 \cdot 10^{-4}$ ;  $K_{vNi} = 4.54 \cdot 10^{-4}$ .

Verification of mathematical model accuracy showed that relative error of component ratios in the compositions of vapour and WF does not exceed 30 % that is due to the assumptions taken during development of this modeling system.

### Conclusions

Thus, the proposed mathematical model enables calculation of not only the relative mass fraction of the toxic component in percent, as it was possible up to now [11], but also calculation of the convective flows of WF components, that allows prediction of the main hygienic index of welding consumables without experimental studies, namely the intensity of WF component formation [12] and determination on its basis of the degree of the risk of harmful action of the process of welding by these consumables on the welder's body.

1. Potapov, N.N. (1989) *Consumables for arc welding*. Vol. 1: Shielding gases and welding fluxes: Refer. Book. Moscow: Mashinostroenie.
2. Landau, L.D., Lifshits, E.M. (1976) *Theoretical physics*. Vol. 5: Statistic physics. Pt 1. Moscow: Nauka.
3. Nesmeyanov, A.N. (1961) *Vapour pressure of chemical elements*. Moscow: AN SSSR.
4. (1976) *Tables of physical magnitudes*: Refer. Book. Ed. by I.K. Kikoin. Moscow: Atomizdat.
5. (1969) *Course of physical chemistry*. Vol. 1. Ed. by Ya.I. Gerasimov. Moscow: Khimiya.
6. Knight, C.J. (1979) Theoretical modeling of rapid surface vaporization with back pressure. *AIAA J.*, **17**, 519–523.
7. Krivtsun, I.V., Sukhorukov, S.B., Sidorets, V.N. et al. (2008) Modelling of the processes of evaporation of metal and gas dynamics of metal vapour inside a keyhole in laser welding. *The Paton Welding J.*, **10**, 16–22.
8. Zhao, H., Debroy, T. (2001) Weld metal composition change during conduction mode laser welding of aluminum alloy 5182. *Metallurg. and Materials Transact. B*, **32B**, 163–172.
9. Mundra, K., Debroy, T. (1993) Calculation of weld metal composition change in high-power conduction mode carbon dioxide laser-welded stainless steels. *Metal. Transact. B*, **24B**, 145–155.
10. Yushchenko, K.A., Levchenko, O.G., Bulat, A.V. et al. (2007) Sanitary and hygienic characteristics of covered electrodes for welding high-alloy steels. *The Paton Welding J.*, **12**, 35–38.
11. Podgaetsky, V.V., Golovatyuk, A.P., Levchenko, O.G. (1989) About mechanism of welding fume formation and prediction of its composition. *Avtomatich. Svarka*, **8**, 9–12.
12. *DSTU ISO 15011-4:2008*: Health protection and safety in welding and related processes. Laboratory method of sampling of fumes and gases. Pt 4: Form for fumes data record. Valid from 2008-08–15. Kyiv: Derzhspozhyvstandart Ukrainy, 2011.

Received 17.11.2016

## RESTORATION SURFACING OF PARTS OF TITANIUM ALLOY VT22

V.P. PRILUTSKY<sup>1</sup>, S.V. AKHONIN<sup>1</sup>, S.L. SHVAB<sup>1</sup>, I.K. PETRICHENKO<sup>1</sup>,  
I.A. RADKEVICH<sup>1</sup>, S.B. RUKHANSKY<sup>1</sup> and S.L. ANTONYUK<sup>2</sup>

<sup>1</sup>E.O. Paton Electric Welding Institute, NASU

11 Kazimir Malevich Str., 03680, Kiev, Ukraine. E-mail: office@paton.kiev.ua

<sup>2</sup>SE «ANTONOV Company»

1 Tupolev Str., 03062, Kiev, Ukraine. E-mail: info@antonov.com

The article gives the results of investigations of application of a flux-cored wire of PPT-22 grade as a filler material and magnetically-impelled arc in argon arc surfacing of worn-out parts of alloy VT22. It is shown, that in restoration of geometric sizes of worn-out surfaces using surfacing, the feasibility appears to control the shape of deposition and to produce the deposited metal with properties at the level of base metal after the standard heat treatment. 6 Ref., 1 Table, 10 Figures.

**Keywords:** alloy VT22, surfacing, titanium flux-cored filler wire, magnetically-controlled arc

One of the significant drawbacks of the most titanium alloys, in particular alloy VT22, is a low wear resistance. Therefore, during service of components and parts the defects of surface are occurred, caused by its wear. These defects are observed in some parts of present passenger and transport aircrafts, in particular in wing mechanization rails of aircraft «AN». Depth of worn-out regions reaches 2 mm (Figure 1). Due to occurrence of these defects it is necessary to replace the worn-out part by a new one, thus leading to large expenses for its manufacture.

One of the methods, which is used for restoration of geometric sizes of surface worn-out zones, is a thermal spraying of coatings [1]. The main drawbacks of these methods are the limiting of thickness of the sprayed coatings, which in many cases is not sufficient for restoration of deep damages, as well as a low adhesion of the sprayed layers, leading to their fracture under the conditions of high contact dynamic loads.



**Figure 1.** Working surface of rail with worn-out regions

The processes of restoration include also a technological process of surfacing. It possesses a high adhesion and allows avoiding those drawbacks which are typical for the above methods. Therefore, it was suggested to apply the process of surfacing by an arc, burning in argon at the tungsten electrode and impelled by the magnetic field for producing the deposited layer [2].

The effect of external transverse variable magnetic field allows controlling the depth of penetration, width and height of deposited layer, and also redistributing the arc heat energy so, that the most part of energy input was consumed for melting of the filler wire.

Probably, due to high content of  $\beta$ -stabilizers, the alloy VT22, is very sensitive to internal stresses, which occur in the heat-affected zone during welding with filler wires, the composition of which is differed from that of alloy VT22 [3,4]. Therefore, it was interesting to use the filler material for surfacing with the same composition of alloying elements, as in base metal, and to apply a standard mode of annealing after surfacing to the entire region of the deposited joint.

The important element of effect on alloy VT22 properties is a heat treatment (HT). Annealing for welded joints of this alloy serves simultaneously as a hardening HT. Depending on the temperature of heating, duration of annealing and cooling rate it is possible to obtain different combinations of strength and ductility. Annealing of alloy VT22 is performed in a two-phase region (750–850 °C) with a subsequent single- or multistep cooling [5]. Such heat treatment leads to maximum heterogeneity of structure with approximately equal amount of  $\alpha$  and  $\beta$  phases.

*Procedure of investigations.* Surfacing on 12 mm thick plates of alloy VT22 was performed by a magnetically-impelled arc. As a filler material, the experimental solid wire VT22 (3 mm diameter) and experimental filler flux-cored wire of PPT-22 (3 mm diameter) were used [6]. Coming from the analysis of literature data, the HT mode was selected, recommended for welded joints: furnace heating up to  $T = 750\text{ }^{\circ}\text{C}$ , 1 h holding, air cooling.

Using microscope Neophot the quality of deposited joints was evaluated after HT on macro- and microsections, on which the deposited metal structure was examined.

*Surfacing with a filler wire VT22.* Results of metallographic examinations of the filler wire VT22 showed that the quality of its surface is poor, there are local defects in the form of cracks, tears and rolling laps on it (Figure 2). These defects occurred in



**Figure 2.** Microdefects of VT22 wire surface ( $\times 200$ )

the process of wire manufacture and can be a source of the deposited metal contamination and, as a consequence, of reducing its quality.

In the metal, deposited by wire VT22, as well as in the fusion zone a large amount of different kinds of macro- (Figure 3) and microdefects (Figure 4) are observed. Mainly, these are discontinuities, cracks, lack of fusion, pores of up to 0.3 mm size. The presence of the mentioned defects can be referred to a poor

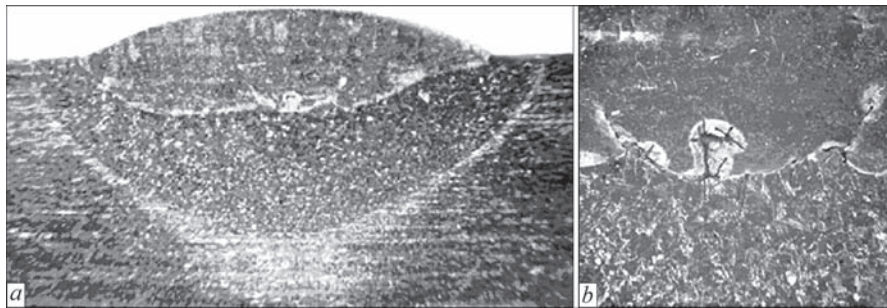


**Figure 3.** Macrosection of joint, deposited by a filler wire VT22 on substrate of VT22 alloy (a) and macrodefects in fusion zone (b)

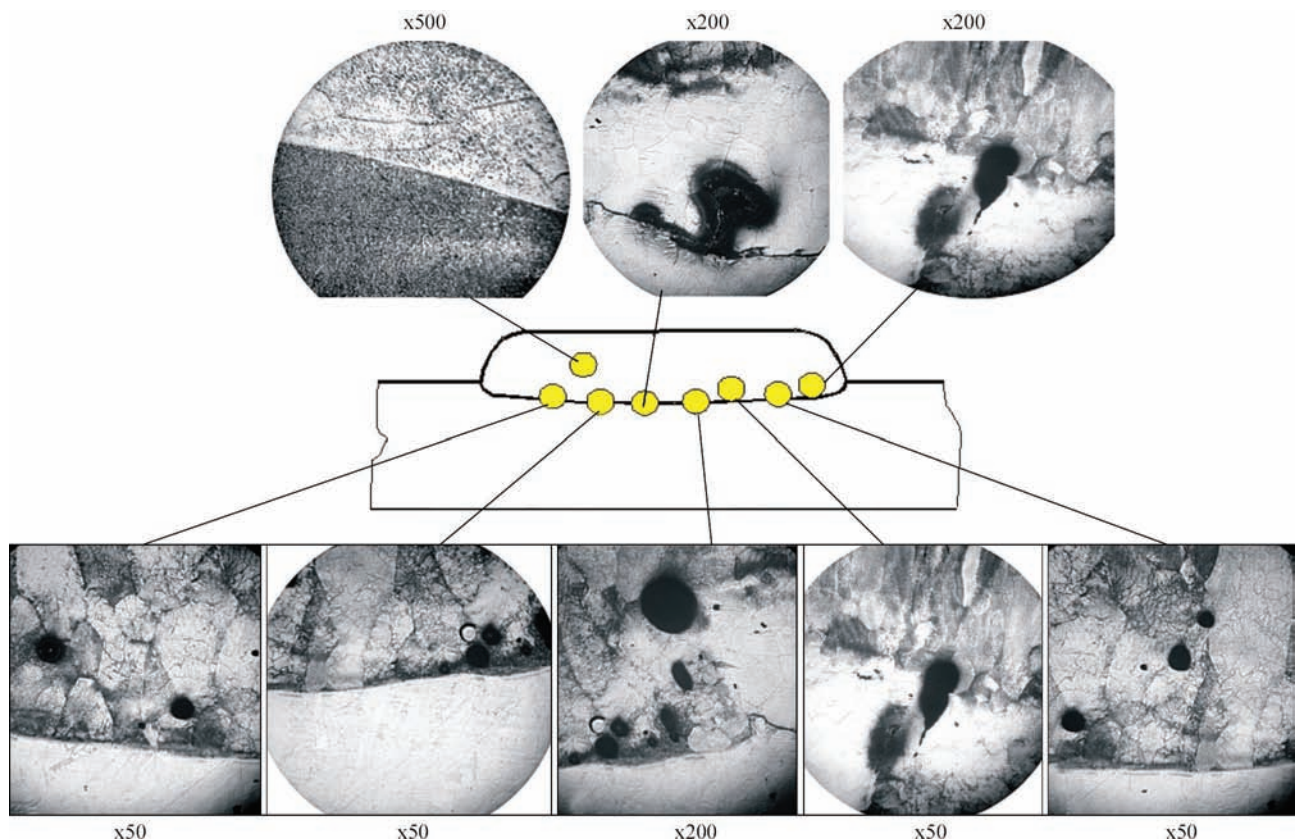


**Figure 4.** Regions of microstructure of deposited metal VT22 near fusion zone

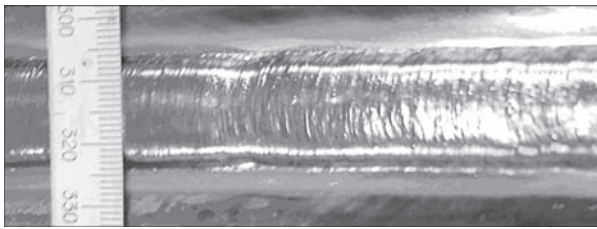


**Figure 5.** Nature of formation of surface of metal, deposited by a flux-cored wire PPT-22 on alloy VT22 plate



**Figure 6.** Macrosection of joint, deposited by a flux-cored wire PPT-22 on VT22 alloy plate in as-surfaced state



**Figure 7.** Radiogram of metal, deposited by a flux-cored wire PPT-22 in as-surfaced state

quality of manufactured filler wire VT22. On the basis of analysis of data, obtained from investigations, the conclusion was made about the non-rationality of application of this wire as a filler material for surfacing.

*Surfacing with a filler flux-cored wire PPT-22.* For making deposits the experimental filler flux-cored wire of PPT-22 grade was used as a filler material. Its design represents a tubular sheath of commercial titanium of VT1-00 grade. Inside the sheath there is a metallic core, consisting of granules of alloy VT22. Appearance of deposited metal is given in Figure 5, macrosection is shown in Figure 6. The made radiographic analysis of deposited specimens showed the absence of pores in them (Figure 7).

Metallographic analysis of the deposited metal did not reveal pores and other defects in it, no microdefects were revealed also in the fusion zone (Figure 8). In the deposited metal a fine-acicular homogeneous structure is formed, the decay of  $\beta$ -phase in grain volume during cooling occurs uniformly (Figure 9).

To stabilize the structure and obtain optimum mechanical properties the joints after surfacing were subjected to HT on the mode: furnace heating at  $T = 750\text{ }^{\circ}\text{C}$ , 1 h holding, air cooling.

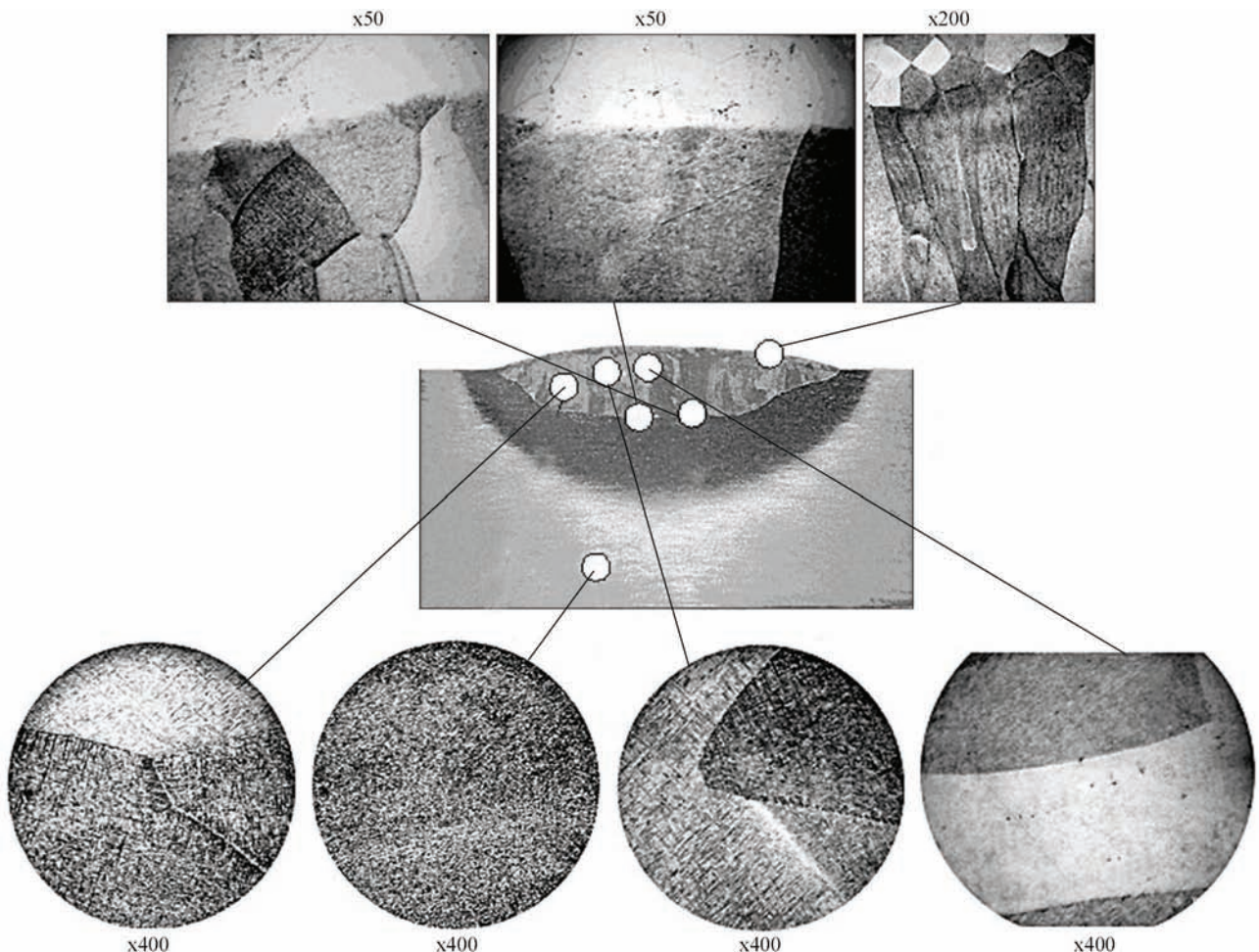


**Figure 8.** Microstructure of regions of joint, deposited by a flux-cored wire PPT-22 on VT22 alloy plate in as-surfaced state

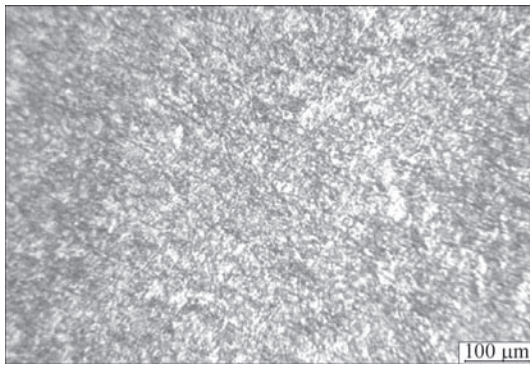


**Figure 9.** Microstructure of metal, deposited by wire PPT-22 in as-surfaced state

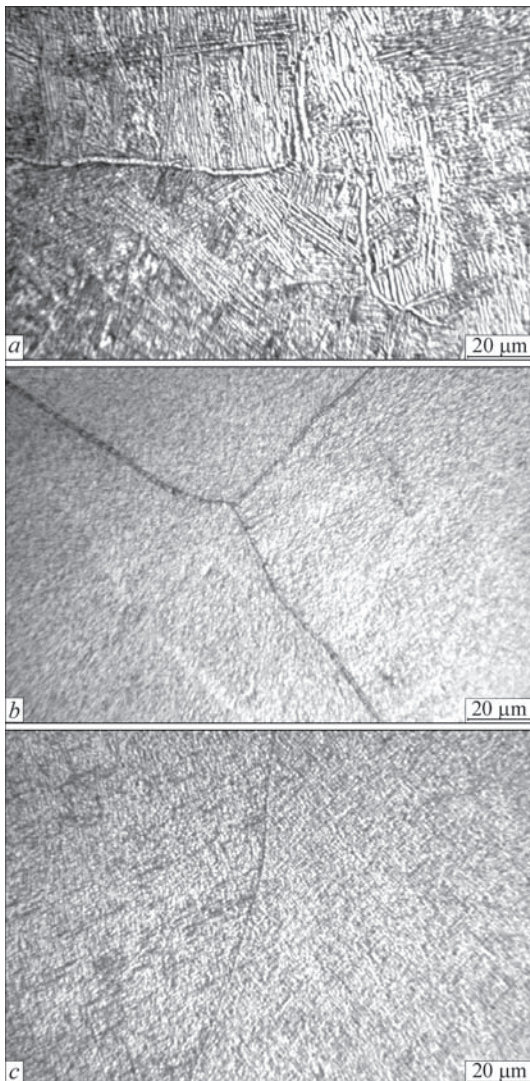


**Figure 10.** Microstructure of metal of joint, deposited by wire PPT-22

The carried out HT caused the change in structure of all the regions of welded joint. In base metal the waviness between  $\alpha$ -plates was observed (Figure 10,

Mechanical properties of deposited and base metal after HT

Metal	$\sigma_r$ , MPa	KCV, J/cm <sup>2</sup>
Deposited metal	1066.0–1133.9	13.4–14.1
	1099.9	13.7
Base metal	930.2–991.5	32.6–35.4
	960.85	34.0

*Note.* Results of 5 tests are given.

a). In the heat-affected zone a sufficiently uniform decay of metastable  $\beta$ -phase with precipitation of dispersed particles of martensitic  $\alpha'/\alpha''$ -phase was occurred. Single fine recrystallized grains, partial recrystallization of  $\beta$ -grain were noted, a subgrain structure was retained (Figure 10, b). Annealing contributed to the formation of more homogeneous and uniform structure of metal in height of deposit (Figure 10, c), than that in a non-annealed specimen.

Analysis of results of mechanical tests (Table) showed that the strength of metal, deposited by the titanium filler flux-cored wire of PPT-22 grade, exceeds negligibly the strength of the base metal, which can exert a positive effect of wear resistance of deposited metal at the tribological tests.

The results of investigations showed that the combined application of filler flux-cored wire of PPT-22 grade and magnetically-impelled arc in argon arc surfacing allow controlling the shape (width and height) of deposit and producing the deposited metal with properties at the level of the base metal after the standard HT. The obtained data allow wire PPT-22 to be recommended for use as a filler material for the restoration surfacing.

- (1984) *Technological recommendations on repair of gas-turbine engine blades and aircraft wing mechanization rails*: Report, 40–56. Kiev: KIIGA.
- Paton, B.E., Zamkov, V.N., Prilutsky, V.P. (1996) Narrow-groove welding proves its worth on thick titanium. *Welding J.*, **5**.
- Gurevich, S.M., Kulikov, F.R., Zamkov, V.N. et al. (1975) *Welding of high-strength titanium alloys*. Moscow: Mashinostroenie.
- Gurevich, S.M., Zamkov, V.N., Kushnirenko, N.A. et al. (1980) Investigation of filler material for welding of ( $\alpha + \beta$ )-titanium alloys. In: *Actual problems of welding of non-ferrous metals*. Kiev: Naukova Dumka.
- Anisimova, L.I., Popov, A.A., Melnikova, V.I. et al. (1977) Influence of heat treatment on structure and properties of titanium alloy VT22. *Fizika Metallov i Metallovedenie*, **44**, Issue 4, 843–845.
- Prilutsky, V.P., Shvab, S.L., Petrichenko, I.K. et al. (2016) Argon-arc welding of titanium VT22 alloy using filler flux-cored wire. *The Paton Welding J.*, **9**, 9–13.

Received 12.12.2016

## EFFECT OF FLUX-CORED STRIP SURFACING MODES ON GEOMETRIC PARAMETERS OF DEPOSITED BEADS

A.P. ZHUDRA, A.P. VORONCHUK, V.O. KOCHURA and V.V. FEDOSENKO

E.O. Paton Electric Welding Institute, NASU

11 Kazimir Malevich Str., 03680, Kiev, Ukraine. E-mail: office@paton.kiev.ua

The effect of parameters of flux-cored strip surfacing modes on geometric dimensions of deposited beads was investigated. The peculiarities of flux-cored strips melting were considered depending on a sheath type and chemical composition of the core. As the objects of investigations the widely applied flux-cored strips PL-AN 101 and PL-AN 179 were selected, which are manufactured on a base of the steel strip-sheath and also the strip PL-AN 111 based on a nickel sheath. The surfacing was carried out in the machine A-874N, equipped with the power source VDU 1201 and the attachment AD 167 within a wide range of modes. It was found that with increase in current from 600 to 1200 A for all the tested grades of flux-cored strips, the growth of a bead width, its height and penetration depth of base metal are characteristic. With increase in current the value of weld shape factor for all the considered types of flux-cored strips decreases. With increase in the arc voltage in the range of 24–38 V the bead width increases and the height is reduced against the growth in volume of base metal. The change in penetration depth and the weld shape factor are ambiguous and depend on the flux-cored strip type. 10 Ref., 1 Table, 4 Figures.

**Keywords:** *flux-cored strip, surfacing modes, penetration depth, geometric parameters of bead, volume of base metal*

At the present time the flux-cored strips are widely applied for strengthening the parts of equipment operating under the conditions of abrasive, gas-abrasive and other types of wear. The application of this electrode material allows producing the deposited metal with a high degree of alloying and carrying out the surfacing process with a high efficiency [1–3].

The important factors influencing the obtaining of the preset chemical composition and hardness of the deposited layer are geometric parameters of bead of deposited metal. In a number of works [4–6] the influence of mode parameters on characteristics of beads being deposited using the cold-rolled electrode strips of different width and chemical composition is considered. It is seen from the carried out investigations that except of current, voltage and surfacing speed, the geometric dimensions of beads are also affected by thickness, width of electrode strip, its chemical composition and the grade of flux being used.

In the works [7, 8] the influence of current and voltage on the geometry of deposited bead during surfacing using flux-cored strip of 45×3 mm section on the currents of 1000–1900 A was investigated. In the works [8, 9] the volume of the electrode metal in surfacing using two-locked flux-cored strip on the currents of 700–1100 A was determined. It was experimentally established that with increase in current in the mentioned range the volume of electrode metal decreases from 0.64 to 0.62 at the speed of 16 m/h and with increase in the speed from 16 to 32 m/h it decreases from 0.63 to 0.57.

Recently, for surfacing of different parts the one-locked flux-cored strip with a tight lock, developed at the E.O. Paton Electric Welding Institute, becomes ever more applied. To develop technological processes of surfacing using this electrode material it became necessary to conduct complex investigations on influence of surfacing mode on geometric parameters of deposited beads, as well as characteristics of melting of flux-cored strips.

For investigations three grades of flux-cored strips PL-Np-300Kh25S3N2G2 (PL-AN 101), PL-Np-500Kh40N-40S2RTs (PL-AN 111) and PL-Np-400Kh20B7M6N-5V2F (PL-AN 179) with the section of 16.5×3.8 mm of one-locked design of the type B were selected according to GOST 26467–85. Such a choice was predetermined by the following considerations: the flux-cored strips PL-AN-101 and PL-AN 111 are the serially manufactured electrode materials. The flux-cored strips PL-AN 101 and PL-AN 179 are manufactured on the base of a steel strip-sheath and PL-AN 111 is manufactured on the nickel one. Furthermore, the core of the flux-cored strip PL-AN 101 is composed mainly of a complex master alloy which stipulates its lower melting temperature. The tests were carried out in the surfacing machine A-874N, equipped with the power source VDU-1201 and the attachment AD-167. The surfacing was carried out by separate beads in one layer at direct current of reverse polarity at a constant value of stickout equal to 50 mm and a rigid external characteristic of the power source. As the base metal the plates of St3 of 30 mm thickness and 300×400 mm size were used. On each of the plates the 6 beads of 200–250 mm length were deposited. To eliminate the influence of preheating, each

successive bead was applied after complete cooling of the previous one. From the middle areas of beads the specimens were cut out applying an anode-mechanical cutting, on which after the subsequent grinding the geometric parameters of deposited beads, the composition and hardness of the deposited metal were determined. In parallel with the surfacing the measurements were also carried out to determine the melting characteristics of the mentioned flux-cored strips. The surfacing modes using all the mentioned strips are given in Table.

For investigations the following geometric parameters of deposited beads were determined (see Figure 1):  $B$  — the width of deposited bead;  $h$  — the penetration depth of base metal;  $C$  — the height of deposited bead, as well as the area of deposited bead over the base metal and the area of penetration base metal were determined.

By calculations according to the formulas the volume of base metal  $\gamma$  and the shape factor of bead  $\varphi$  were determined:

$$\gamma = \frac{F_p}{F_b + F_p},$$

where  $F_p$  is the area of penetration of base metal;  $F_b$  is the area of deposited bead over the base metal

$$\varphi = \frac{B}{h},$$

where  $B$  is the width of deposited bead;  $h$  is the penetration depth of base metal.

The obtained results are presented in a graphic form. Moreover, it should be indicated out that to each point on the diagram the mean value of not less than five measurements and calculations produced on them is corresponded.

Figure 2 shows the change in geometric parameters of deposited bead depending on current. As the current increases from 600 to 1200 A for all the tested grades of flux-cored strips the growth of bead width (Figure 2, *a*), height (Figure 2, *b*) and penetration depth of base metal (Figure 2, *c*) is characteristic. Regarding the flux-cored strip PL-AN 101, the growth in width and height of the bead is observed at the currents of up to 900 A. The further increase in current does not result in the change of these parameters but the area of the deposited bead is increased. In our opinion, this is explained by a great fluidity of molten metal of weld pool, which in its turn is associated with the type of alloy being deposited and the use of the complexly-alloyed master alloy as a powder-filler. The values of weld shape factor for all the considered flux-cored strips are reduced with increase in current (Figure 2, *d*).

In the current range from 600 to 800 A for the strips PL-AN 101 and PL-AN 179 a sharp increase in volume of base metal from 0.45 to 0.5–0.53 is observed, and for the flux-cored strip PL-AN 111 in the same range a sharp decrease from 0.6 to 0.55 is observed. The volume of base metal for all the three flux-cored

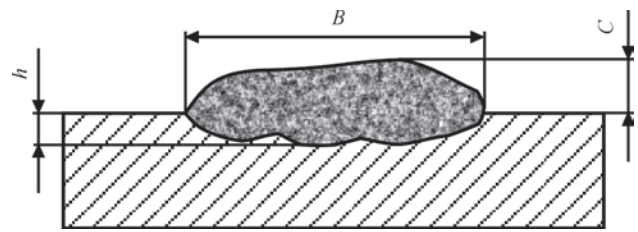
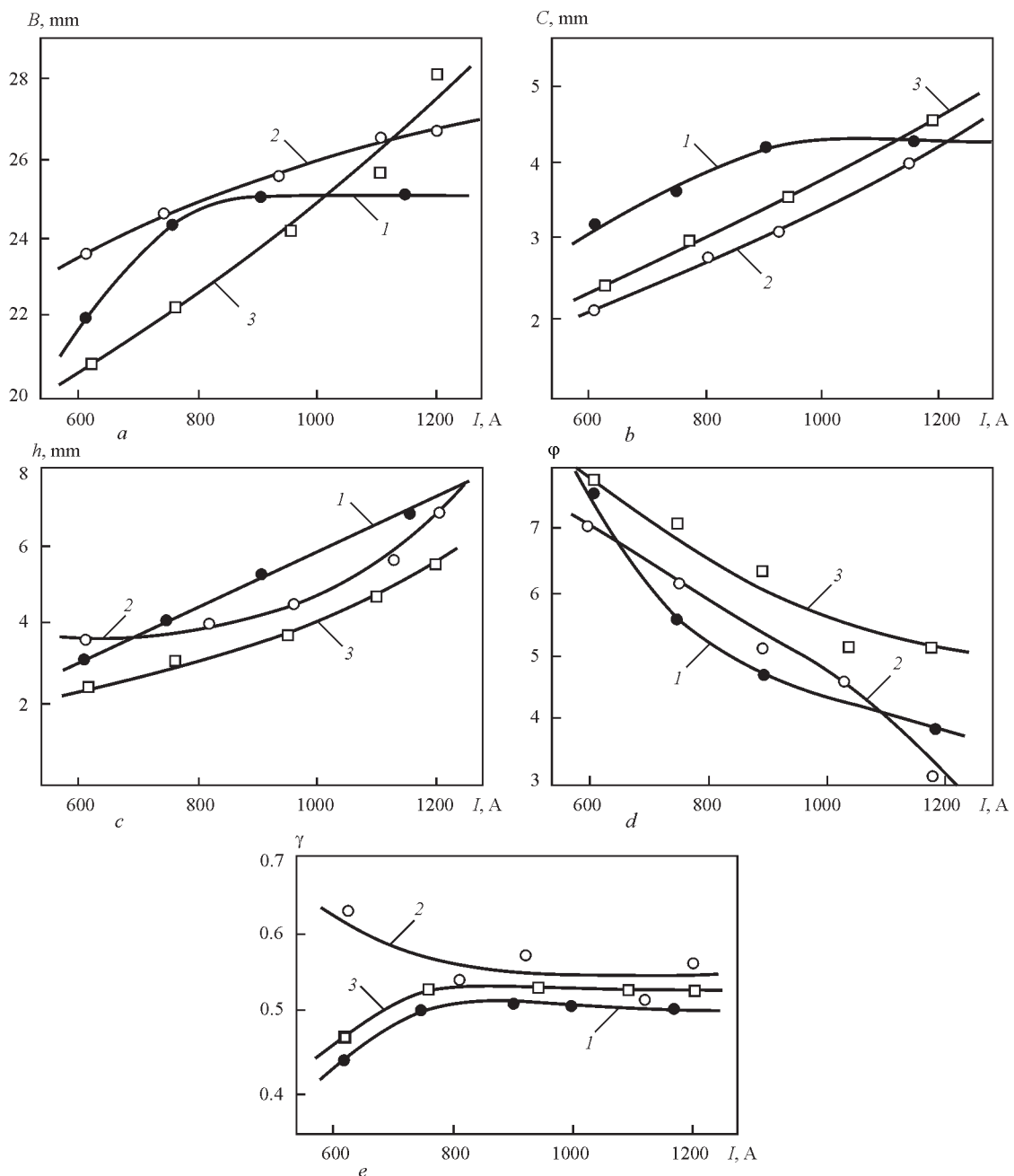


Figure 1. Cross-section of bead deposited using flux-cored strip strips with further increase in current in the range of 800–1200 A remains almost constant, equal to 0.5–55 (Figure 2, *e*). Such ambiguous behavior of this parameter for different flux-cored strips, in our opinion, can be explained by differences in the nature of their melting caused in the first turn, by the strip-sheath material. So, the flux-cored strip PL-AN 111 is manufactured using nickel strip-sheath having a high specific resistance, which contributes to a more significant preheating of flux-cored strip at the stickout. At the lower values of current, consequently at a lower feed speed of the electrode material, in the total heat balance the increasingly important role belongs to heat evolution at the electrode stickout consumed for its preheating [10]. In melting of flux-cored strips PL-AN 101 and PL-AN 179 with a steel strip-sheath, having a lower ohmic resistance, the melting of the electrode metal is carried out mainly due to heat power of the arc. After reaching the certain values of current, which is 800 A in the considered case, the character of change in deposited beads parameters for different flux-cored strips becomes almost the same. At the same time for the tested electrode materials the heat balance of the arc becomes constant, consumed for melting of electrode and the base metal. We believe that a more precise explanation of the nature of change in volume of base metal can be obtained after additional investigations of changes in flux-cored strip resistance depending on temperature and other parameters influencing the nature of melting electrode materials.

Figure 3 presents the geometric parameters of deposited beads depending on arc voltage. With increase in voltage in the range of 24–38 V the bead

#### Surfacing modes

Current, A	Voltage, V	Surfacing speed, m/h
600 ± 25	32 ± 1	32 ± 1
750 ± 25	32 ± 1	32 ± 1
900 ± 25	32 ± 1	32 ± 1
1150 ± 25	32 ± 1	32 ± 1
1200 ± 25	32 ± 1	32 ± 1
900 ± 25	24 ± 1	32 ± 1
900 ± 25	28 ± 1	32 ± 1
900 ± 25	36 ± 1	32 ± 1
900 ± 25	40 ± 1	32 ± 1
900 ± 25	32 ± 1	19 ± 1
900 ± 25	32 ± 1	40 ± 1
900 ± 25	32 ± 1	48 ± 1
900 ± 25	32 ± 1	55 ± 1



**Figure 2.** Change in geometric parameters of deposited bead: width (a), height (b), penetration depth of base metal (c), weld shape factor (d), volume of base metal (e) depending on current in surfacing using flux-cored strips: 1 — PL-AN 101; 2 — PL-AN 111; 3 — PL-AN 179

width increases from 21–22 to 29–31 mm depending on grades of flux-cored strips (Figure 3, a).

The height of the bead (Figure 3, b) for all the strips decreases and the volume of base metal (Figure 3, c) is growing from 0.45–0.5 to 0.6. Regarding the penetration depth (Figure 3, d) and the weld shape factor (Figure 3, e), their change is ambiguous and depends on the tested grade of a flux-cored strip. Thus, the penetration depth in using the strip PL-AN 111 is increased in proportion to the voltage in the whole range. Whereas in surfacing applying the strips PL-AN 101 and PL-AN 179 at voltage increase from 24 to 32 V the growth of penetration depth of base metal and the reduction of this value in the range of 32–38 V

occurs. Moreover, it is expressed particularly strongly for the flux-cored strip PL-AN 101.

In our opinion, this is connected both with the nature of melting the electrode material with different strip-sheaths as well as with different properties of liquid molten metal.

The lowest value of weld shape factor corresponds to the voltage of 28 V for all the tested grades of flux-cored strips (Figure 3, e).

In the range of minimum and maximum values of arc voltage the weld shape factors are increased. The influence of surfacing speed on geometric parameters of deposited bead is presented in Figure 4. With increase in the surfacing speed from 19 to 55 m/h

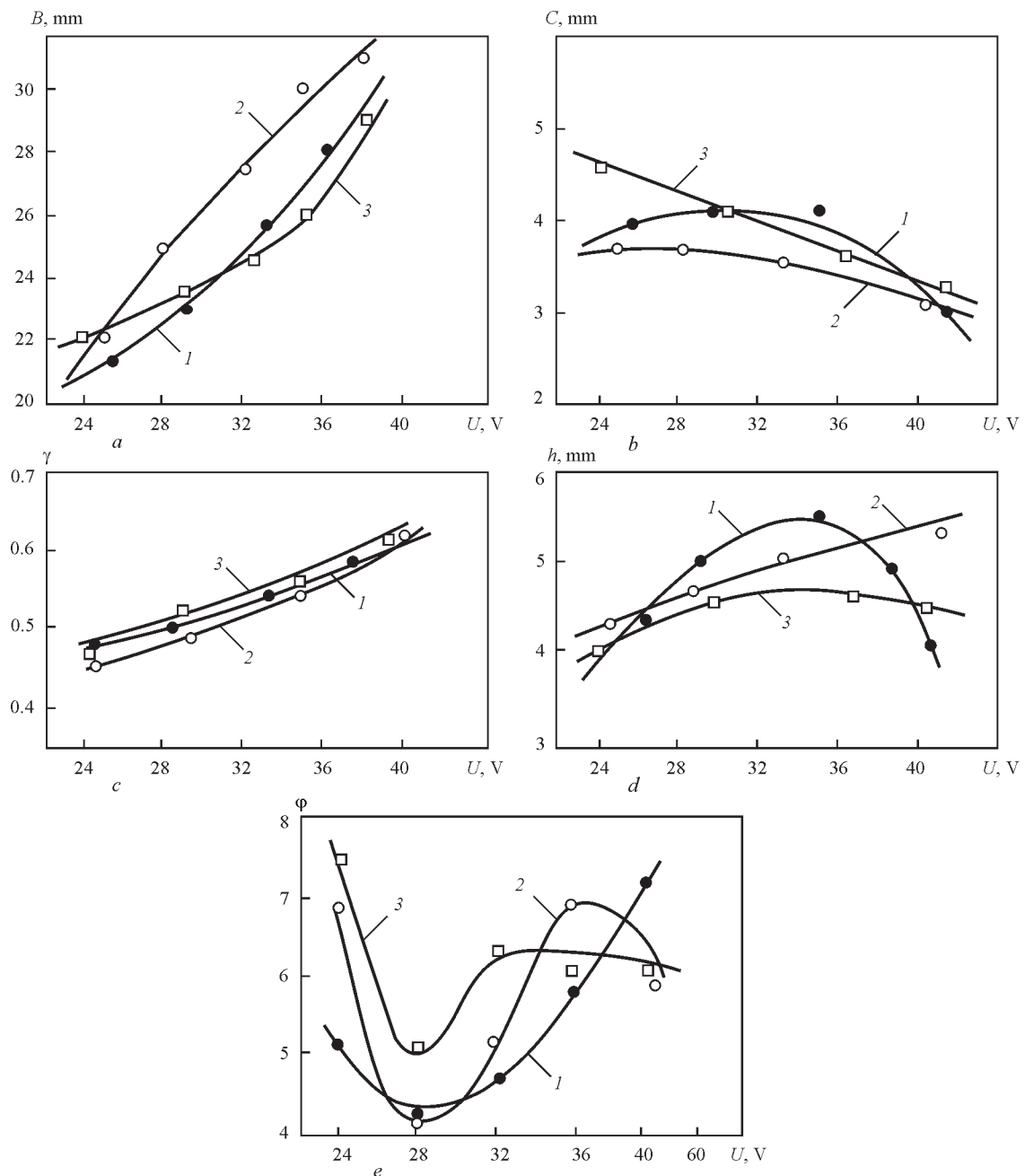


**Figure 3.** Change in geometric parameters of deposited bead: width (a), height (b), volume of base metal (c), penetration depth of base metal (d), weld shape factor (e) depending on voltage in surfacing using flux-cored strips: 1 — PL-AN 101; 2 — PL-AN 111; 3 — PL-AN 179

the bead width is reduced from 30–32 to 20.5 mm (Figure 4, a), the height — from 4–5 to 2–3.5 mm (Figure 4, b), the penetration depth — from 5.5–6.5 to 3–4.5 mm (Figure 4, c). At the same time the volume of base metal increases with increase in the speed from 19 to 20 m/h (Figure 4, d). The further increase in the surfacing speed does not influence the volume of base metal. The weld shape factor has the lowest values at 40 m/h speed for flux-cored strips PL-AN 101 and PL-AN 111. The lowest value of weld shape for flux-cored strip PL-AN 179 is observed at the surfacing speed of 19 m/h (Figure 4, e).

Considering the obtained results in general, the following should be noted. The geometric param-

eters of deposited beads, characteristics of melting the flux-cored strips, and consequently, the composition and hardness of the deposited metal, except surfacing modes, are significantly influenced by the composition of the powder-filler and strip-sheath material. Thus, in surfacing using flux-cored strip PL-AN 111, manufactured on the base of a nickel strip-sheath, all the investigated characteristics are rather different from the data obtained in surfacing using flux-cored strips PL-AN 101 and PL-AN 179, manufactured of a steel strip-sheath. This, obviously, can be explained by a higher ohmic resistance of a nickel strip-sheath. At the same time, due to a larger voltage drop at the electrode stickout the more intensive heating of the

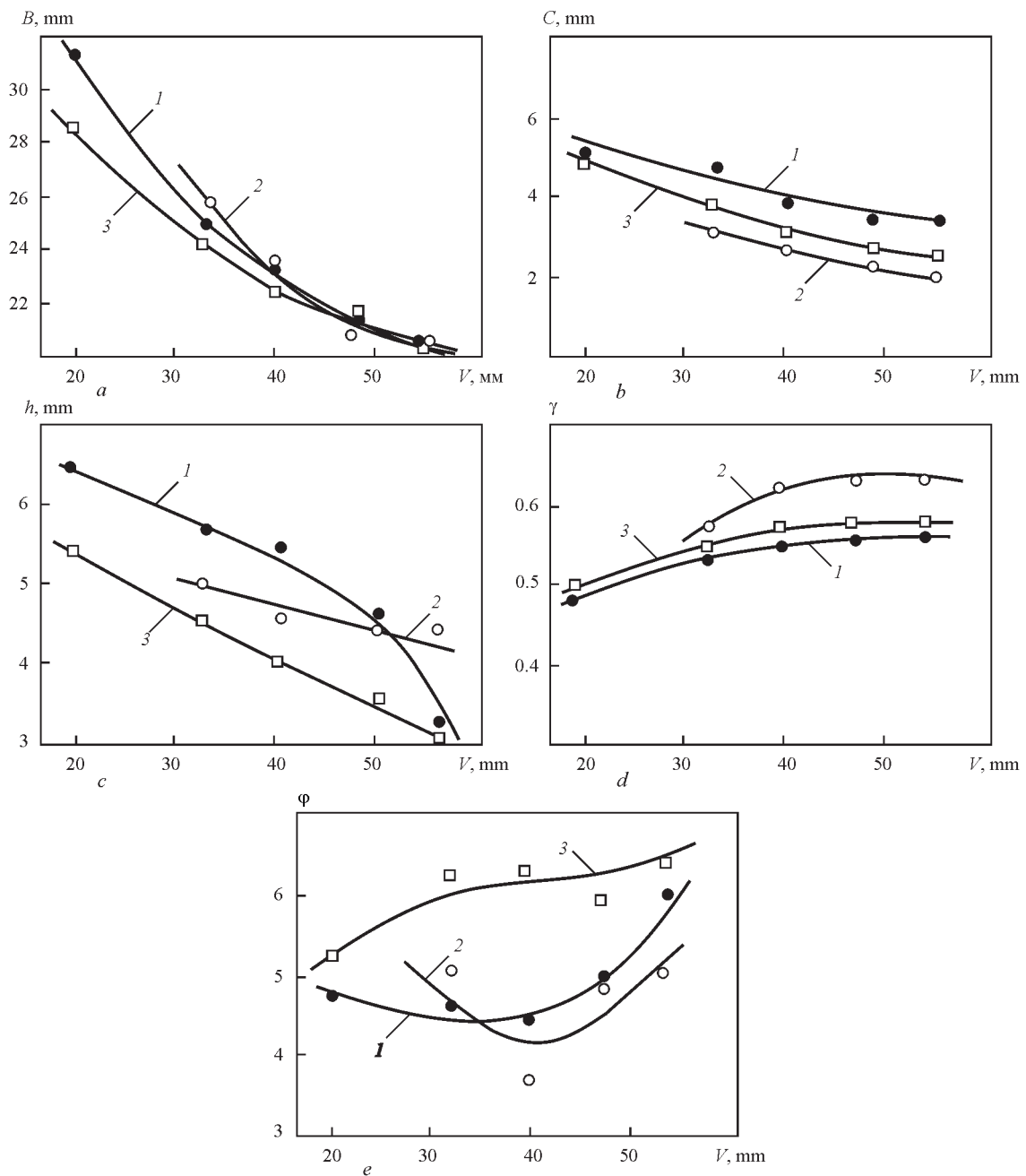


**Figure 4.** Change in geometric parameters of deposited bead: width (a), height (b), penetration depth (c), volume of base metal (d), weld shape factor (e), depending on change of speed in surfacing using flux-cored strips: 1 — PL-AN 101; 2 — PL-AN 111; 3 — PL-AN 179

flux-cored strip occurs at the stickout, which in its turn increases the efficiency of its melting by arc, i.e. leads to a more efficient use of the arc heat power.

1. Danilchenko, B.V., Shimanovsky, V.P., Voronchuk, A.P. et al. (1989) Surfacing of wearing parts with self-shielded flux-cored strips. *Avtomatich. Svarka*, **5**, 38–41.
2. Zhudra, A.P., Voronchuk, A.P. (2010) Wear-resistant flux-cored strip surfacing. *Svarshchik*, **6**, 6–9.
3. Zhudra A.P., Voronchuk, A.P. (2012) Cladding flux-cored strips (Review). *The Paton Welding J.*, **1**, 39–44.
4. Belov, Yu.M. (1961) Influence of mode of automatic submerged arc surfacing with strip electrode on bead section. *Svarochn. Proizvodstvo*, **12**, 6–8.
5. Kravtsov, T.T. (1978) *Electric arc strip electrode surfacing*. Moscow: Mashinostroenie.

6. Kazartsev, V.I., Kryazhov, V.M., Baranov, Yu.M. (1968) Penetration of base metal in electrode strip surfacing. *Avtomatich. Svarka*, **3**, 53–55.
7. Nikolaenko, M.R., Kuznetsov, L.D., Kortelev, G.A. (1976) Transfer of electrode metal and homogeneity of properties of deposited layer in flux-cored strip electrode surfacing on forced modes. *Svarochn. Proizvodstvo*, **6**, 33–34.
8. Kuznetsov, L.D., Nikolaenko, M.R., Grinberg, N.A. (1980) Geometrical characteristics of bead in flux-cored strip submerged arc surfacing on forced modes. *Avtomatich. Svarka*, **9**, 58–59.
9. Belousov, E.F., Zelenkin, Yu.A., Rykov, A.M. (1973) Automatic flux-cored strip surfacing of sealing surfaces of stop valves. *Svarochn. Proizvodstvo*, **3**, 46–47.
10. Paton, B.E. (1949) Process of electrode melting in automatic submerged arc welding. *Trudy po Avtomat. Svarke pod Flyusom*, **4**, 22–38.

Received 02.12.2016

# NUCLEAR MAGNETIC SPECTROSCOPY STUDY OF THE STRUCTURE OF LIQUID GLASSES FOR WELDING ELECTRODES

A.E. MARCHENKO<sup>1</sup>, N.V. SKORINA<sup>1</sup>, M.O. KISELEV<sup>1</sup> and V.V. TRACHEVSKY<sup>2</sup>

<sup>1</sup>E.O. Paton Electric Welding Institute, NASU

11 Kazimir Malevich Str., 03680, Kiev, Ukraine. E-mail: office@paton.kiev.ua

<sup>2</sup>Technical Center of NASU

13 Pokrovskaya Str., 04070, Kiev, Ukraine. E-mail: trachev@imp.kiev.ua

Nuclear magnetic spectroscopy was used to study the structure of silicon-oxygen anions (SOA) in the composition of monobasic (Li, Na, K) and binary (LiNa, LiK, and NaK) liquid glasses. It is found that combinations of different forms of connection reflect the structure of silicon-oxygen anions present in the solution, which determines the change of liquid glass viscosity, depending on their chemical composition. Structure of SOA of monobasic liquid glasses is determined by the kind of modifier ion. The larger its size, the weaker is its destructive action on SOA, with preservation of a larger number of bridge bonds, ensuring a higher level of liquid glass viscosity. Binary mixtures of liquid glasses at certain ratios of alkali oxide fractions, demonstrate synergism of viscosity. The fraction of bridge bonds is higher in such glasses. Synergic increase of viscosity is more pronounced in LiK glasses than in LiNa and NaK analogs, although viscosity of monobasic glasses, from which the mixtures were prepared, was the same. 11 Ref., 3 Tables, 3 Figures.

**Keywords:** arc welding, welding electrodes, manufacturing technology, liquid glass, liquid glass structure, application of NMR spectroscopy technique

Modern production of welded structures makes increasing requirements to metallurgical, technological, sanitary-hygienic, and service characteristics and quality of coated electrode manufacturing. Many of them are directly connected to the kind and chemical composition of liquid glasses, used as electrode coating binder. Solution of such a multivector problem usually is a compromise. For this reason, binary, for instance, NaK liquid glasses, began to be applied in electrode production. These glasses favourably combine useful characteristics of their components. However, other properties of the combined binder, important for the characteristics of coatings and welding electrodes, often deteriorate. For instance, lowering of water-holding capacity of the binder, electrode coating hygroscopicity and hydrogen content in the deposited metal, is accompanied by lowering of coating strength, and deterioration of sanitary-hygienic characteristics of electrodes. Although combined liquid glasses have been used in local and foreign electrode production for a long time, the cause of the above peculiarities has not been established. Electrode developers are acutely aware of the lack of information about liquid glass structure and properties that would help them solve these problems.

In many silicate technologies the structure of glasses in general and of liquid glasses, in particular, is studied, using a combination of such spectroscopy

methods, as infrared (IR), combined light scattering (CLS), X-ray diffraction (XRD), X-ray emission (XES), Laser Raman, extended X-ray-absorption fine structure (EXAFS), and X-ray photoelectron spectroscopy (XPS) [1].

Over the last decades these have been effectively complemented by nuclear magnetic spectroscopy (NMRS) [2-6], which considers liquid glass structure in terms of the ratio of the fractions of bridge and non-bridge oxygen in the composition of silicon-oxygen anions (SOA).

The cited published sources do not provide replies to the questions we are interested in. Many of the investigation techniques used in them are not available to us.

We applied NMR<sup>29</sup>Si technique to study the structure of monobasic (Li, Na, K) and binary (LiNa, LiK, and NaK) liquid glasses, used in welding electrode production.

This technique is based on the phenomenon of resonance absorption of electromagnetic waves by atomic nuclei of the tested substance placed into an external magnetic field [7]. In the case of hydrogen atom nucleus the principle of NMRS looks as follows. The proton has its own spin and magnetic moment. Spatial orientation of proton magnetic vector spin can either coincide with the direction of intensity vector of constant magnetic field, around which  $\mu$  will precess, or it can be opposite to it.

**Table 1.** Kinds of connection combined in liquid glass SOA structure

$Q^4$	$Q^3$	$Q^2$	$Q^1$	$Q^0$
(O) Si	(O) Si	O <sup>-</sup>	O <sup>-</sup>	O <sup>-</sup>
Si(O)-Si-(O)Si	Si(O)-Si-O <sup>-</sup>	Si(O)-Si-O <sup>-</sup>	Si(O)-Si-O <sup>-</sup>	O-Si-O <sup>-</sup>
(O)Si	(O)Si	(O)Si	O <sup>-</sup>	O <sup>-</sup>

Proton field energy  $E$  is greater in the first of the mentioned states than in the second one. If energy is added to the proton, which happened to be in these states by its irradiation by variable electromagnetic field quanta of corresponding frequency, the proton will go into a state with greater energy during pulse action time of 2  $\mu$ s, while its spin will be directed normal to constant field vector.

In a sample with a large number of mobile protons, an averaged pattern is observed, reflecting the behaviour of an ensemble of resonating nuclei.

In practice, fixed magnetic field intensity is usually used, and the range of frequencies of irradiating pack is varied. Then, the resonance occurs at their certain ratio, which is registered in NMR time scale at detection of the features of energy absorption and subsequent relaxation at interaction with the environment.

When recording the information, extracted by NMR technique, it should be taken into account that:

- signals of atoms, included into the composition of certain functional groups, are observed in strictly defined spectral regions;
- integral intensities of peaks are proportional to the quantity of resonating atoms of different nature;
- nuclei spaced at 1–4 bonds from each other, are capable of causing multiplicity of analytical signals as a result of superfine interactions.

Signal position in NMRS spectra is characterized by the value of their chemical shift relative to the reference signal, coupled with NMR electronic shielding. The unit of chemical shift is part per million (ppm) of instrument frequency. If the substance spectrum is too complicated, it is interpreted using quantum-chemical modeling of electron density distribution between characteristic fragments of the selected coherent structure.

Oxygen atoms in tetrahedrons, differing by atomic ratios  $Si:(O)_{4-x}:(OSi)_x$ , are the main structural motif of silicon-oxygen anions (SOA) in liquid glasses and are fragments with bridge Si–O–Si ( $O_b$ ) or non-bridge Si–O ( $O_n$ ) bonds. In the latter of the mentioned forms of the bond, oxygen modifications are terminal ones and are coordinated by modifier cations (Li, Na, K, Ca). Depending on  $O_n/O_b$  ratio, 5 types of  $SiO_4$  tetrahedrons are distinguished, which are designated by  $Q^n$  symbol, where  $n$  is the degree of connection, i.e. number of bridge atoms of oxygen per one atom of silicon in SOA. Depending on cation type (Li, Na, K or their binary combinations), modulus and concentration of dissolved silicate,  $n$  index can vary from 0 up to 4. The higher the value of this index, the greater is the number of bridge (bound) atoms of oxygen  $O_b$  in SOA structure (Table 1).

**Investigation procedures, substance compositions and properties of liquid glasses.** Values of chemical shift are determined at room temperature in NMR-spectrometer of AVANSE 400 model, BRUKER, Germany. Intensity of signals of structural groups  $Q^n$  in NMR<sup>29</sup>Si of primary analytical spectra was the source of information about the structure of liquid glasses SOA. Absorption due to material, surrounding the measurement zone, was taken into account in idle measurements. Interpretation of NMR-<sup>29</sup>Si spectra by the degree of connection  $Q^n$ , recorded from liquid glass samples, was conducted after preliminary isolation of the above background from the spectrum.

Chemical composition, data on density and viscosity of monobasic liquid glasses are given in Table 2. Table 3 gives a comparison of connection indices, found at testing monobasic liquid glasses and binary mixture samples made from them. In Figure 1 such a

**Table 2.** Chemical composition, density and viscosity of monobasic liquid glasses

Glass kind	Modulus	Weight fraction, %				Glass properties	
		SiO <sub>2</sub>	Li <sub>2</sub> O	Na <sub>2</sub> O	K <sub>2</sub> O	$\rho$ , kg·m <sup>-3</sup>	$\eta$ , mPa·s
Li	2.77	25.52	4.60	–	–	1313	325
Na	3.09	28.54	–	8.40	1.70	1433	325
K	3.67	26.37	–	1.66	8.93	1422	360

**Table 3.** Chemical composition, density and viscosity of combined liquid glasses

Number	Second component fraction, wt. %	Fraction of connections, %			Viscosity, $\eta$ , mPa·s
		$Q^3$	$Q^4$	$\Sigma Q^3 + Q^4$	
LiNa liquid glasses					
1	0	38.3	26.5	64.8	325
2	16.3	43.5	23.4	66.9	770
3	33.3	43.4	22.7	66.1	795
4	50.0	36.9	30.8	67.7	815
5	66.7	41.1	21.0	62.1	620
6	83.7	37.8	18.4	56.2	435
7	100	38.1	16.0	54.1	325
LiK liquid glasses					
1	0	38.5	26.5	65.0	325
2	16.3	37.8	25.0	62.8	1750
3	33.3	33.0	36.9	69.9	2115
4	50.0	38.4	26.9	65.3	6140
5	66.7	40.0	26.4	66.4	20800
6	83.7	40.5	27.4	67.9	1300
7	100	41.3	14.0	55.3	360
NaK liquid glasses					
1	0	38.6	15.4	54.0	325
2	16.3	43.5	10.3	53.8	395
3	33.3	44.5	11.4	55.9	595
4	50.0	45.3	12.6	57.9	545
5	66.7	47.0	8.0	55.0	445
6	83.7	47.3	8.8	56.1	440
7	100	42.0	12.8	54.8	360

comparison is given in the graphic form (glass numbers are the same as in Table 3).

As follows from the above data, viscosity of a number of initial monobasic liquid glasses was approximately the same (320–360 MPa·s). Binary mixtures of these glasses demonstrate synergism of viscosity: after mixing, mixture viscosity rises, compared to anticipated additive value. The greater the difference of dimensions of modifier ions in initial glasses, the more clearly is the synergism of their viscosity manifested.

The given data allow making the following generalizations.

SOA structure of monobasic liquid glasses is determined by the kind of modifier ion. The greater its size, the smaller its destructive action on SOA structure: a greater number of bridge bonds is preserved  $Q^4$ .

In liquid glass mixtures, where the greatest synergic increase of viscosity was manifested, the fraction of bridge bonds rises, compared to the fraction of the respective forms of connection in monobasic glasses. An exception are NaK liquid glasses, where potassium component causes lowering of  $Q^4$  yield, starting from small additions, also in the synergic composition.

Change of connections strictly follows the stoichiometry of equations of exchange reaction for LiNa-4 mixture, and less strictly — for LiK-5:

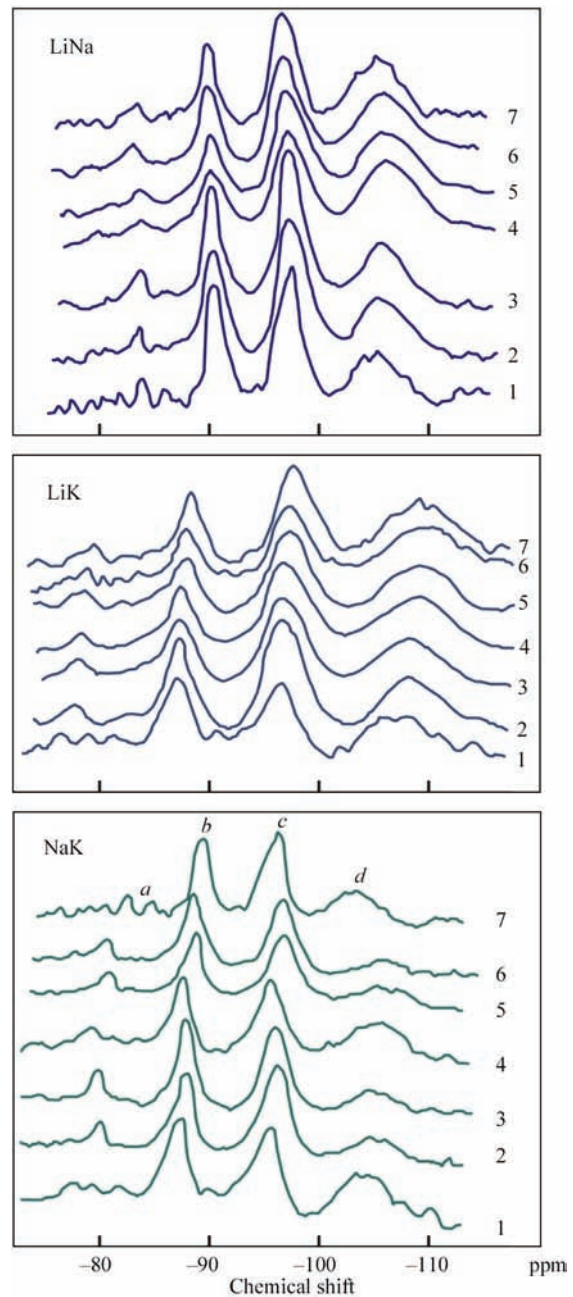


**Figure 1.** Evolution of NMR<sup>29</sup>Si parameters of combined NaK, LiK and LiNa liquid glasses, depending on the ratio of monobasic components in their composition; *a*, *b*, *c*, *d* are the values of integral intensities of signals with values of chemical shift, characteristic for  $Q^1$ ,  $Q^2$ ,  $Q^3$ ,  $Q^4$



The above glasses demonstrate the highest degree of viscosity synergism.

For NaK glasses the synergic effect is manifested to the lowest degree, and form stoichiometry does not obey equation (1). Signals from forms with different connections differ not only in intensity, but also in width, particularly,  $Q^4$ . It is possible that they combine not one, but 2 to 3 kinds of connections. Correct separation of superpositions into individual components requires application of special techniques.

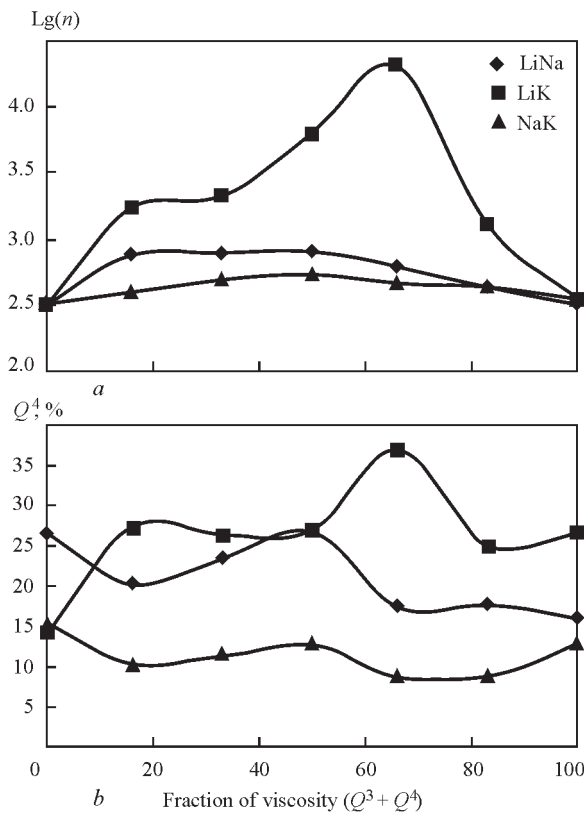


**Figure 2.** Influence of 2<sup>nd</sup> component concentration on viscosity of LiNa, LiK and NaK liquid glass mixture (a), as well as on fraction of  $Q^4$  connections (b) in SOA structure

Qualitative connection between viscosity and fraction of  $Q^4$  forms in the structure of glasses, responsible for the degree of SOA polymerization, is illustrated in Figure 2. A finer correlation between SOA viscosity and structure can be established, if we use not  $Q^4$  yield, but  $(Q^3 + Q^4)$  sum as the structural index. In Figure 3 such a relationship is demonstrated in the graphic form. Natural coordinates were used for LiNa and NaK liquid glasses with a small synergic effect. For LiK liquid glasses, in which the range of viscosities, associated with synergic effect, was expanded by more than 20 times, because of the large difference in the dimensions of cations (and, therefore, SOA), the logarithmic scale of viscosities was applied.

Directly proportional dependence between viscosity of LiNa, NaK glasses and summary fraction of connection forms ( $Q^3 + Q^4$ ) indicates that both the SOA forms contribute to formation of viscosity effect, competing in structure formation. The difference in the ratio of dimensions of K and NA ions, greater than that of Na and Li ions, can account for larger slope inclination in the graph of the first straight line, than in that of the second. For binary LiK glasses with cations, much more different from each other in their dimensions, synergic increase of viscosity is manifested to the greatest extent.

Established regularities allow a more detailed consideration of the mechanism of synergic effect in the

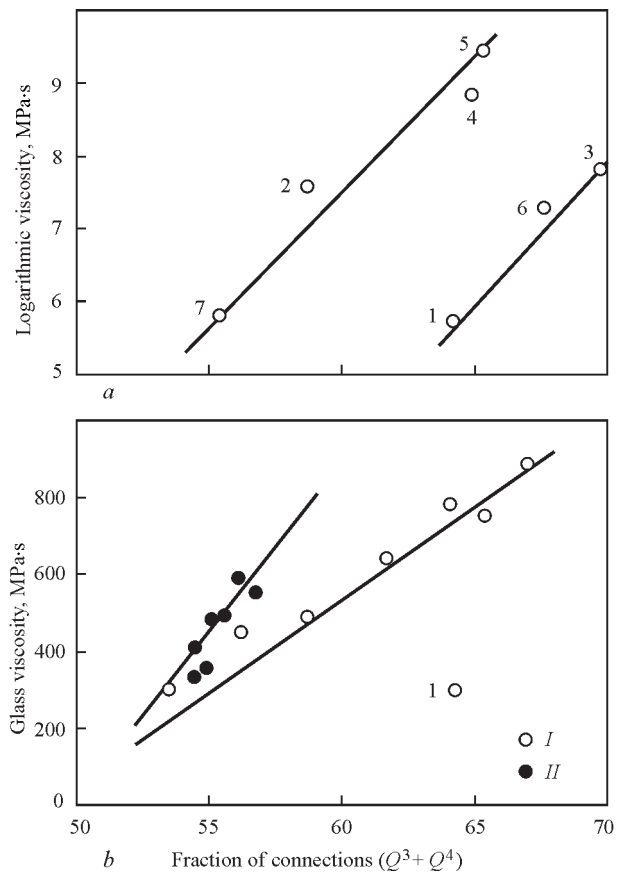


**Figure 3.** Dependence of binary LiK (a), as well as LiNa (b, I) and NaK (b, II) liquid glasses on summary fraction of forms of connection ( $Q^3 + Q^4$ ). Figures near the points designate numbers of liquid glass samples

case of melts ( $K_2O-Li_2O-SiO_2$ ) [8]. Energy stability of  $LiO_2$  is higher than that of  $K_2O$ . Owing to a greater fraction of connection forms  $Q^4$ , the system with lithium oxide is characterized by lower basicity than the system with  $K_2O$ . As a weak base cation  $((LiOH)_y(H_2O)_x)Li^+$  tetramers dominate in concentrated water solutions of  $LiOH$ ,  $Li^+$  tends to coordinate in its environment the silicon-oxygen structural units with  $Q^2$  and  $Q^1$  connections, the yield of which in single-component lithium glasses is insignificant. Lithium cation realizes this ability to a greater extent in liquid glasses with two cations, where it dominates in the competition with K ions.

In its turn,  $K^+$  environment will be made up by silicon-oxygen groups  $Q^3$  and  $Q^4$ . Exchange reaction, allowing for competitive coordination and mutual transformation of  $Q^n$  forms, is as follows:



As a result of exchange of silicon-oxygen groups, the lithium component of the mixture will increase, and the potassium component will lower its modulus. Presence of several SOA modifications, each being in cation affected area, hinders their redistribution at shear, and this leads to the respective increase of viscosity.

A weaker manifestation of synergism of viscosity in experiments with LiNa and NaK liquid glasses, is attributable to smaller difference in the dimensions and acid-base characteristics of the compared alkali cations. At higher initial viscosity of monobasic liquid glasses, the synergism of viscosity of their mixtures is manifested to a greater degree [9, 10].

Position of points 1, 3 and 6, which is particularly noticeable in the given logarithmic interpretation of variation of LiK mixture viscosity (Figure 3), is also attributable to the influence of SOA dimensions and acid-base characteristics. For this purpose it is necessary, based on NMR data, to precisely identify not only the forms with different coordination environment, but also their possible isomerization. The fact that viscosity of liquid glass mixture can have not only positive, but often also negative deviation from additive values, particularly, if it was prepared using solutions with initial components with different moduli, was confirmed experimentally [9, 10].

Investigation results allow interpreting the causes for the revealed features of liquid glass influence on water-holding capacity of coatings, hydrogen content in the metal, deposited with low-hydrogen electrodes, and sanitary-hygienic characteristics of electrodes for welding high-alloyed chromium-nickel steels, proceeding from the concepts of structural changes in liquid glasses based on connections in SOA [11].

## Conclusions

1. Complex investigation of monobasic (Li, Na, K) and binary (LiNa, LiK and NaK) liquid glasses, using methods to obtain multilevel information about structural-functional transformations in silicates, allowed revealing discrete structure of alkali liquid glasses. SOA dimensions are determined by dimensions of cations, encapsulated by them. There is a close relationship between the structure-forming ability of various forms of connection, present in SOA structure and viscosity of water solutions formed by them.

2. Structure of SOA of monobasic liquid glasses is determined by the kind of modifier ion. The larger its size, the weaker is its destructuring influence on SOA,

with preservation of greater number of bridge bonds  $Q^4$ , providing a higher level of liquid glass viscosity.

3. In binary mixtures of liquid glasses, manifesting synergism of viscosity at certain ratios of alkali oxides, the proportion of bridge bonds is greater, than in monobasic glasses. Synergic increase in viscosity is manifested to the greatest degree in LiK glasses. There exists a directly proportional relationship between the viscosity of binary liquid glasses and summary fraction of connection forms ( $Q^3 + Q^4$ ): in the regular coordinate grid for LiNa and NaK glasses, showing slight synergism of viscosity, and in the logarithmic coordinate grid for LiK, characterized by stronger effect of synergism.

1. Uchino, T., Sakka, T., Iwasaki, M. (1991) Interpretation of hydrated states of sodium silicate glasses by infrared and Raman analysis. *J. Am. Ceram. Soc.*, 74(2), 306–313.
2. Bukermann, W.A., Mueller-Warmuth, W., Frichat, G.H. (1992) A further  $^{29}\text{Si}$  MAS NMR study on binary alkali silicate glasses. *Glastechn. Ber.*, 65(5), 18–21.
3. Maekawa, H., Maekawa, T., Kawamura, K. et al. (1991) The structural groups of alkali silicate glasses determined from  $^{29}\text{Si}$  MAS — NMR. *J. Non-Cryst. Sol.*, 127, 53–64.
4. Brykov, A.S., Danilov, V.V., Aleshunina, E.Yu. (2008) State of silicon in silicate and silicon-containing solutions and their binding properties. *Zh. Prikladnoj Khimii*, 81(Issue10), 1589–1593.
5. Brykov, A.S. (2009) *Silicate solutions and their application*. St.-Petersburg.
6. Malyavsky, N.I. (2003) Alkaline-silicate heating materials. Properties and chemical principles of production. *Ros. Khim. Zhurn.*, 47(4), 39–45.
7. Fedotov, M.A. (2009) *NMR of inorganic compounds solutions*. Novosibirsk.
8. Anfilogov, V.N., Bykov, V.N., Oslipov, F.F. (2005) *Silicate melts*. Moscow: Nauka.
9. Marchenko, A.E., Skorina, N.V. (1981) *Liquid glasses — structured liquids*. Information. Kiev: Naukova Dumka, Issue 2, 106–109.
10. Marchenko, A.E. (1989) Combined alkaline silicates in production of low-hydrogen electrodes. In: *Proc. of 2<sup>nd</sup> Int. School of Countries-Members of CMEA on Metallurgical and Technological Problems of Electrodes with Basic Coating* (Sofia, November 1989). Kiev: Naukova Dumka, 1989, 123–130.
11. Marchenko, A.E., Skorina, N.V. (2013) Influence of technological factors in manufacture of low-hydrogen electrodes on hydrogen content in the deposited metal. *The Paton Welding J.*, 8, 13–24.

Received 18.12.2016

# PRODUCTION OF WELDING CONSUMABLES BY ENTERPRISES OF CORPORATION «PLAZMATEK»

V.P. SLOBODYANYUK

PJSC «PlazmaTek»

18 Maksimovich Str., 21036, Vinnitsa, Ukraine. E-mail: info@plasmatec.com.ua

Information about PJSC «PlazmaTek», the leading manufacturer of welding consumables in Ukraine and CIS, history and plans of development, products being manufactured, as well as some peculiarities of the technology of their manufacture is described.

**Keywords:** arc welding, welding consumables, coated electrodes, production of welding consumables

In 2016 the Public Joint Stock Company «PlazmaTek» celebrated the 15<sup>th</sup> Anniversary. The activity of the PJSC «PlazmaTek» began on the base of «Agromash» enterprise of agricultural machine building in village Rudnitsa of Vinnitsa region, which manufactured a small amount of welding electrodes ANO-4 for repair purposes in its industry branch. Over the next 15 years the great investments were contributed for the enterprise development, a radical technical modernization and reorganization of the production was made, the volumes of products were increased (Figure 1, *a, b*).

At present, the PJSC «PlazmaTek» represents a modern multi-profile company with annual turnover

of 50 million of euro and staff of 1340 persons (Figure 2). As to selling the welding consumables the corporation occupies the leading positions in CIS. Additionally to the electrode production a unique complex was constructed for manufacture of copper-plated welding wire of 10 million euro cost. It was completed with the Swedish technological equipment, having a vacuum plasma dressing of a rolled wire and designed for manufacture of 10 thousand tons of wire per year (Figure 3). On the base of treatment plant in Rovno region the enterprise on production of raw materials for manufacture of welding electrodes, such as mica-muscovite, fluorspar, kaolin and quartz sand, was

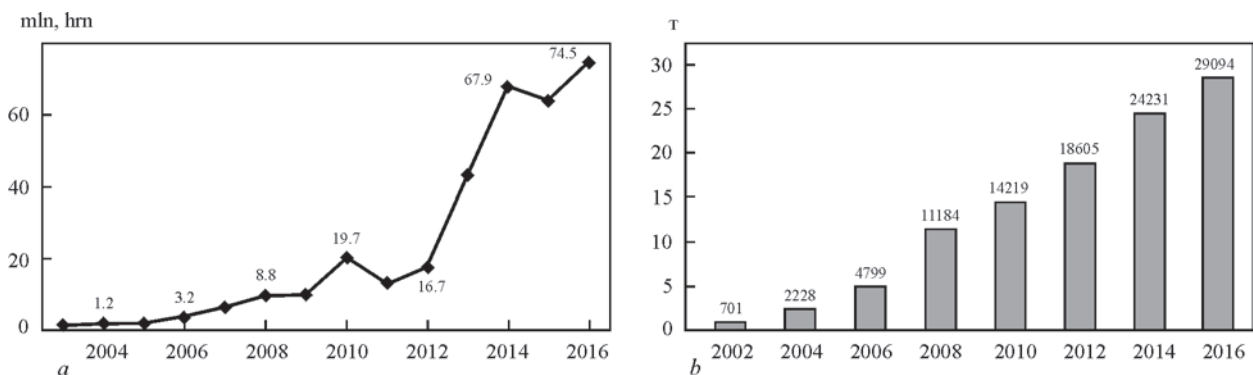


Figure 1. Investments into the corporation development (*a*) and volumes of production of electrodes (*b*) in 2003–2016



Figure 2. Panorama of industrial buildings of corporation

established and is functioning now. The enterprise has the unique technological equipment and necessary monitoring-analytical devices. Being designed at the beginning for satisfying the needs inside the company only, it was further reoriented also for the sale.

At present, the production capacities, functioning in Ukraine and Belarus, are designed for electrode manufacture in the volume of 46 thousand tons per year. They are delivered to dealers by own transport from the trade-logistic centers, providing services to customers at the territory of countries occupying the area of 21 million km<sup>2</sup>. Now the PJSC «PlazmaTek» exports the welding electrodes to more than 20 countries at different continents. The share of company «PlazmaTek» at the main markets is, %: 46 in Ukraine, 32 in Belarus, 46 in Romania, 41 in Moldova, 10 in Russia, etc.

The PJSC «PlazmaTek», having its representations in Europe, in the nearest future has an intention to open them in UAE, USA and Brazil, and also to construct plants for the electrode production in Kazakhstan and Azerbaijan, transforming gradually into the international corporation.

In the electrode production of the PJSC «PlazmaTek» the system of the quality management is functioning during 10 years, which was worked out and certified in accordance with provisions of DSTU ISO 9001. The general structure of the quality management system is given in Figure 4.

Since 2006 the PJSC «PlazmaTek» is successfully manufacturing the rutile-cellulose electrodes ANO-36 (E46 RS type by GOST 9467–75), developed at the E.O. Paton Electric Welding Institute of the NASU and realizing them under the trademark MONOLITH. Since 2007 their promotion as a competitor to electrodes OK 46.00 began at the market of Europe. For admission to the European market the electrodes ANO-36 passed the certification in the Institute of Welding in Gliwice (Poland) for conformity to the requirements of the International standard ISO 2560. In 2008 the volume of production of electrodes ANO-36 surpassed the level of 10 thousand tons (90 % of total production of electrodes by the enterprise at that moment). Nowadays, alongside with them approximately 8 % of electrodes with a basic coating, about 2 % of special electrodes for welding of stainless steels with a rutile-basic coating, as well as electrodes for welding of cast iron and for surfacing are produced. All the electrodes as to the properties and quality level are in compliance with the requirements of the European and International standards.

In 2009 the right was obtained to mark the electrodes ANO-36, manufactured by the PJSC «PlazmaTek», as CE grade, confirming their conformity



Figure 3. New technological line for manufacture of copper-plated welding wire

to standards of quality and safety of the European Union. At the same year the system of the quality management of the PJSC «PlazmaTek» was certified in accordance with ISO 9001 by the TUF Rayland European Body on certification.

Technological scheme of production of electrodes includes, together with conventional components, the additional components, required under market conditions, such as management of resources, including processes of buying raw and other materials and interaction with customers, analysis of market and providing services to customers of products (Figure 5).

Now, the production of electrodes is equipped with required technological, analytical, test equipment and devices, mainly of the domestic manufacture. Their technical characteristics provide the production of a wide assortment of grades, types and sizes of electrodes, which are in demand at the market. There is equipment, which is not traditional at the domestic

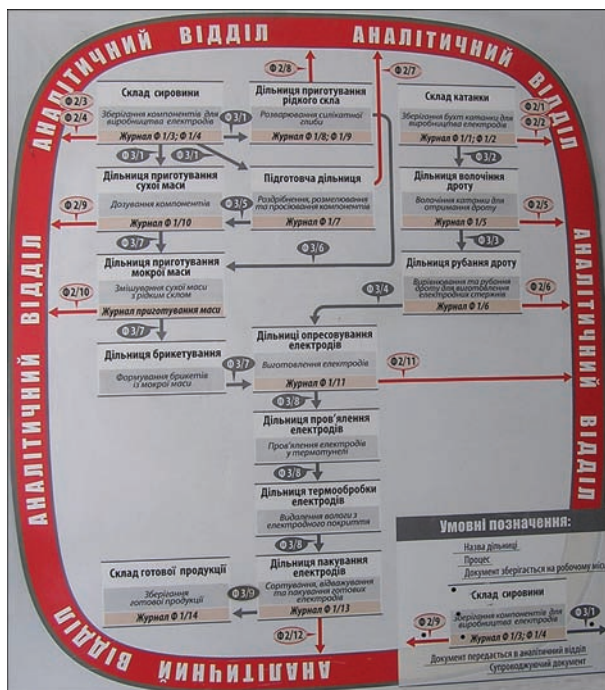


Figure 4. Structure of the quality management system according to DSTU ISO 9001



**Figure 5.** Cargo transport of company for delivery and fast communication with the customer of products

conditions. For example, to provide the quality of electrodes by coating thickness variation the 4-, 5-, 6- and 8-fold drawing mills, operating from a rolled wire, and modern and cutting machine tools AR-04 of «Velma» Company are included into the technological chain of manufacture of rods, and for sieving the powder materials the vibration sieves Sv-0.8 and Sv-1.2 are used.

For dry mixing the charge and preparation of a coating mass the intensive counter-flow mixers of SGI 060, SI 10-1A and SI 20 models of «Velma» Company are used.

The electrodes are manufactured in six technological lines:

- the first line is equipped with an electrode coating unit AOE-4, modernized by «Velma» company to update hydraulic systems and a press head, its rod feeding machine tool, briquetting press and dressing machine;

- the second and third lines are equipped with presses PEO 2000 of «Velma» Company with regular auxiliary equipment (briquetting press, rod feeding machine tool, dressing machine);

- the fourth line is equipped with press PEO 1000 of «Velma» Company and regular completing parts; general view of line is given in Figure 6;

- the fifth line is equipped with electrode coating press of OB 2775 model, manufactured by the Pilot



**Figure 6.** Line of manufacture of electrodes in press PEO 1000

Plant of Welding Equipment of the E.O. Paton Electric Welding Institute;

- the sixth line is equipped with a vertical press of «Bruno Berner» Company and designed for manufacture of special-purpose electrodes.

In all the lines for electrode manufacture the devices for individual marking and deposition of a special coating on electrode edges for arc exciting are mounted, and also there are electromagnetic and mechanical devices for selective monitoring of coating thickness variation.

Heat treatment of electrodes is performed in a conveyor three-pass furnace, three thermal tunnels, as well as in 7 electric chamber-type furnaces with a working space volume of 5 m<sup>3</sup>, manufactured by Sarnensk plant of bridge structures.

Packing of electrodes is still performed manually into cardboard boxes of 0.5; 1.0; 2.5 and 5.0 kg mass and into thermo-shrinkable film.

The electrodes, designed for realization through a retail trade, are supplied in a special packing.

At present, two lines on packing of electrodes into tubes of own manufacture of 1.0 and 2.5 kg mass are mounted and started operation, their automation is planned. The works are carried out for implementation of vacuum packing of electrodes into a foiled film.

Technological and testing laboratories perform control of characteristics of liquid glass and grain composition of powders of electrode coatings, chemical composition of wire and deposited metal, mechanical properties and hardness of weld metal, etc. For this purpose, there is a set of devices and test machines. In particular, areometers, viscometers, diffraction scattering machine, X-ray spectrometer «Spectromax» (Germany) (Figure 7), rupture machine R5M, pendulum hammer 2010 KM-30 (Figure 8), etc.

There is a workshop on manufacture of specimens for testing the weld metal properties. Measuring industrial laboratory of the PJSC «PlazmaTek» was ac-



**Figure 7.** X-ray spectrometer «Spectromax»



**Figure 8.** Rupture machine R5M and pendulum hammer 2010 KM-30

credited for carrying out measurements in the sphere of competence of State metrological inspection.

Over many years the PJSC «PlazmaTek» is closely cooperated with the E.O. Paton Electric Welding Institute in optimizing and updating of the technology of manufacture of ANO-36 electrodes, in training of personnel, creation of the quality management system, corresponding to the provisions of standard DSTU ISO 9001, in testing of new raw materials, including those, the production of which is mastered in the treatment plant, included into the PJSC «PlazmaTek» structure. Figure 9 gives optical characteristics (in relative units) of domestic and foreign mica-muscovite. Comparison of structure confirms the possibility of use of the national raw material in technological purposes.

The PJSC «PlazmaTek» is a member of the International Association «Electrode» and the Society of Welders of Ukraine (SWU). Results of joint works are published in welding journals, at the E.O. Paton

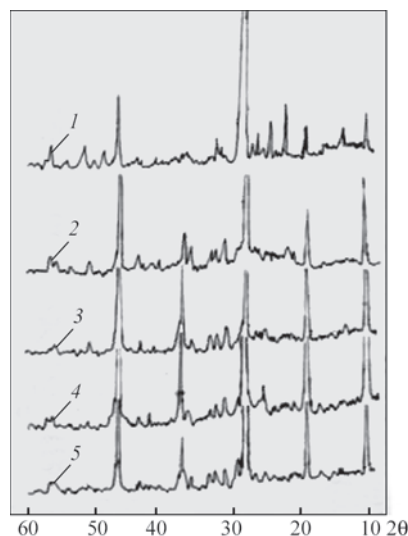


**Figure 9.** Comparison of structure of specimens of mica-muscovite: 1–3 — test samples; 4, 5 — samples of Indian and Russian mica of grade SME-315

Electric Welding Institute, and also in publications of Association «Electrode» and SWU [1–4].

1. Slobodyanyuk, V.P., Skorina, N.V. (2011) Manufacture of electrodes PJSC PlasmaTek. In: *Proc. of 6<sup>th</sup> Int. Conf. on Welding Consumables of CIS Countries: Welding Consumables. Development. Technology. Manufacture. Quality. Competitiveness* (Krasnodar, 6–9 June, 2011). Krasnodar, 2011, 116–123.
2. Slobodyanyuk, V.P., Skorina, N.V. (2011) Manufacture of electrodes PJSC PlasmaTek. *Svarshchik*, **6**, 18–25.
3. (2011) PJSC PlasmaTek — 10 years. *Visnyk Tov. Zvarnykiv Ukrainy*, **2**, 19.
4. Slobodyanyuk, V.P., Skorina, N.V. (2013) Technological properties of new raw material for manufacture of welding electrodes. In: *Proc. of 7<sup>th</sup> Int. Conf. on Welding Consumables of CIS Countries: Welding Consumables. Development. Technology. Manufacture. Quality. Competitiveness* (Krasnodar, 17–21 June, 2013). Krasnodar, 2013, 148–155.

Received 16.12.2016

# CONTROL OF GRANULOMETRIC COMPOSITION OF POWDERS APPLIED IN MANUFACTURE OF WELDING CONSUMABLES

Z.A. SIDLIN

OJSC «TEKhPROM»

57 Gilyarovskiy Str., 107966, Moscow, Russia. E-mail: techprom-ru@yandex.ru

The industrial experience on development of requirements to the analysis of granulometric composition of consumables, applied in the electrode coatings was described. The importance of selecting the method of analysis and the applied equipment was noted. The conclusion on importance of unification of analysis procedures at the manufacturers of consumables and suppliers of powders was made. 8 Ref., 3 Tables.

**Keywords:** arc welding, coated electrodes, production of electrodes, dry charge, powders, granulometric composition, control

The growing competition with the leading world producers of welding consumables specifies ever-increasing requirements to the stability of technological process of their manufacture, which, in its turn dictates the growth of requirements to the reliability of data on characteristics of the applied components. The requirements to high speed of data acquisition grow also. Of course, the above-said belongs to granulometric composition of components as well.

It is known that granulometric composition of dry charge components is the most important and often determining factor in manufacturability of electrodes during their manufacture and application. The rational requirements to it should take into account the ability of ore mineral components at their mixing with liquid glass to provide producing the covering masses with the necessary properties; chemical activity of a number of metals and ferroalloys in the liquid glass environment; the differences in coarseness of different metals and ferroalloys, intended for alloying of deposited metal and/or deoxidizing of molten metal [1]. At the same time the brand requirements to granulometric composition should be based on reliable real data and take into account the specific technological features of a particular enterprise.

At the department of the E.O. Paton Electric Welding Institute, created and headed by Prof. I.K. Pokhodnya over many years, many research and practical works were carried out devoted to technological problems of technology for production of welding consumables. Of course, the problems associated with granulometry of powders, in particular those considered in the work [2], were also studied. However, in

these works the methods of analysis of coarseness of materials were not covered. Until recently, the manufacturers of welding consumables at the territory of the former Soviet Union carried out crushing, grinding and preparation of electrode coating components and flux-cored wires in the own crushing-grinding divisions.

The transition to producing the components in the form of finished powders requires not only a clear formulation of user's requirements to their granulation, but also unification or harmonization of procedures for determination of particle sizes with the supplier. The delicacy of the problem lies in the fact that granulometric composition is often «know-how» of welding consumables manufacturers. In the same cases when in the technical literature the data on coarseness of different materials are given, they are represented, as a rule, in general form. Thus, in the work [3] it is pointed out that the amount of material on the sieves 045, 0355 and the upper limit of granulation of minerals in the «basin» of sieve 005 (according to GOST 6613) is approximate. In the [4] it is indicated that the sieve analysis is carried out mainly during setting up the grinding modes, and the given data on granulometric composition are approximate. Sometimes the indications on requirements to coarseness prepared to application of components can be found in the branch documentation of a limited use.

The some enterprises, producing electrodes, gained a considerable experience and statistics, on the basis of which the requirements to granulometric composition of different materials used as electrode coating components were developed. The most famous of them are the data of the Moscow Pilot Welding Plant (MOSZ), which are the basis of norms of many domestic enter-

prises [1]. It was particularly emphasized, that at each enterprise, producing electrodes, the requirements to granulometric composition should be specified taking into account the specifics of production.

Let us precise that such specifics, except of taking into account the nomenclature of the produced electrodes, their type and size series, physical nature of the used components and their nomenclature, structural characteristics and capabilities of the main technological equipment, characteristics of a binder, etc., should consider the characteristics of testing equipment used to determine the granulometric composition. After all, in fact the accuracy of sieve analysis is determined by the quality of fractionation and precision of sieves and its reliability is determined also by the quality of sampling and its careful performance.

The data of MOSZ are true in carrying out the sieve analysis in the device of the model 029 (basic technical characteristics: number of sieves oscillations is 300 rpm, number of strikes of a striker is 180 strikes/min), where the material is sieved through the

system of rotating and shaking sieves in a semi-automatic mode. The other widespread device is the model 01412 which is the electromagnetic vibrator with the frequency of sieves oscillation being  $50 \text{ s}^{-1}$  at the amplitude of 0.1–1.0 mm. In the vibrostand PE 6700 used by one of the suppliers of finished powders (Table 1, C), the number of oscillations amounts to 12–25 Hz at the amplitude of 0.25–4.00 mm. The principle of operation of the device is the rendering of reciprocal oscillations in vertical plane to the sieves fixed at the desktop.

No wonder that during the control of one and the same batches of powders of different materials using different equipment the results are also different (Table 1). At the same time the determinations were performed in the devices of 029 model at two different enterprises (Table 1, A and B), and the obtained results were similar. In this case the difference of data on the sieve 016 can be attributed to the accuracy of grids and that will be discussed below.

**Table 1.** Results of determination of granulometric composition of materials applying different equipment. Remnant on sieves (in % from the mass of initial sample)

Number	Description of material, model of device	Index of enterprise	Numbers of sieves according to GOST 6613–86						
			0315	02	016	01	0063	005	–005
1	Ferroboron PE6700	C	0	N/D	N/D	N/D	91.5	7.6	0.9
	(029) 1	A	0.6	13.8	10.6	24.2	11.8	8.6	30.0
	(029) 2	B	0	22.44	0.57	28.27	15.93	7.36	24.58
	01412	A	0	22.16	8.53	23.40	15.52	7.70	22.68
2	Metallic manganese PE6700	C	0	N/D	N/D	N/D	84.5	11.7	3.8
	(029) 1	A	0	17.2	12.6	22.6	8.0	5.0	33.6
	(029) 2	B	0	17.09	0.95	29.31	16.76	9.09	27.22
	01412	A	0	14.53	8.78	26.18	14.30	12.1	24.16
3	Ferroniobium PE6700	C	0	N/D	N/D	N/D	78.2	9.9	11.89
	(029) 1	A	0	7.8	8.6	25.2	11.2	8.2	37.6
	(029) 2	B	0	9.38	0.68	28.92	20.22	12.10	28.69
	01412	A	0	8.78	6.11	25.78	19.31	13.64	25.59
4	Ferromanganese PE6700	C	0	N/D	N/D	N/D	85.37	10.62	4.01
	(029) 1	A	0.2	11.6	10.4	22.0	9.6	9.2	37.0
	(029) 2	B	0	20.48	1.53	26.35	14.80	10.54	24.58
	01412	A	0	18.33	0.37	64.62	10.54	5.54	0.15
5	Ferrosilicium PE6700	C	0	N/D	N/D	N/D	81.4	13.4	5.2
	(029) 1	A	0	20.2	12.2	23.4	8.2	5.0	30.2
	(029) 2	B	0	22.34	0.36	28.22	15.56	6.78	25.97
	01412	A	0	20.02	8.43	23.33	14.59	8.49	24.38
6	Ferrotitanium PE6700	C	0	N/D	N/D	N/D	75.38	14.97	9.65
	(029) 1	A	3.6	22.6	12.4	22.4	8.0	5.8	24.6
	(029) 2	B	2.69	21.63	7.45	20.74	16.63	8.20	22.46
	01412	A	1.42	20.06	8.09	23.72	16.42	10.88	19.45
7	Ferrochrome PE6700	C	0	N/D	N/D	N/D	81.85	13.49	4.66
	(029) 1	A	4.6	22.4	9.6	19.0	7.8	6.4	28.8
	(029) 2	B	2.75	21.40	6.07	17.22	14.15	8.13	29.1
	01412	A	1.12	21.98	6.59	19.73	12.92	10.75	25.82
8	Metallic chrome PE6700	C	0.06	N/D	N/D	N/D	90.3	3.3	6.34
	(029) 1	A	1.3	23.6	13.6	26.8	8.4	5.2	20.2
	(029) 2	B	3.08	26.99	7.43	27.87	14.26	5.13	13.45
	01412	A	2.52	27.90	10.40	27.70	12.79	5.40	11.56

Note. N/D — no data.

**Table 2.** Results of sieve analysis of powders of different materials

Number	Description of material, model of device	Index of enterprise	Numbers of sieves according to GOST 6613–86						
			0315	02	016	01	0063	005	–005
1	Ferroniobium	A	–	26.50	5.58	28.47	14.57	6.64	20.13
		B	–	24.20	12.5	24.0	12.2	3.9	21.9
2	Ferrochrome	A	0.06	1.52	12.68	46.81	20.90	6.63	11.27
		B	–	0.6	13.7	55.7	15.1	3.5	11.1
3	Nickel	A	0.08	0.55	0.95	90.75	4.55	1.24	1.82
		B	–	0.6	1.8	93.7	1.7	1.2	0

Table 1 presents the data on control of domestic materials, but the similar results were obtained also during control of powders of the Swedish Company MRT in the device of the model 029 at the enterprises A and B (Table 2).

It is noteworthy that in the branch technological documentation and in the majority of standards the types and models of devices for sieve analysis are not specified. The more precise control of technological processes in the electrode production also requires obtaining the data about granulometric composition of that part of powders, which have sizes smaller than 50  $\mu\text{m}$ , which can not be determined using conventional vibrating methods. This is explained by the fact that for the particles of such sizes the forces of adhesion and cohesion are comparable with their mass, sharply increasing at the further reduction in sizes. This results in conglutination of particles, clogging of sieve meshes, hindered sieving and obtaining the erroneous data [5]. The possibilities of analysis of granulometric composition of powders using dry method are expanded by electrostatic sieving realized, for example, in domestic devices Elsa-M and Gran [6].

One of the most advanced equipment is of the Company «Fritch» (Germany), which reliably proved itself over many years of practice. For example, the vibrating screen Analysett 3 with a vertical movement of high-quality analytic sieves provides a measurement of particles in the range from 63  $\mu\text{m}$  to 20  $\mu\text{m}$ . The laser diffraction measuring devices of the series Analysett 22 using the physical principle of fluctuation of electromagnetic waves, provide the ability to measure particles from 0.1  $\mu\text{m}$ , moreover, the model Analysett 22 NanoTek also simultaneously detects

the shape of particles. The software Autosieve allows carrying out automatic processing of results, including graphical representation, calculation of statistical values, calculation of values, keeping data bank [7]. Unfortunately, until now the Russian enterprises do not have such equipment in their disposal.

The metal grids used for sieving materials are delivered according to the standards GOST 2715 «Metallic wire grids. Types, basic parameters and dimensions» and according to GOST 6613 «Wire cloth grids with square meshes». To control the granulometric composition in electrode production, the grids according to GOST 6613 are mainly used, manufactured of non-ferrous metals and alloys. The systematization of grids for welding production was carried out by the authors of work [8].

Briefly the grids are designated by the number corresponding to the inside size of a mesh side in mm. The abbreviated notation for the meshes being smaller than 1.0 mm is made without a comma separating the integer part from the fractional one and zeros after significant digits are omitted. For example, a grid with an inside size of 0.315 mm of a mesh is designated with the number 0315, and a grid with an inside size of a mesh of 0.100 mm with the number 01. Formerly in the USSR and even now in a number of countries the number of a grid denoted the number of meshes accounted per 1 linear inch (mesh). Depending on the number of a grid the standard provides a different type of interweaving of wires of base and filling: in linen one the interweaving is through one wire and in serge one the interweaving is through two wires:

**Table 3.** Results of sieve analysis of powders of the company MRT

Number of grid	Nominal sides of mesh, $\mu\text{m}$	Accuracy of manufacture					
		H		B		K	
		Maximum deviation from nominal value, $\mu\text{m}$	Share, %	Maximum deviation from nominal value, $\mu\text{m}$	Share, %	Maximum deviation from nominal value, $\mu\text{m}$ (interval)	Share, %
005	50	34	$\leq 8$	25	$\leq 5$	13–23	$\leq 5$
01	100	60		40		19–34	
0315	315	151		79		40–67	
04	400	180		96		47–78	

Number of grid	Type and order of interweaving
004–0063	Serge 2/2
0071–014	Serge 2/2 or linen 1/1
016–2.5	Linen 1/1

The grids are distinguished by the manufacture accuracy: N — normal, H — high, R — reference, differing, first of all, by tolerances on maximum deviation of size of a mesh side from the nominal value. As an example, Table 3 shows the corresponding data for several grids applied in the electrode production.

Unfortunately, according to the survey of enterprises-manufacturers that we conducted, in the country only the grid of normal manufacturing accuracy is produced, namely which is mostly applied in the sieves used in installations, including those produced by the OJSC «Litmashpribor». The aforementioned should be taken into account when considering the results of the analysis. At the same time, as in industrial sieves the grids of normal accuracy are used, it becomes unnecessary to adjust granulometric composition according to the data of analysis for practical application.

A unified approach to standardization of requirements on granulometric composition is absent even in the state standards on the materials of electrode coatings. Also in the most of standard documentation on electrode coating materials delivered in a powder form, the procedures for determination of granulometric composition are insufficiently described. Even in a separate standard such as GOST 19724, for example, which covers the method for determination of granulometric composition of fluorspar, including flotation concentrate, it is only specified that the mechanical shaker and grids according to GOST 6613 are applied. The analysis of pulverized quartz according to GOST

8077 should be performed in a wet method using the similar grids; during analysis of mica according to GOST 14327 the use of the sieving mechanical analyzer at the frequency of not less than 280 oscillations per minute, etc. is prescribed (GOST 19572).

It follows from the above mentioned that it is necessary to unify the methods for determination of granulometric composition at the enterprises-manufacturers of welding consumables and manufacturers of powder materials, as well as to include the norms on granulometric composition to the contracts for delivery of powder materials with the agreement of acceptance test procedures. During cooperation with the major domestic supplier of powder ferroalloys OJSC «MELDIS-FERRO» the practical realization of such approach allowed eliminating the misunderstandings encountered before and provided a stable and coordinated work in the future.

1. Sidlin, Z.A. (2009) *Manufacture of electrodes for manual arc welding*. Kyiv: Ekotekhnologiya.
2. Marchenko, A.E. (2014) Effect of charge grain composition on rheological characteristics of compounds for low-hydrogen electrodes. *The Paton Welding J.*, **6/7**, 163–171.
3. Blagoveshchenskaya, V.V., Gololobov, B.A., Strogova, V.Ya. (1966) *Technology of manufacture of arc welding electrodes*. Moscow-Leningrad: Mashinostroenie.
4. Garnik, I.I., Piolunkovsky, G.M. (1975) *Manufacture of metallic electrodes*. Moscow: Metallurgiya.
5. Kouzov, P.A. (1974) *Principles of analysis of dispersion composition of industrial dusts and crushed materials*. Leningrad: Khimiya.
6. Starostin, G.A., Krashennnikov, V.M., Stetsovsky, A.P. et al. (1985) Advanced devices for determination of granulometric composition of powder materials. *Nauchno-Tekhn. Dostizheniya, Intersect. Coll.*, **2**, 72–77.
7. *Fritch Company brochures*, FRG.
8. Gridin, A.A., Tarkhov, N.A. (1981) Systematization of meshes and recommendations on set of sieves for determination of granulometric composition of powder materials in welding production. *Svaroch. Proizvodstvo*, **10**, 25–28.

Received 18.11.2016

# FLUX-CORED WIRE FOR WEAR-RESISTANT SURFACING OF THIN-SHEET STRUCTURES

A.A. BABINETS and I.A. RYABTSEV

E.O. Paton Electric Welding Institute, NASU

11 Kazimir Malevich Str., 03680, Kiev, Ukraine. E-mail: office@paton.kiev.ua

The electric arc surfacing of wear-resistant layers on sheet structures of less than 4 mm thickness is connected with a risk of occurrence of burn-outs and excessive deformation of sheets due to their high penetration. One of the possible ways to decrease penetration is the selection of an optimum method of surfacing and development of appropriate technologies and surfacing materials. It was experimentally found, that to provide a minimum penetration with account for a quality formation of deposited metal is possible by using the open-arc surfacing with a flux-cored wire of less than 1.6 mm diameter. The application of the developed technology and technique of surfacing using an improved self-shielding flux-cored wire PP-AN198 provided a quality formation of the deposited metal, absence of burn-outs, pores and other defects, as well as reduced the residual deformations in surfacing of sheets of 3 mm thick steel St3 to minimum. The obtained results can be used in selection of surfacing materials and technologies for surfacing the wear-resistant layers on thin-sheet structures, which are operating in mining and metallurgical industries under the conditions of different types of abrasive wear. 8 Ref., 1 Table, 3 Figures.

**Keywords:** arc surfacing, flux-cored wire, thin-sheet structures, penetration, deformations, deposited metal

Due to their versatility, the flux-cored wires found a wide application for mechanized and automatic arc surfacing in different branches of industry. First of all, it is explained by a sufficiently simple adaptation of their chemical composition to the composition and properties of the parts being surfaced, high stability of arc burning, relatively low spattering of the electrode metal and a good formation of deposited layers [1–6].

One of the promising directions for application of flux-cored wires is their use for surfacing of thin-sheet structures (thickness of sheets  $\leq 4$  mm), operating in mining and metallurgical industries under conditions of different types of abrasive wear.

The main problems in surfacing of thin-sheet structures consist in a possible occurrence of burn-outs and large deformations of these structures. To solve these problems it was decided to apply the surfacing flux-cored wires of a small diameter (1.2–1.6 mm) and minimum possible modes of surfacing, at which a stable process and quality formation of the deposited layers will be provided [7].

For experiments the flux-cored wire PP-AN198 of Fe–C–Cr–Mn–Si system of alloying, developed at the E.O. Paton Electric Welding Institute, was taken as a prototype.

Thus, the aim of the present work was the optimizing the charge composition of the flux-cored wire PP-AN198 for producing the required composition of the deposited metal at a minimum diameter of the wire and development of technique and technology of sur-

facing, providing a good formation of the deposited layer and absence of defects like burn-outs, pores and other types in it.

It is known that the method of surfacing (under flux, in shielding gas and with open arc) effects greatly the value of penetration and quality of deposited metal formation even during surfacing at similar conditions and application of wire of the same grade and diameter [8].

Coming from this, it was necessary, first of all, to find out at which method of surfacing it is possible to obtain a minimum penetration of the base metal at the formation of high quality deposited beads. For experiments, six test batches of the flux-cored wire PP-AN198 of 1.6 and 1.8 mm diameter were manufactured for surfacing under flux, in shielding gas and with open arc. In prior series of experiments the surfacing was performed on plates of steel St.3 and wide range of modes by current (150–300 A) and voltage (20–28 V) at constant surfacing speed of 30 m/h.

Figure 1 gives the experimental data of penetration depth of base metal for wires of 1.6 mm diameter (solid lines) and 1.8 mm diameter (dashed lines) during surfacing by three different methods: under flux (*a*), in shielding gas (*b*), and with open arc (*c*). It is seen from Figure 1 that with increase in current and voltage the penetration depth of the base metal is also increased. Here, it is possible to provide a minimum penetration with account for the quality formation of deposited metal during open-arc surfacing using flux-cored wire of 1.6 mm diameter. Coming from the obtained results

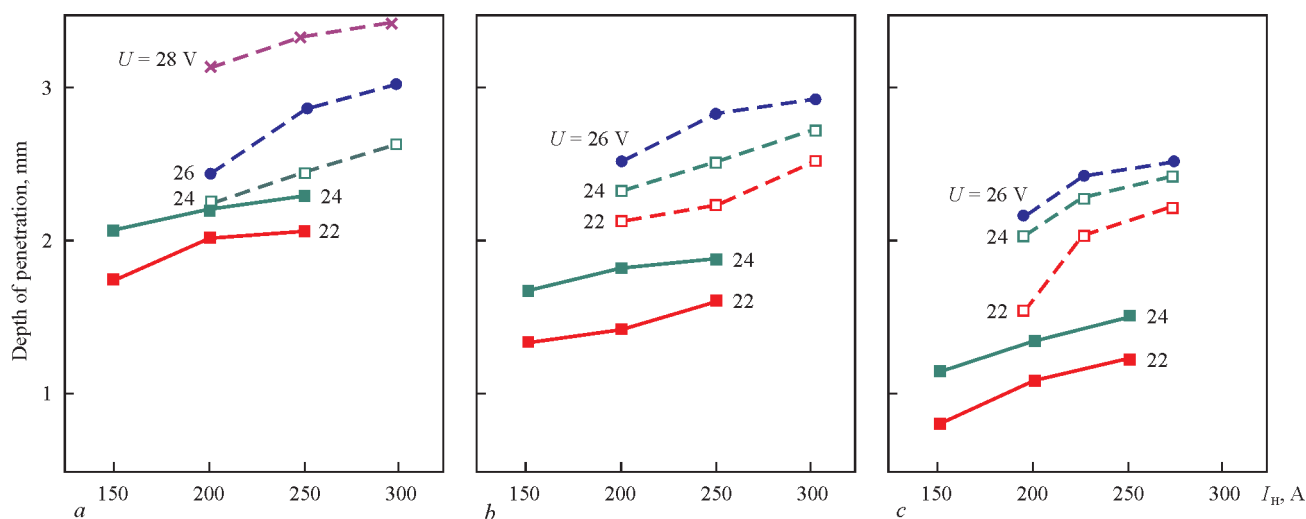


**Figure 1.** Effect of current on penetration depth in surfacing under flux (*a*), in shielding gases (*b*) and using open arc (*c*) (solid lines — wire of 1.6 mm diameter; dashed lines — wire of 1.8 mm diameter)

it was decided to continue the works using this type of the flux-cored wire.

To provide a reliable protection of the welding pool and produce the quality deposited metal at minimum possible modes, it was necessary to select properly a gas-slag-forming system of the flux-cored wire.

For this purpose, four test variants of self-shielding flux-cored wires PP-AN198 of 1.6 mm diameter with different systems of gas-slag-forming components were manufactured:  $\text{CaO} + \text{TiO}_2 + \text{MgO} + \text{CaF}_2 + \text{Al}_2\text{O}_3$  (wire with designation PP-Op-1);  $\text{CaO} + \text{MgO} + \text{CaF}_2 + \text{Al}_2\text{O}_3$  (PP-Op-2);  $\text{CaO} + \text{CaF}_2 + \text{Al}_2\text{O}_3$  (PP-Op-3) and  $\text{CaO} + \text{Al}_2\text{O}_3 + \text{C}_6\text{H}_{10}\text{O}_5$  (PP-Op-4).

During the process of surfacing by the mentioned wires the expert evaluation of welding-technological properties of self-shielding flux-cored wires of all four types was carried out (nature of metal transfer, value of spattering, covering of deposited beads with a slag, etc). In this case the following system of estimates was used. The metal transfer was characterized by numbers: 1 — fine-drop; 2 — coarse-drop; 3 — mixed; spattering was also evaluated in numbers: 1 — small; 2 — medium; 3 — high; the degree of covering with a slag was evaluated in percents; the presence of pores was characterized by two indices: available and

no available; formation of deposited metal was characterized as good, fair or poor.

To evaluate the welding-technological properties the surfacing of specimens at similar current of 160–180 A and surfacing speed of 30 m/h was performed. Since the decisive effect on pores formation and quality of deposited beads during surfacing by the flux-cored wires with an open arc is exerted by voltage [4], the latter it was varied from 20 V and higher up to the appearance of pores in the deposited metal or up to deterioration of the quality of formation for each type of the flux-cored wire (Table).

From the results of experiments it was found that among four flux-cored wires the self-shielding flux-cored wire PP-AN198 (Op-1) possesses the best complex of welding-technological properties and, therefore, it was used further for surfacing of thin sheets.

As was mentioned above, one of the main problems during surfacing of sheets of <4 mm thickness is the probability of burn-outs formation. This probability is increased in the process of surfacing due to the growth of temperature of the sheet being deposited and its deformation, which results in increased gap between the sheet and the surface of the surfacing table. As in the work the sheets of relatively small size (3×400×600 mm) were used, then to reduce their

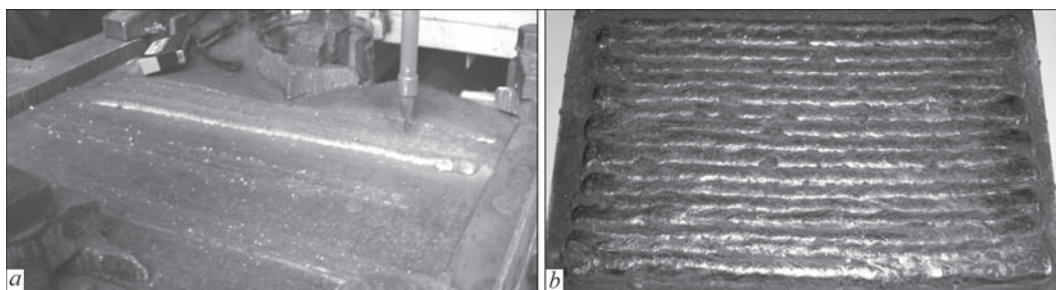


**Figure 2.** Process of surfacing of 3 mm thick steel plate fixed on water-cooled copper table (*a*) and appearance of deposited plate (*b*)

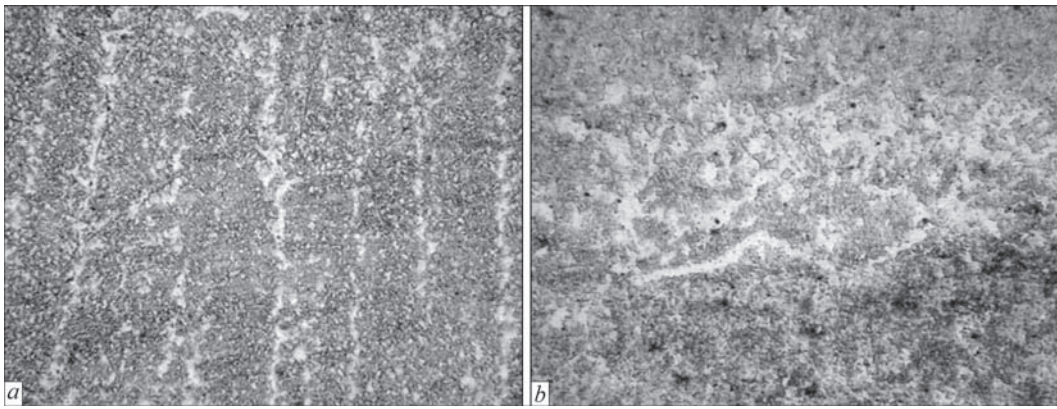


**Figure 3.** Microstructure ( $\times 250$ ) of metal deposited using self-shielding flux-cored wire PP-AN198 (a) and zones of its fusion with steel St3 (b)

Results of evaluation of welding and technological properties of test self-shielding flux-cored wires of type PP-AN198

Designation of wire	Voltage, V	Type of transfer, numbers	Spattering, numbers	Covering with slag, %	Pores	Quality of formation
PP-AN198 (Op-1)	20	2	1	100	No	Good
	22	3	2	100	No	Good
	24	3	2	100	Available	Fair
PP-AN198 (Op-2)	20	3	1	100	No	Fair
	22	3	2	80	Available	Poor
PP-AN198 (Op-3)	20	3	1	100	No	Good
	22	3	2	100	No	Fair
	24	3	3	80	Available	Fair
PP-AN198 (Op-4)	20	2	1	90	No	Good
	22	3	2	90	No	Fair
	24	3	3	90	Available	Poor

temperature and deformation a device with a cooled copper table was used, where the sheets were fixed by means of clamping straps (Figure 2, a).

For experiments on optimizing the technology of arc surfacing of 3 mm thick sheets of steel St3, the flux-cored wire PP-AN198 (Op-1) of 1.6 mm diameter was manufactured. In manufacture of flux-cored wire the strip of steel 08kp (rimmed) of production of «Zaporozhstal» metallurgical plant was used as a sheath. The strip has a relatively low elongation values ( $\sim 25\%$ ), so it was not possible to manufacture the wire of a smaller diameter. The experience shows that using a strip of foreign production, the elongation of which is at the level of 40 % the surfacing flux-cored wire with the diameter of 1.2–1.4 mm can be manufactured.

The surfacing of 3 mm thick sheets of steel St3 using the flux-cored wire PP-AN198 (Op-1) of 1.6 mm diameter was carried out at the following modes: current 160–180 A, voltage 21–22 V; surfacing speed of 30 m/h; overlapping of adjacent beads was 50 %. Figure 2, b shows the appearance of the sheet deposited using above-mentioned technology. The visual inspection revealed that on the surface of the deposited sheet the burn-outs, pores, cracks and other defects were absent.

The metallographic examinations of specimens of deposited metal and its fusion zone with the base metal were carried out. It was found that the microstructure of the upper layer of metal, deposited using wire PP-AN198, consists of ferrite, concentrated along the boundaries of crystallites and martensite-sorbite mixture with a small amount of chromium carbides located in the body of crystallites (Figure 3, a). Ferrite fringes at the boundaries of crystallites have a width of 10–20  $\mu\text{m}$ . The width of crystallites is 40–75  $\mu\text{m}$ . The hardness of the upper deposited layer is  $HV1-2970-3090$  MPa.

In the structure of deposited metal near the boundary of fusion with the base metal the amount of ferrite component is somewhat higher, than near the surface, respectively, its hardness is lower, i.e.  $HV1-1930-1980$  MPa. Along the fusion line of base metal with the deposited one the discontinuous ferrite band is formed (Figure 3, b). Thus, the metallographic examinations confirmed also producing of a quality joint and the absence of defects both in the deposited metal as well as in the fusion zone.

### Conclusions

1. It was found that for electric arc surfacing of thin-sheet structures ( $\delta \leq 4$  mm) it is necessary to use the

self-shielding flux-cored wires of the diameter of  $\leq 1.6$  mm and the minimum surfacing modes, providing the absence of burn-outs and a good formation of deposited beads.

2. The device was manufactured and techniques and technology for surfacing of steel sheets of 3 mm thickness using self-shielding flux-cored wire PP-AN198 of 1.6 mm diameter of improved composition were developed. The application of these technologies and surfacing materials allows producing thin bimetallic sheets on which the burn-outs, pores and other defects are absent and residual deformations are reduced to a minimum.

1. Pokhodnya, I.K., Suptel, A.M., Shlepakov, V.N. (1972) *Flux-cored welding*. Kiev: Naukova Dumka.
2. Pokhodnya, I.K., Yavdoshchin, I.R., Paltsevich, A.P. et al. (1994) *Metallurgy of arc welding, interaction of metal with gases*. Kiev: Naukova Dumka.
3. Pokhodnya, I.K., Shlepakov, V.N., Maksimov, S.Yu. et al. (2010) Research and developments of the E.O. Paton Electric Welding Institute in the field of electric arc welding and surfacing using flux-cored wire (Review). *The Paton Welding J.*, **12**, 26–33.
4. Yuzvenko, Yu.A., Kirilyuk, G.A. (1973) *Flux-cored surfacing*. Moscow: Mashinostroenie.
5. Ryabtsev, I.A. (2004) *Surfacing of machine parts and mechanisms*. Kyiv: Ekotekhnologiya.
6. Kondratiev, I.A., Ryabtsev, I.A. (2014) Flux-cored wires for surfacing of steel hot mill rolls. *The Paton Welding J.*, **6/7**, 95–96.
7. Lankin, Yu.N., Ryabtsev, I.A., Soloviov, V.G. et al. (2014) Effect of electric parameters of arc surfacing using flux-cored wire on process stability and base metal penetration. *Ibid.*, **9**, 25–29.
8. Babinets, A.A., Ryabtsev, I.A., Panfilov, A.I. et al. (2016) Influence of methods of arc surfacing with flux-cored wire on penetration of base metal and formation of deposited metal. *Ibid.*, **11**, 17–22.

Received 23.11.2016

# ADHESION-ACTIVE HIGH-TEMPERATURE WEAR-RESISTANT SURFACING CONSUMABLES KMKh AND KMKhS

A.M. KOSTIN<sup>1</sup>, V.A. MARTYNENKO<sup>1</sup>, A.B. MALY<sup>2</sup> and V.V. KVASNITSKY<sup>3</sup>

<sup>1</sup>Admiral Makarov National University of Shipbuilding  
9 Geroev Stalingrada Ave., 54025, Mykolaiv, Ukraine. E-mail:university@nuos.edu.ua

<sup>2</sup>SE GTSPC «Zorya-Mashproekt»

42-a Bogoyavlensky Ave., 54018, Mykolaiv, Ukraine. E-mail:office@zorya.com.ua

<sup>3</sup>NTUU «Igor Sikorsky KPI»

37 Pobedy Ave., 03056, Kiev, Ukraine. E-mail:kvas69@ukr.net

Adhesion-active high-temperature wear-resistant composite surfacing consumables KMKh and KMKhS were developed. They provide for significant increase of wear resistance of contact surfaces of parts of hot gas path in gas turbine engines. It is determined that additional introduction of chromium carbide in alloy based on solid solution of cobalt, alloyed by molybdenum, chromium, boron and silicon, promotes for stabilization of its structure and properties with simultaneous decrease of melting temperature of composition. Boron and silicon provide for increase of adhesion alloy activity in deposition on contact surfaces and form uniformly distributed thermodynamically stable high-dispersion complex silicides and borides. Wear resistance tests show that average value of wear intensity of working surfaces, deposited with new KMKh and KMKhS consumables, are 3–4 times lower under conditions of operation in oxidizing medium at critical temperatures, than the surfaces deposited with known commercial alloys. High characteristics of wear resistance and possibility of work under critical temperatures allowed recommending developed composite consumables and technology of their surfacing to commercial application. 10 Ref., 3 Tables, 1 Figure.

**Keywords:** surfacing, adhesion-active wear-resistant composite consumables, high-temperature alloys, structure, phase composition, wear intensity

One of the main problems of ship machine building is rise of efficiency, safety and life of gas turbine engines (GTE). First of all, these parameters are determined by wear of the contact surfaces of working blades, which are operated under extreme conditions at high operating loads and temperatures.

Currently there is a wide range of wear-resistant consumables for surfacing on the contact surfaces with base metal melting or without it.

The main criteria of their serviceability are melting temperature and possible methods of deposition of high-temperature alloys on the contact surfaces. On practice, mentioned criteria can have mutually exclusive effect that significantly complicates or makes impossible simultaneous choice of optimum composition of surfacing alloy and method of formation of wear-resistant layer, which could satisfy specific requirements of particular manufacturer [1].

Aim of present work is a development of new adhesion-active high-temperature wear-resistant composite consumables, providing significant rise of life of the contact surfaces of parts of GTE hot gas path.

It is known fact that ship gas turbine building uses high-temperature nickel alloys of ChS88U-VI, ChS70U-VI and other types for construction of turbine working blades. These alloys are strengthened with

disperse precipitations of  $\gamma'$ -phase  $Ni_3(Al, Ti)$ , having tendency to coagulation in process of contact interaction at high-temperatures, that results in formation of favorable conditions for wear increase, including due to intensification of oxidation processes in a depleted surface layer by alloying elements. These alloys refer to the materials with unsatisfactory process weldability, therefore temperature of their heating during deposition of wear-resistant layer on the contact surface should not exceed  $1220 \pm 10$  °C. Otherwise, it is impossible to eliminate rapid decrease of base metal strength as a result of  $\gamma'$ -phase degradation and formation of cracks in deposition zone [2]. In this connection, alloys used for strengthening of the contact surfaces, should have melting temperature not more than  $1220 \pm 10$  °C at deposition in form of melt. With higher temperature of melting of wear-resistant consumable its deposition is carried out by brazing, but turbine blade design does not always allow application of this effective method.

Thus, wear-resistant alloys can be comfortably divided on two groups by melting temperature before and after  $1220 \pm 10$  °C.

It is extremely difficult problem to develop the alloys, relating to the first group and having necessary level of wear resistance at operating temperatures (to

900 °C) and capable to withstand short-term heating to 1150 °C which is close to solution temperature of strengthening  $\gamma'$ -phase in the base metal.

Alloys of the first group include KBNKhL-2 composition having nickel-cobalt matrix with content, wt.% of nickel 35.5–36.5; cobalt 20.5–21.5; chromium 24.5–25.5; chromium carbide 11.5–12.5; chromium boride 2.5–3.5 and boron 2.9–3.1 [3]. High relative wear resistance of alloy is provided by strengthening of nickel-cobalt matrix with chromium carbides and borides. A disadvantage of alloy is its low melting temperature (~1070–1090 °C) that does not provide alloy with possibility to withstand short-term thermal loads at temperatures up to 1150 °C.

All other known alloys can be referred to the second group that significantly complicates their application in surfacing on the contact surface. For example, there is cobalt-based V3K-r alloy, having in its composition, wt.%: 28.0–32.0 of chromium; 7.0–11.0 of tungsten and 1.6–2.0 of carbon as main alloying elements and additionally alloyed in small amount by Si, Mn, Ni, B, Fe. Alloy strengthening is provided by formation of tungsten and chromium carbides [4]. Temperature of stable operation of this alloy does not exceed 600 °C.

Cobalt-based alloy Stellite 12 has similar composition, it includes as main alloying elements, wt.%: chromium 28.0–31.0; tungsten 7.2–9.2, carbon 1.55–1.75 and additionally Ni, Si, Fe and Mo. Alloy strengthening takes place as a result of formation of tungsten and chromium carbides [5]. Operating temperature of this alloy also doesn't exceed 600 °C.

There is nickel-based alloy Kh0N50Yu5T2, having, wt.%: 32.0–36.0 of chromium; 5.0–6.0 of aluminum; 1.4–2.1 of titanium; 1.2–1.6 of carbon as the main alloying elements and additionally boron and iron in small amount. High relative wear resistance of this alloy is provided by formation of Ni<sub>3</sub>(Al, Ti) intermetallics and chromium and titanium complex carbides. Such a strengthening mechanism is of low efficiency due to instability of  $\gamma'$ -phase under conditions of effect of significant contact loads at increased temperatures in oxidizing medium. This promotes for rise of intensity of alloy wear that is its significant disadvantage.

Aviation engineering successfully applies cobalt-based alloy KhTN-61, containing, wt.%: 19.0–

21.0 of chromium, 15.0–16.0 of niobium; 2.7–3.3 of tungsten; 1.8–2.2 of molybdenum; 0.8–1.2 of aluminum and 1.95–2.30 of carbon, strengthened by disperse precipitations of niobium monocarbides and having high wear resistance exceeding that of nickel-based alloys due to resistance of strengthening phase [6]. Significant disadvantage of this alloy is its low high-temperature resistance and loss of properties in melting (melting temperature 1340±10 °C). Deposition of this alloy on the contact surfaces is possible only by brazing.

Similar composition has cobalt-based alloy KhTN-62, containing, wt.%: 5.0–25.0 of chromium; 13.5–17.0 of niobium; 6.0–12.0 of tungsten; 2.0–3.5 of aluminum; 2.0–5.0 of iron; 1.6–1.9 of carbon. Alloy has increased high-temperature resistance, however relatively low content of carbide phase (NbC) results in significant decrease of alloy wear resistance that is substantial disadvantage and does not provide in full all necessary complex of properties.

A basis of development of new adhesion-active high-temperature wear resistant composite consumables is a problem of providing a necessary level of their wear resistance at operating temperatures (to 900 °C), capability to withstand temporary thermal loads in oxidizing medium at temperatures to 1150 °C and possibility of deposition in form of melt on the contact surfaces at temperatures of their heating not more than 1220±10°C.

New high-temperature wear-resistant consumables KMKh and KMKhS, which correspond to the requirements given in works [7, 8], were developed together with SEG TSPC «Zorya-Mashproekt».

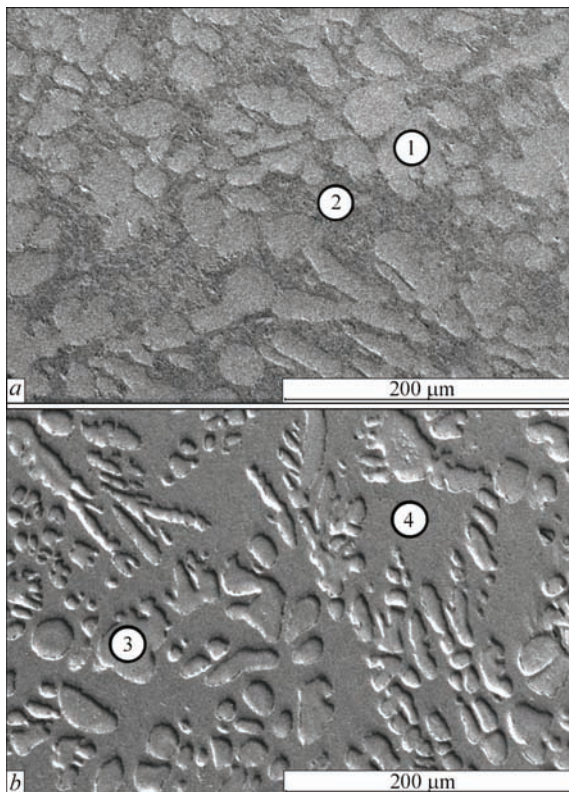
Table 1 gives composition and melting temperature of KMKh and KMKhS alloys.

Philosophy of the new materials design is based on application of cobalt-based solid solution alloyed by molybdenum and chromium as a matrix. It can withstand contact and thermal loads to 1000 °C temperature with additional implementation of boron and silicon, which reduce melting temperature and increase adhesion activity of the alloys to necessary level during deposition on the contact surfaces in liquid state. Besides, after solidification boron and silicon actively form uniformly distributed, thermodynamically stable, high-disperse strengthening phase, consisting of complex silicides and borides. This pro-

**Table 1.** Properties of KMKh and KMKhS alloys

Alloy grade	Composition, wt.%							Melting temperature*, °C
	Co	Cr	Mo	Si	B	Ni	Cr <sub>3</sub> C <sub>2</sub>	
KMKh	Base	17–18	27–28	2.8–3.2	0.8–1.2	–	–	1185 <sup>+5</sup>
KMKhS	Same	17–18	27–28	2.8–3.2	0.8–1.2	2.8–3.2	1.9–2.1	1165 <sup>+5</sup>

\*Melting temperature was determined by means of high-temperature differential thermal analysis.



Microstructure of KMKh (a) and KMKhS (b) alloys

vides for necessary high level of alloys wear resistance. Dosed additives of chromium carbides in KMKhS alloy somewhat reduce melting temperature in comparison with KMKh alloy and stabilize its structure and properties.

**Table 2.** Phase composition of KMKh and KMKhS alloys

Alloy grade	Interplanar spacing (experimental data), $d_{hkl}$	Interplanar spacing (reference data), $d_{hkl}$	Phase [9]
KMKh	2.046	2.040	Co
	1.775	1.770	
	0.219	0.219	CoB
	0.185	0.183	
	0.237	0.237	Mo <sub>2</sub> B
	0.220	0.219	
KMKhS	0.237	0.237	MoSi
	0.219	0.220	
KMKhS	0.198	0.197	CoSi
	0.181	0.183	
	2.047	2.040	Co
	1.776	1.770	
	0.219	0.219	CoB
	0.185	0.183	
KMKhS	0.237	0.237	Mo <sub>2</sub> B
	0.220	0.219	
KMKhS	0.237	0.237	MoSi
	0.219	0.220	
KMKhS	0.198	0.197	CoSi
	0.181	0.183	
KMKhS	0.238	0.237	Cr <sub>2</sub> C <sub>6</sub>
	0.218	0.219	

Figure shows microstructure of the alloys, produced by vacuum-induction melting in vacuum of around  $10^{-2}$  Pa with further annealing during 1 h at 1100 °C temperature. The alloys have regular double-phase structure, density and homogeneity of which rise at transfer from KMKh to KMKhS alloy. Hardness of KMKh alloy makes around 710–715 units ( $HV_{10}$ ) and that of alloy KMKhS is 735–740 units. Average microhardness ( $H_{\mu 50}$ ) of constituent phases for KMKh alloy corresponds to 4771 MPa (zone 1, Figure) and 2365 MPa (zone 2) and that for alloy KMKhS is 6661 MPa (zone 3) and 3213 MPa (zone 4), respectively.

X-ray structure analysis of the alloy samples indicate that basis of both alloys is a solid solution of alloyed stable cubic cobalt ( $\beta$ -modification), which is uniformly reinforced with disperse precipitations of strengthening phases: CoB, Mo<sub>2</sub>B, MoSi and CoSi. Alloy KMKhS, besides, contains chromium carbides Cr<sub>2</sub>C<sub>6</sub> (Table 2). All identified phases have alternating stoichiometric composition and contain in different relationship alloys' element-components.

Comparative wear resistance tests of commercial alloys and new composite consumables KMKh and KMKhS were carried out using known procedure [10] under conditions of high-temperature fretting on gas-dynamic bench allowing complete reconstruction of operating conditions of the contact surfaces of turbine blades in the engine on loads, acceleration levels, heating and cooling rates, vibration frequency as well as gas medium. Aircraft kerosene TS-1 was used as a fuel.

Wear intensity was determined in wear resistance testing of studied samples:  $J_v = V/N$ , where  $J_v$  is the volumetric intensity of wear-out, mm<sup>3</sup>/cycle; V is the volume of worn material, mm<sup>3</sup>; N is the number of loading cycles (derivative of samples' oscillations). Other parameters corresponded the following conditions, namely static contact load 50 MPa; amplitude of relative movement of samples — 0.169 mm; oscillation frequency — 2500 min<sup>-1</sup>; test time — 2 h; temperature in area of contact of studied samples ~ 1150 °C.

Studied samples of high-temperature nickel alloy ChS88U-VI with 22×12×2 mm platform size were deposited by a layer of wear-resistant consumable of 2 mm thickness with further annealing at 1100 °C temperature in  $10^{-2}$  Pa vacuum during one hour for stress relief. All surfacing consumables were used in form of rods of 2×2 mm section. Commercial surfacing consumables Kh30N50Yu5T2 and V3K-r were deposited by tungsten argon-arc welding (welding code 141), at that microcracks in a base to deposit-

**Table 3.** Results of testing of wear resistance of deposited samples

Tested material	Kh30N50Yu5T2	V3K-r	KBNKhL-2	KMKh	KMKhS
<u>min-max</u> average	<u>7.718–14.408</u> 10.126	Fractured		<u>1.817–3.750</u> 2.761	<u>1.548–2.894</u> 2.372
Wear intensity, $J_v$ , mm <sup>3</sup> /cycle	Based on testing 40 min			Based on testing 2 h	

ed metal transition zone conditionally were considered as unacceptable defects. Surfacing by stellite KBNKhL-2 and new adhesion-active surfacing consumables KMKh and KMKhS was carried out using oxyacetylene flame of normal regulation with GS-2 torch, nozzle No.2 (welding code 311). Surface for deposition and surfacing rods were fluxed by spirit solution of PV200 flux (relationship 1:7). After surfacing the samples were cleaned from flux remains using galvanic method, mechanically treated and tested by non-destructive fluorescence method. Wear tests were carried out on pairs of identical samples with area of mutual contact of around 50 % (12–14 mm<sup>2</sup>). The results of tests are given in Table 3.

Analysis of test results showed that the commercial high-temperature wear-resistant alloys V3K-r and KBNKhL-2 did not withstand contact loads and completely fracture under heating to ~1150 °C. The samples deposited by commercial alloy Kh30N50Yu5T2 can work under such conditions only for limited time due to intensive wear. Developed new adhesion-active materials KMKh and KMKhS demonstrate significantly higher wear resistance at that average value of intensity of their wear based on two hours testing is 3–4 times lower than that in the surfaces deposited by commercial alloy Kh30N50Yu5T2 based on 40 minutes testing. Dosed additives of chromium carbides (in around 2 wt.% amount) in KMKhS alloy simultaneously with decrease of alloy melting temperature (by ~20 °C) result in rise of its wear resistance in comparison with KMKh alloy by 15–20 %. High wear resistance characteristics and possibility of operation under effect of critical temperatures allowed recommending developed composite consumables and technology of their surfacing on platforms of blades of ship gas turbine engines to commercial application at SE GTSPC «Zorya-Mashproekt».

## Conclusions

1. Commercial high-temperature wear-resistant alloys, used in ship machine building, such as V3K-r, KBNKhL-2, Kh30N50Yu5T2 do not withstand contact loads and fracture under conditions of heating to critical temperatures.

2. Proposed new adhesion-active composite consumables KMKh and KMKhS can withstand critical temperatures up to 1150°C as well as demonstrate at that high wear resistance, satisfying the operation and repair requirements of current ship GDE.

- Kostin, A.M., Butenko, A.Yu., Kvasnitsky, V.V. (2014) Materials for strengthening of gas turbine blades. *The Paton Welding J.*, **6/7**, 132–134.
- Kostin, A.M., Butenko, A.Yu., Maly, A.B. (2012) Analysis of materials for strengthening of turbine blade platforms (Review). *Vestnik NUK*, **5**, 137–141. <http://ev.nuos.edu.ua/ru/material?publicationId=19317>
- Altukhov, A.A., Gavrillov, O.V. (2004) Application of heat-resistant consumable KBNKhL-2 for surfacing of gas turbine parts. *Svarshchik*, **2**, 22–23.
- Pejchev, G.I., Zamkovoij, V.E., Andrejchenko, N.V. (2009) Comparative characteristics of wear-resistant alloys for strengthening of blades platforms of gas turbine engines. *Vestnik Dvigatelsestroeniya*, **2**, 123–125.
- Som, A.I., Ishchenko, V.Yu., Maly, A.B. (2004) Stellite plasma-powder surfacing with of pipe clamps. *Svarshchik*, **2**, 18–19.
- Dmitrieva, G.P., Cherepova, T.S., Kosorukova, T.A. et al. (2015) Structure and properties of wear-resistant alloy based on cobalt with niobium carbide. *Metallofizika i Novejschie Tekhnologii*, **37(7)**, 973–986.
- Kostin, O.M., Martynenko, V.O., Maly, O.B. et al. *Wear-resistant high-temperature composite alloy based on cobalt*. Pat. 107286 Ukraine. Int. Cl. C22C 19/07, C22F 1/10. Fill. 21.12.2015; Publ. 25.05.2016.
- Kostin, O.M., Martynenko, V.O., Maly, O.B. et al. *Wear-resistant high-temperature composite alloy based on cobalt*. Pat. 111213 Ukraine. Int. Cl. C22C 19/07, C22C 29/00. Fill. 22.03.2016; Publ. 10.11.2016.
- Mirkin, L.I. (1979) *X-ray testing of machine-building materials*: Refer. Book. Moscow: Mashinostroenie.
- Ivshchenko, L.J., Andrienko, A.G. (1996) Method of tribological tests under conditions of cyclic force and temperature loading. *Metaloiznavstvo ta Obrobka Metaliv*, **3**, 62–65.

Received 09.12.2016

# STATE-OF-THE ART AND TENDENCIES IN DEVELOPMENT OF WELDING ELECTRODE MARKET IN UKRAINE

S.V. PUSTOVOJT, N.V. SKORINA and V.S. PETRUK

E.O. Paton Electric Welding Institute, NASU

11 Kazimir Malevich Str., 03680, Kiev, Ukraine. E-mail: office@paton.kiev.ua

Welding as the main technology of joining materials is an intrinsic component of the industrial sector of economy, integrated into production process of basic industries. The paper presents systematized economic-statistical information about the state-of-the art and development of welding electrode market in Ukraine, the indices of their production volumes and export-import operations. Capacities of Ukrainian manufacturers allow both satisfying the demand for welding electrodes in the internal market, and supplying their products to the external market. 12 Ref., 3 Tables, 11 Figures

**Keywords:** *welding, welding production, welding electrodes, technologies, market state, prospects*

Processes of globalization in the world and their influence on internal markets necessitate performance of studies of welding equipment market in Ukraine, in order to identify promising directions of development of welding production in view of its high importance to national economy, as welding as a method to produce permanent joints of metals and non-metals is the basic technology in many industrial sectors and in construction.

Economic-statistical analysis of the state of world and regional markets of welding equipment in Ukraine and prospects for their development is given in [1–7]. These investigations allow finding optimum ways for successful functioning of Ukrainian manufacturers to satisfy the demand for their products under the conditions of tough competition not only in external, but also in the internal markets. To ensure stable functioning of Ukrainian manufacturers of welding materials under these conditions, it is necessary to quickly respond to constantly changing requirements of the users through improvement of the already manufactured products which are in demand in the market and developing new ones [8, 9]. An important element in

planning the enterprise activity is evaluation of the competitiveness of the produced welding materials in each area of their application [10].

Welding materials manufacturing is the leading component of welding production in Ukraine. Capacities of Ukrainian enterprises-manufacturers of welding materials, in particular, welding electrodes, allow both satisfying internal market needs, and supplying their products to external markets [11]. This is promoted by availability of raw material base for producing general-purpose electrodes, used for welding carbon and low-alloyed steels (ANO-4, ANO-21, MR-3 grades with rutile coating, as well as electrodes with basic coating of UONI-13 type). This is due to the fact that their products were in demand in many enterprises of mechanical engineering complex, in construction and other spheres of production (Figure 1). Demand for special electrode grades for welding in power engineering, welding of pipelines, high-alloyed steels, non-ferrous metals, cast iron and for surfacing operations during Soviet times was satisfied mainly by supplies from Russia.

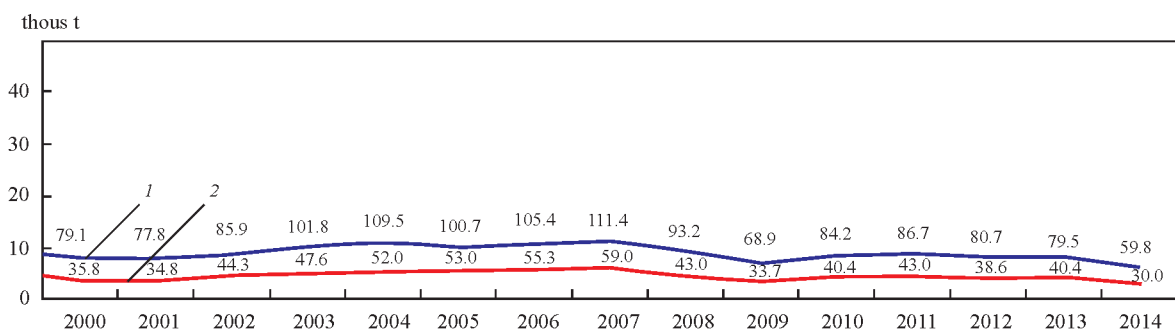


**Figure 1.** Dynamics of welding material and electrode production: 1 — WM production volume; 2 — electrode production volume; 1990 — 429.9 (WM), 162.4 (welding electrodes); 1995 — 93.4 and 54.2, respectively

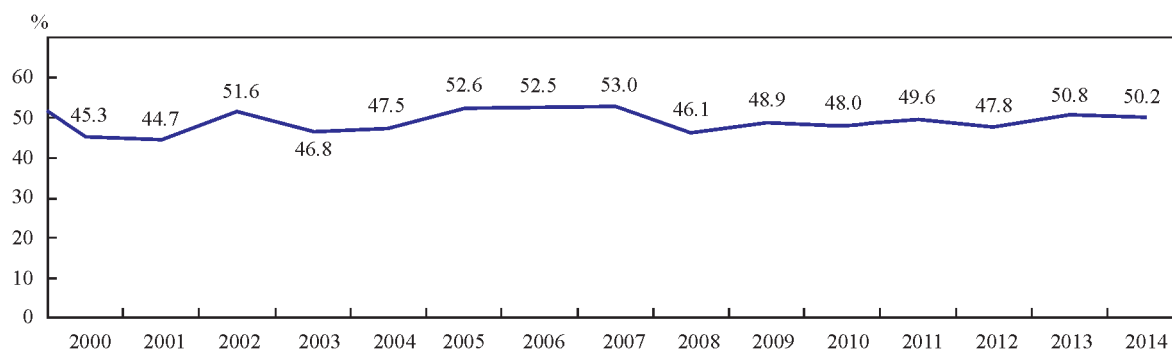


Figure 2. Share of welding electrodes in overall volume of welding material production; 1990 — 37.88, 1995 — 58 %

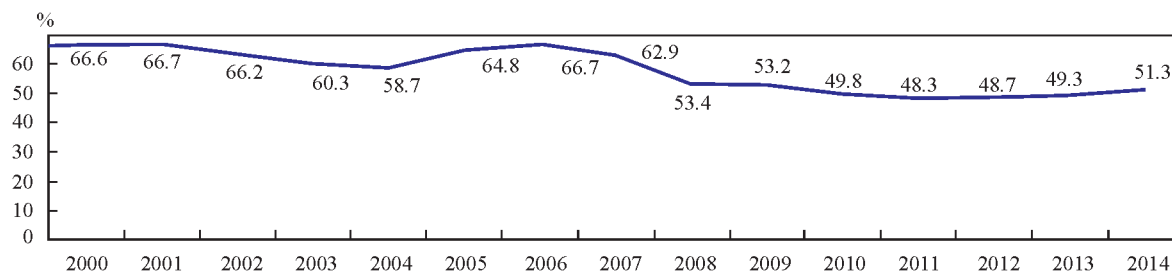


Figure 3. MAW share (by deposited metal); 1990 — 41.98; 1995 — 65.1 %

Long-term economic crisis in CIS countries led to a considerable reduction of the volumes of welding material production, including welding electrodes. Starting from 1995, the scope of production of welding materials and electrodes was stabilized in the new range. During the years of growth of industrial production in Ukraine and CIS countries (main sales markets) the output of welding materials and welding electrodes increased. During the years of economic and financial crisis a decline of production of welding materials and electrodes was observed, both in Ukraine, and in the world. Such an almost synchronous change of production volumes was caused by that the proportion of welding electrodes material the

main part of welding material output structure (Figure 2).

Increase of the proportion of welding electrode output is related to increase of the scope of work, performed using manual arc welding (Figure 3), in connection with the change in the structure of industrial production (Table 1), namely reduction of the share of mechanical engineering (to 6.4 %), as a result of reduction in the output of key product kinds (Table 2), in manufacturing of which automatic and mechanized welding is extensively used. With stabilization of economic processes in the country and growth of industrial production the share of manual arc welding by deposited metal somewhat decreases, but it remains

Table 1. Proportion of the main industries in overall scope of production, %

Industry	1990	1995	2000	2005	2008	2010	2012	2013	2014	2015
Power generation	3.2	11.0	15.2	15.9	17.8	21.3	24.5	24.6	24.6	21.9
Mining and metallurgical complex	12.1	23.4	29.8	30.4	31.4	28.9	26.5	26.1	27.4	29.6
Mechanical engineering	30.5	16.0	13.4	12.7	13.3	10.9	10.2	10.0	7.2	6.4
Light industry	10.8	2.8	1.7	1.1	0.9	0.8	0.7	0.7	0.8	0.9
Food industry	18.6	15.1	17.7	16.3	15.2	18.1	18.2	18.5	21.2	21.8

Table 2. Output of some industrial products

Product type	1990	1995	2000	2005	2010	2011	2012	2013	2014	2015
Finished rolled stock; mln. t	38.6	16.6	22.6	32.2	29.2	31.0	29.3	29.1	23.8	21.3
Steel pipes, mln. t	6.5	1.6	1.7	2.4	2.0	2.4	2.3	1.8	1.6	1.0
Metal cutting machines, thous. pcs	37.0	6.0	1.3	0.4	0.1	0.1	0.1	0.1	0.07	0.04
Press-forming equipment, thous. pcs	10.9	1.4	0.4	0.1	0.05	0.022	0.051	0.011	0.007	0.008
Welding equipment, thous. pcs	49.6	18.3	16.2	25.4	16.9	18.1	22.8	18.2	13.0	—
Excavators, thous. pcs	11.2	2.3	0.2	0.6	0.11	0.12	0.08	0.05	—	0.03
Tractors, thous. pcs	106.0	10.4	4.0	5.5	5.2	6.4	5.3	4.3	4.1	4.2
Cars, buses, thous. pcs	196.0	67.4	31.9	196.6	82.9	104.4	73.3	50.4	26.8	—
Precast concrete, mln. m <sup>3</sup>	23.3	5.6	2.0	3.2	1.9	2.3	2.1	2.0	1.9	1.7

**Table 3.** Application of arc welding processes, % (by deposited metal)

Country	Welding process	1965	1975	1985	1995	2000	2005	2012	2015
Western Europe	MAW		58	34	18	15	12	8.9	10
	CO <sub>2</sub>	74	31	56	70	71	75	63.9	56
	FCW		2	3	6	6.5	6.5	19.1	22
	ASAW		9	7	6	7.5	6.5	8.1	13
USA	MAW		53	42	25	19.5	15	10.3	11
	CO <sub>2</sub>	71	25	38	54	54	58.5	61.4	56
	FCW		13	13	19	19	19.5	22.1	23
	ASAW		9	7	7	7.5	7	6.2	10
Japan	MAW		67	44	22	14	12	7.3	8.8
	CO <sub>2</sub>	85	20	39	52	54	54.5	49.5	45.9
	FCW		1	11	25	25	27	35.9	35.1
	ASAW		9	10	7	7	6.5	7.3	10.2
Ukraine	MAW	63	52.4	44.9	65.1	66.6	64.8	48.9	
	CO <sub>2</sub>	9.5	23.7	35	26.5	23.3	16.1	32.5	
	FCW	0.5	3.2	3.4	0.9	0.5	3.2	1.4	
	ASAW	27	20.7	16.7	7.5	9.6	15.9	17.2	

*Note.* MAW — manual arc welding, CO<sub>2</sub> — gas-shielded welding; FCW — flux-cored wire welding, ASAW — automatic submerged-arc welding.

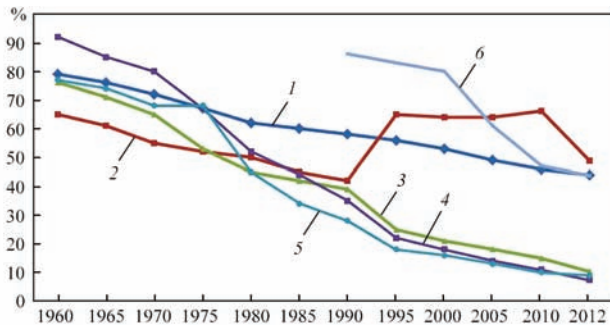


**Figure 4.** Share of manual arc welding in the world countries (% by deposited metal): 1 — RF; 2 — Ukraine, 3 — USA; 4 — Japan; 5 — Western Europe; 6 — China

high, compared to economically developed countries (Tables 3 and Figure 4).

Data given in Figure 4 show that the proportion of manual arc welding in Ukraine, which was equal to 64 % in 1965, was lower than that in economically developed countries (80–90 %). By 1990 it was on the

level of 42 % that is comparable with the indices for the USA and Japan. Over the recent years, the share of manual arc welding in Ukraine increased significantly for the above reasons. Wide application of MAW also influenced the scope of welding electrode market: volume of their production and consumption in Ukraine increased (see Figures 2 and 3).

Figure 5 presents the dynamics of production, export, import and apparent consumption of welding electrodes in the internal market. The basic needs for electrodes of mechanical engineering enterprises and construction are satisfied by their production by Ukrainian manufacturers. At present 14 welding electrode manufacturing enterprises are really operating in Ukraine, although in 1990s their number was up to one hundred. The main manufacturers currently are: PJSC «Plasmatek» (Vinnitsa), Mashzavod «Pobeda truda» Vistek (Bakhmut, Donetsk region), «Sumy-Electrode» Ltd. (Sumy), PWI Pilot Plant of

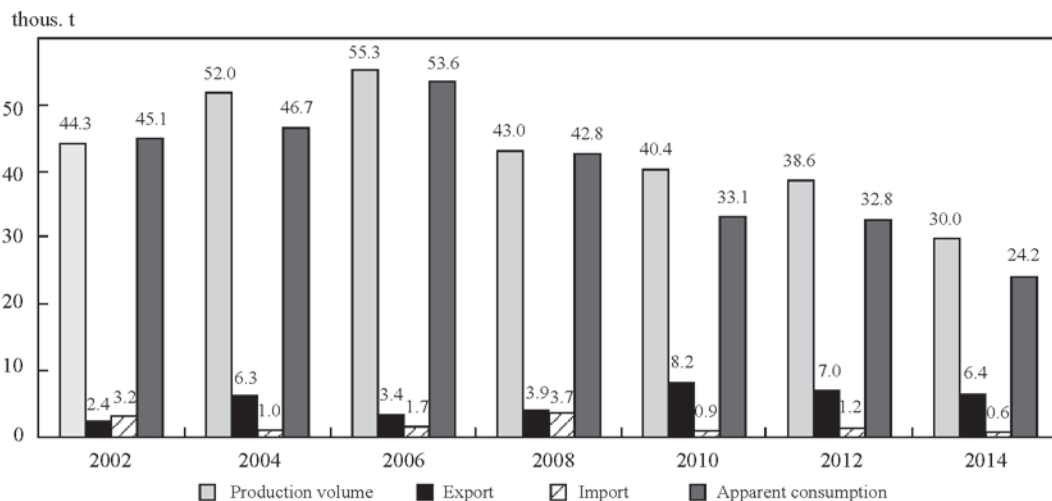


**Figure 5.** Scope of domestic consumption of electrodes in Ukraine, thous. t

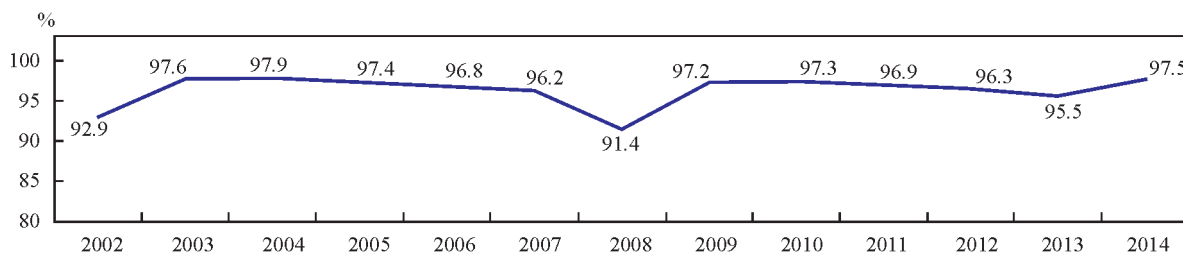


Figure 6. Share of Ukrainian manufacturers in the internal market

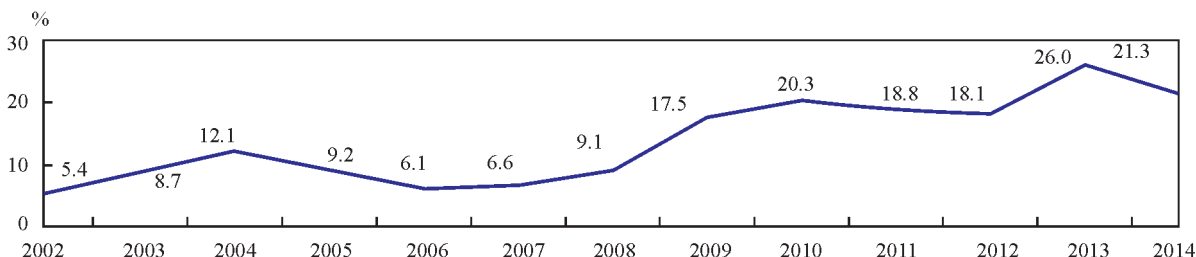


Figure 7. Export share in overall production volume

Welding Consumables (Kiev), «Galelektroservis» Ltd. (Lvov), «II BadmAtd» (Dniepr), «Gansa» Ltd. (Krivoj Rog).

Ukrainian manufacturers take up leading positions in the internal market. Their share in the internal market is higher than 90 % (Figure 6).

Dynamics of exports share in the overall volume of welding electrode production for 2002–2014 [12] is shown in Figure 7. Export volumes largely depend on economic condition in the main regional sales markets. During the years of growth of industrial production the demand for products of Ukrainian manufacturers grows in these markets, and volumes of export operations are increased, respectively. Due to devaluation of the national currency (hryvnia) during the years of financial crisis, Ukrainian products become more marketable and competitive that promotes export.

From 2002 till 2014 the import share in internal market structure was equal to about 4 %, on average, but in some years this figure was up to 8.6 %.

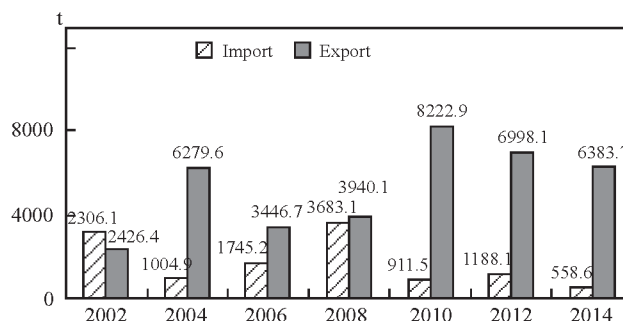


Figure 8. Dynamics of export-import of welding electrodes

Dynamics of export-import operations in the product group of welding electrodes is shown in Figure 8. Volumes of export supplies of welding electrodes are much larger than those of import. This ensures a positive foreign trade balance in this product group, and electrode manufacturing plants promote foreign currency flow into the country and maintenance of hryvnia rate.

The main regional associations on export-import operations are CIS and EU countries. These countries

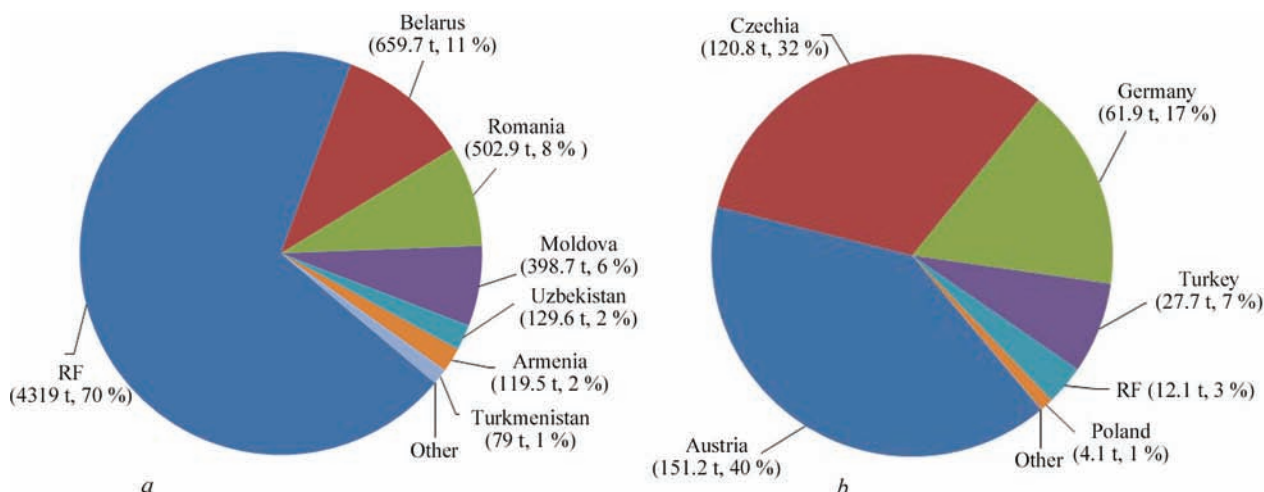
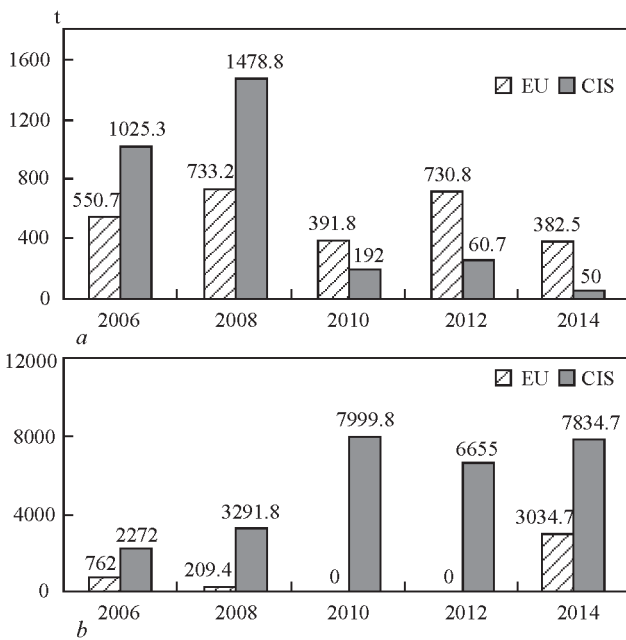


Figure 9. Geography of export-import operations in product group of welding electrodes for 2015: a — export; b — import



**Figure 10.** Dynamics of export-import operations with CIS and EU countries; *a* — import; *b* — export

account for 70–90 % of export-import volume (Figure 9). Dynamics of export-import operations with CIS and EU countries is shown in Figure 10.

CIS countries are the main region for export of Ukrainian manufacturing plants. Such plants as «Plasmatek» and «Sumy-Electrode» became the leading exporters. General purpose electrodes of UONI 13/45, UONI 13/55, MR-3, ANO-4, ANO-21, and ANO-36 grades are mainly supplied to the markets of these countries. Proportion of special electrodes is relatively small and includes four electrode grades for welding high-alloyed steels — TsL-11, OZL-18, EA-400/10U and EA-395/9, two grades of electrodes for cast iron welding — TsCh-4 and MNCh-2 and two surfacing electrode grades T-620 and T-590.

Volume of import from these countries in 2009–2014 decreased significantly and became an order of magnitude smaller than export indices. Mostly special purpose electrodes are imported. Reduced imports became possible as a result of import substitution of a number of electrode grades. The majority of plants have mastered production of special grades of welding electrodes, but their share in the general product volume grows, and is becoming the dominant one in some enterprises («Sumy-Electrode» Ltd., «Gefest», WeldingTek). PJSC «Plasmatek» and «Sumy-Electrode» Ltd. developed and put into production several grades of electrodes with rutile coating for welding high-alloyed steels, which correspond to the best foreign analogs.

Over the recent years leading enterprises of Ukraine developed and mastered production of mod-

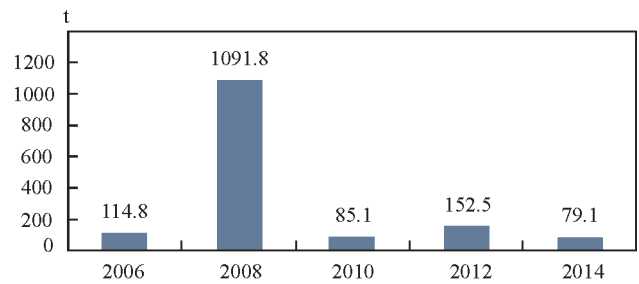


**Figure 11.** Dynamics of welding electrode supplies from China

ern electrode grades with rutile and basic coating, which in terms of quality correspond to the level of the best foreign grades (ANO-36, Monolit RTs, MD6013, Proton E6013, UONI-13/55 Plasma, etc.).

Starting from 2009, EU countries account for a considerable volume of import in product group of welding electrodes. The main suppliers are leading world companies, such as ESAB and BOHLER, which mainly supply high-quality electrodes for pipeline welding (OK 53.70, OK 74.30, FOX EV560, FOX PIPE, Phoenix 7018), which are not available in Ukraine, as well as electrodes with rutile coating for welding high-alloyed steels, having excellent welding-technological properties. Ukrainian analogs of these electrodes (for instance, TsL-11, OZL-8, etc.) are significantly inferior to them by their welding-technological properties.

Dynamics of supply of welding electrodes from China in 2005–2008 should be noted. Annual increase of import during this period was equal to 250–600 % (Figure 11). After a sharp drop in welding electrode sales in 2009, by 2013 the volumes of import practically reached the pre-crisis period indices. Mainly general purpose electrodes of ANO-21 type (E6013 type to AWS) were supplied from China. Due to a low content of manganese in the metal deposited with above-mentioned electrodes, however, the users had some complaints against them. Owing to hryvnia devaluation, supplies of welding electrodes from China have practically ceased.

Known Turkish Companies «ASKA-NYAK» and «GEDIK» performed supplies of general purpose welding electrodes with rutile and basic coating, as well as electrodes with rutile coating for welding high-alloyed steels, and electrodes for welding cast iron and copper. The above electrodes have a good balance of quality and cost.

Decline in industrial production in Ukraine in 2014–2015 as a result of political and economic crisis, led to a drop in demand for welding electrodes, and to reduction in their supplies from EU countries, Turkey and China, respectively.

## Conclusions

Welding is a leading technological process in Ukrainian industry, and the national market of welding electrodes is developing dynamically.

Production capacities available in Ukraine allow satisfying the domestic needs of mechanical engineering enterprises for most of the items in product group of welding electrodes.

Further stable and effective development of welding electrode production and improvement of their competitiveness is possible at application of the results of fundamental and applied research, available high potential, active transfer of high welding technologies and other innovations.

1. Bernadsky, V.N., Mazur, A.A. (1999) State-of-the-art and prospects of world welding market. *Avtomatich. Svarka*, **11**, 49–55.
2. Bruno Pekkari (2006). *Svetsaren*, **3**, 12–16.
3. Bernadsky, V.N., Makovetskaya, O.K. (2007) Welding fabrication and welding equipment market in modern economy. *The Paton Welding J.*, **1**, 35–39.
4. Makovetskaya, O.K. (2011) Modern market of welding equipment and materials. *Ibid.*, **6**, 18–32.
5. Makovetskaya, O.K. (2012) Main tendencies at the market of welding technologies in 2008–2011 and forecast of its development (Review). *Ibid.*, **6**, 32–38.
6. Zadolsky A.N., Pin Ma (2009) Review of welding production market in Ukraine. *Biznesinform*, **5**, 33–39.
7. Middeldorf, K., Hofe, D. von (2009) Tendencies of development of material joining technologies. *Mir Tekhniki i Tekhnologij*, **11**, 12–16.
8. Yavdoshchin, I.R., Folbort, O.I. (2011) New information on «old» electrodes. *The Paton Welding J.*, **1**, 48–49.
9. Marchenko, A.E., Skorina, N.V., Kostyuchenko, V.P. (2011) State-of-the-art of development and manufacture of low-hydrogen electrodes with double-layer coating in CIS countries (Review). *Ibid.*, **1**, 41–44.
10. Shlepakov, V.N. (2011) Current consumables and methods of fusion arc welding (Review). *Ibid.*, **10**, 26–29.
11. (2015) *Economic-statistic review of welding production and market of welding equipment of Ukraine in 1990–2014*. Kyiv: PWI.
12. *Foreign economic activity of Ukraine in 2002–2015*. Kyiv: PWI.

Received 08.12.2016

## PRODUCTION OF FLUX-CORED WIRES IN «TM.VELTEK» COMPANY

In 1993 in Kiev on the initiative of the group of colleagues of the E.O. Paton Electric Welding Institute the joint Russian-Ukrainian enterprise OJSC «SP TM.VELTEK» was founded. The successful start of production of flux-cored wires in the new political and economic conditions of the 90s was provided due to the support of the «Dnepropetrovsk Hardware Production Association», whose management treated the idea of restoring the production of flux-cored wires with understanding. In 2001, the production of flux-cored wires was allotted into a separate division: the company OJSC «TM.VELTEK».

The close cooperation with leading research centers, including those in the field of welding and a high professionalism of engineering and technical staff and workers allowed mastering a stable classical technology of production of welding and surfacing flux-cored wires and wires for electric arc spraying to perfection.

Over the period of work of the company the complex of measures on repair and modernization of basic equipment, in particular, the production lines for flux-cored wires and the charge division, was realized. The modern types of products delivery were mastered. The technologies of manufacturing flux-cored wires of diameters from 1.0 to 6.0 mm were updated.

The efforts of the enterprise allowed preserving a significant part of the market of welding consumables of Ukraine for domestic producers and providing the consumers with quality materials at reasonable prices. The practice of work of the enterprise includes rendering consulting advice on the choice of material, the optimal technology and equipment for its realization, providing engineering support of the production process. In some cases, the enterprise produces flux-cored wires according to technical specifications, individually agreed with the customer. The weldability of the already mastered grades is constantly improved and new grades of wires are developed, which have no analogues.

Regardless of the nomenclature and volumes of batches, the high scientific and technical potential

of the enterprise allows fulfilling the orders in the shortest terms and with the required quality. This allowed occupying a large enough share of the market in Ukraine, ensuring stable fulfillment of foreign contracts and becoming a permanent partner for many enterprises.

As to their purpose and technical characteristics the flux-cored wires of grade VELTEK are not inferior to the products of leading foreign companies, which is confirmed by their high estimate at the domestic and foreign exhibitions, recognition by the leading enterprises of Ukraine and CIS, the continuous expansion of application areas and growth of sales volumes despite the ever-changing economic and political conditions. Over the years of work the enterprise acquired the status of a reliable partner at the market of welding consumables in Ukraine, Russia, Belarus, Uzbekistan and other CIS countries, Lithuania, Latvia and also the Czech Republic, India.

Since 2004, at the enterprise the quality management system was realized certified by UkrSEPRO and the Russian Maritime Register of Shipping, which meets the requirements of DSTU ISO 9001:2009 (ISO 9001:2008, IDT). The certificates of conformity UkrSEPRO on more than 100 grades of welding and surfacing flux-cored wires, the Certificate of approval of welding consumables of the Russian Maritime Register of Shipping, the Certificate of approval of welding consumables Lloyds Register and the Certificate on approval of welding consumables of the Register of Shipping of Ukraine were obtained.

The flux-cored wires of grade VELTEK are used in a wide range of industries: at the railway enterprises, at the integrated works of mining and metallurgical complex, at the plants of metal structures, at the machine-building plants of mine, transport, hoisting equipment, in shipbuilding, diesel locomotives and carriage engineering. Below the nomenclature of a wide range of flux-cored wires for welding and surfacing, manufactured by the OJSC «TM.VELTEK» is briefly given.



The enterprise OJSC «TM VELTEK» produces flux-cored wires for welding of low-carbon and low-alloyed steels (PP-AN1, PP-AN4, PP-AN8, PPs-TMV6, PPs-TMV8, PPs-TMV29, PPs-TMV7, PPs-TMV10N), low-alloyed high-strength (VeT PPs-TMV57) and heat-resistant steels (VeT PPs-TMV14, VeT PPs-TMV15), as well as for welding of high-manganese steels of the type 110G13L in combination with low-alloyed and alloyed structural steels (VELTEK-N210U, VELTEK-215, VeT PPv-TMV11). The last wires can also be used for surfacing of buffer layers before application of hard-alloy coating. Also, the OJSC «TM.VELTEK» produces a large amount of surfacing flux-cored wires, which are applied in different industries and are designed for restoration of different types of worn-out parts of machines.

The flux-cored wires, applied at the railway enterprises (VELTEK-N250, VELTEK-N290, VELTEK-N351, VELTEK-N490, VELTEK-285) are designed for surfacing of thrust bearings of trolleys and wheels of railway cars, axles, shafts, surfacing and repair of defective areas of tracks and automatic couplers of car devices.

The flux-cored wires, applied for restoration and strengthening surfacing (VELTEK-N290, VELTEK-N300-RM, VELTEK-N350-RM, VELTEK-N351, VELTEK-N370-RM, VELTEK-N380, VELTEK-N450, VELTEK-N455, VELTEK-N475) are designed for restoration surfacing of seats of

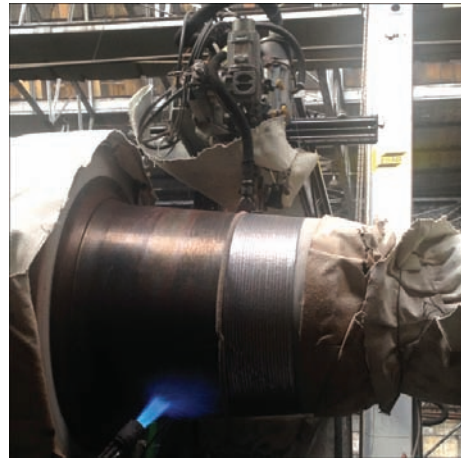


axles, shafts, necks of MCCB rollers, as well as for strengthening surfacing of tractor rollers and caterpillar tracks, rollers of roller conveyors, bandages, crane wheels, brake pulleys, gear teeth, support rollers, etc.

The flux-cored wires, applied at large metallurgical plants for parts, subjecting to significant specific pressures and wear at the elevated temperature (VELTEK-N390, VELTEK-N410, VELTEK-N415, VELTEK-N420, VELTEK-N460, VELTEK-N462, VELTEK-N465, VELTEK-N470, VELTEK-N472, VELTEK-N480, VELTEK-N495, VELTEK-N500-RM, VELTEK-N505-RM, VELTEK-N550-RM, VELTEK-N555, VELTEK-N565), are designed for surfacing of MCCB rollers, plungers of hydraulic presses, hot rolling rolls of pipe rolling and section rolling mills, knives of hot and cold metal cutting, punching and pressing tools, sealing surfaces of general industrial fitting valves.

The surfacing flux-cored wires, applied for restoration and strengthening surfacing of manganese steels of 110G13L type and parts, operating under the conditions of high specific pressures (VELTEK-N200, VELTEK-N220U, VELTEK-N230, VELTEK-N240, VELTEK-N245, VELTEK-N285) are designed for surfacing of railway frogs, crushing jaws, parts of





shot blast blades, beats of hammer mills, heavy-loaded crane wheels, for restoration of sizes and correction of defects of 110G13L steel casting.

The wires are produced, applied for deposition of buffer layer before the strengthening surfacing: VELTEK-N210U, VELTEK-N215, VeT PPs-TMV11. The flux-cored wires, applied for surfacing of parts, operating under the conditions of impact-abrasive wear (VELTEK-N552, VELTEK-N575, VELTEK-N600, VELTEK-N620) are designed for surfacing of teeth and buckets of mining excavators for operation at rocky soils and frozen conditions, scoops of drags, grader blades, blades of bulldozers, mills for grinding of hard materials, crushers, asphalt mixers, rotors of vertical hammer crushers, roller presses, parts of dredgers and pulp pumps.

The flux-cored wires, applied for surfacing of parts, experiencing a strong abrasive wear (VELTEK-N560, VELTEK-N580, VELTEK-N605, VELTEK-N617, VELTEK-N640, VELTEK-N634, VELTEK-N635, VELTEK-N650), are designed for surfacing the parts of agriculture, worn-out parts of mining and metal-

lurgical enterprises, construction and road machinery, screws, parts of mixers, smoke extractor blades, casings and impellers of dredgers, parts of cement and concrete pumps, etc. The flux-cored wires, applied for surfacing of parts experiencing a strong abrasive wear in combination with a high temperature (VELTEK-N479, VELTEK-N630, VELTEK-N690) are designed for surfacing of protective surfaces of charging tapers and bowls, screens and grinders of agglomeration plants, coke dumping mechanisms, parts of mining and processing plants and plants for pellets formation, cutting edges and teeth of rotor excavators, blades of mixers, worm conveyors, grinders of cement clinker, concrete and cement pumps and other parts, worn out by friction, operating at elevated temperatures. Also, the enterprise manufactures flux-cored surfacing wires in accordance with GOST 26101–84.

A.A. Golyakevich, L.N.Orlov, V.N. Upyr